Master Thesis in Inorganic Chemistry

Design and Synthesis of Ruthenium based Olefin Metathesis Catalysts

Åsmund Singstad

Kjemisk Institutt

Universitetet i Bergen

1.6.2010

i Forord

Med denne oppgaven settes punktum for en nesten fem år lang æra ved Kjemisk institutt ved Universitetet i Bergen. Tiden har gått fort, fagene vært mange og inntrykkene av uendelig antall. Sett på det rent faglig, lurer jeg på om utdanningen min rent termodynamisk har vært spontan?

La oss først vurdere systemet; nemlig meg. Fra mitt ståsted har ikke prosessen virket i nærheten av spontan og jeg ønsker heller ikke at den skal være det. Jeg har forbrukt store mengder energi for å komme meg til et høyere akademisk nivå. Barrierene har vært mange og harde. Heldigvis har jeg fått hjelp av gode katalysatorer til å senke disse barrierene. Disse har vært kvantekjemikeren Phd. Student Yury Minenkov som har hjulpet og lært meg *mye* om beregningskjemi, dr.scient. Nicolas Merle som har bidratt med sine unike kunnskaper i eksperimentell organometallisk kjemi, krystallkongen Professor Karl Wilhelm Törnroos, biveileder Professor Hans-René Bjørsvik, hovedveilederen min Professor Vidar R. Jensen og i aller høyeste grad min biveileder dr.scient. Giovanni Occhipinti, som har brukt mye av sin *verdifulle tid* til å lære opp en uerfaren eksperimentell kjemiker. Mellom de harde transisjonstilstandene har jeg fått hjelp av kjemivennene mine til å stabilisere og ta vare på mellomliggende tilstander. De som fortjener omtale er ”molarmusene” fra museet Line, Randi og Rhiannon, Alexander, Marit og Fredrik.

Fra utsiden kan kanskje mastergraden min ha virket spontan, selv om det har vært mange medspillere som har prøvd å få orden på utdannelsen min. De som fortjener å nevnes er fjorårets foreleser Professor Knut Børve, Professor Leif J. Sæthre og Professor emeritus Jon Songstad for deres unike kunnskaper. Ros fortjener og Atle Aaberg som har hjulpet med NMR og som endte NMR-krigen, Lisbeth Glærum med tilgang til alle tenkelig kjemikalier, Egil Nodland for hjelp med MS og IR, Steinar Vatne for tilgang til eksotiske gasser og løsemidler, Elaine Olsson og Wouter Heyndrickx for sporadisk hjelp med systematiseringen av teoretisk informasjon.

Jeg ønsker at utdannelsen min skal ha vært ikke-spontan, siden jeg da er at da har jeg opparbeidet meg potensial til å få noe til å skje i etterkant av utdannelsen min, og ikke bare sluntret bort fem år av livet mitt…

Jeg vil også takke alle som har tatt seg tid til å lese gjennom oppgaven min og har gitt meg verdifulle tips og tilbakemeldinger. Tusen takk Vidar, Giovanni og Sigrid.

Takk til familien min, som har prøvd å interessere seg for det jeg har drevet med, selv om de lite har forstått. Og tilslutt tusen hjertelig takk til min elskede Sigrid som har holdt ut med sene middager og en til tider fraværende kjæreste i årene som har gått!

ii Abstract

The present Master thesis seeks to develop new unsymmetrical ruthenium-based olefin metathesis catalysts and therein a better understanding of olefin metathesis catalysis with unsymmetrical active complexes. Such catalysts have a potential for chemoselectivity and in best case, stereoselectivity. Two different classes of catalysts, coordinated by a hemilabile amine ligand and by a novel N-heterocyclic carbene (NHC) ligand respectively, have been investigated. Two new amine-based olefin metathesis catalysts have been synthesized and tested. In addition, quantum chemical calculations to study the catalysts were performed to give a better knowledge about their behaviour in catalytic olefin metathesis. Prior to the main calculations a validation study was performed to identify the most accurate and effective method of optimizing geometries. The catalysts are shown to be temperature dependent catalysts (latent catalysts) with high thermal stability, which makes them interesting for some industrial applications. The results from the experiments and the calculations are combined to give a better understanding of the catalyst and their properties. However, the analysis of the results for the amine-based catalysts, suggests a limited potential for *E/Z*-stereoselectivity. To explore a different potentially stereoselective design, a novel sterically demanding bidentate NHC ligand was synthesized. Unfortunately, any attempt to synthesize a corresponding olefin metathesis failed. Instead, we succeeded to synthesize a novel iridium(I) complex containing the novel bidentate NHC ligand. The iridium complex could have potential for catalytic hydrogenation by further adjustments.

iii Abbreviations

AC	active complex state
CM	cross metathesis
COD	cyclooctadiene
DFT	density functional theory
Equiv	molar equivalents
Et	ethyl
Et-DIPA	ethyl diisopropylamine
Ether	diethylether
EtOAc	ethyl acetate
H_2IMes	1,3-dimesityl-4,5-dihydro-imidazol-2-ylidene
HR-MS	high resolution mass spectroscopy
KBTSA	potassium bistrimethlysilylamide
MAINDE	mean all internuclear distance error
MCB	metallo-cyclobutane
Me	methyl
MEP	minimal energy path
MS	mass spectrometry
NHC	N-heterocyclic carbene,
NHC-phehoxy	bidentate NHC-phenoxy chelating ligand
NMR	nuclear magnetic resonance
olefin	alkene; old terminology.
PC	precatalyst state
PCy_3	tricyclohexylphosphine
Ph	phenyl ring
πC	π-complex
PPh_3	triphenylphosphine
RCM	ring closing metathesis
ROMP	ring opening metathesis polymerization
THF	tetrahydrofuran
TLC	thin layer chromatography
TMS	tetramethylsilane

iiii Numeration

G1, G2	Grubbs first and second generation catalyst.
H1,H2	Grubbs-Hoveyda first and second generation catalyst
I1-I5	imine based catalysts
L0-L16	amine ligand numberation used in chapter five
A1-A3	amine based olefin metathesis catalysts used in chapter three and five
A10,A13, A16	suggested new amine based catalysts
5	bidentate NHC ligand synthesized
6	silver complex of 5
9	iridium complex of 5

Table of contents

1 Introduction

1.1 Olefin metathesis

The phenomenon later called olefin (alkene) metathesis was first discovered and published in the Journal of American Chemical Society by Montague and co-workers 50 years ago.[1] Olefin metathesis is a chemical reaction where carbon-carbon double bounds are redistributed.[2] Montague and co-workers described the polymerization of norbornene using an aluminium and titanium catalyst, which showed an unusual ring opening reaction.[1] In 1964 a fairly detailed work described this redistribution of carbon-carbon double bond starting from simple alkenes and ending up with a more complex mixture of different alkenes.[3] This work was the first sign of what was later called cross metathesis,[4] which has proven to be a simple method to make expensive alkenes from cheap feedstocks. These works showed a new catalytic reaction. This reaction would at a later stage prove to be of real importance in organic chemistry, and so important that the work of the most important researchers in the field won the Nobel price in Chemistry in 2005.[5]

The general accepted mechanism for catalysed olefin metathesis was projected as early as in 1971 by Chauvin and Hèrisson.[6] For this work Yves Chauvin was included in the Nobel price in Chemistry in 2005. The reaction is basically an entropy driven equilibrated reaction,[7] but there are some exceptions; ring opening metathesis polymerization (ROMP) of sterically strained small cycloalkenes.[8] The general reaction mechanism for olefin metathesis is shown in Scheme 1.1. The 14-electron methylidene complex **I** is generally the active catalyst beyond the first cycle. Indeed, in the first metathesis reaction the alkylidene moiety (=CHR) of the initial catalyst is exchanged with the methylidene moiety ($=CH_2$) of the substrate, which usually is a terminal olefin. For ruthenium based catalysts, namely those investigated in this work, the first catalytic cycle is also preceded by the dissociation of a dative ligand that transforms the inactive 16-electron precatalyst into the active 14-electron alkylidene catalyst (initiation step).[9] After the initiation the propagation phase starts and after the formation of the methylidene complex **I,** a new alkene can be coordinated and the metallo-cyclobutane (MCB) **II** is formed. In the next step the MCB loses an ethylene molecule and a *new* metal alkylidene forms **III**. This active complex can once more coordinate a new alkene and form the corresponding MCB **IV**. In the next step the MCB loses another alkene, and the catalyst is back at the starting point **I**. All the steps in the catalytic cycle are in principle reversible, with some exceptions,[9] example goes ring opening metathesis polymerization of norbornene.

Scheme 1.1: Catalytic cycle proposed by Chauvin in 1970.

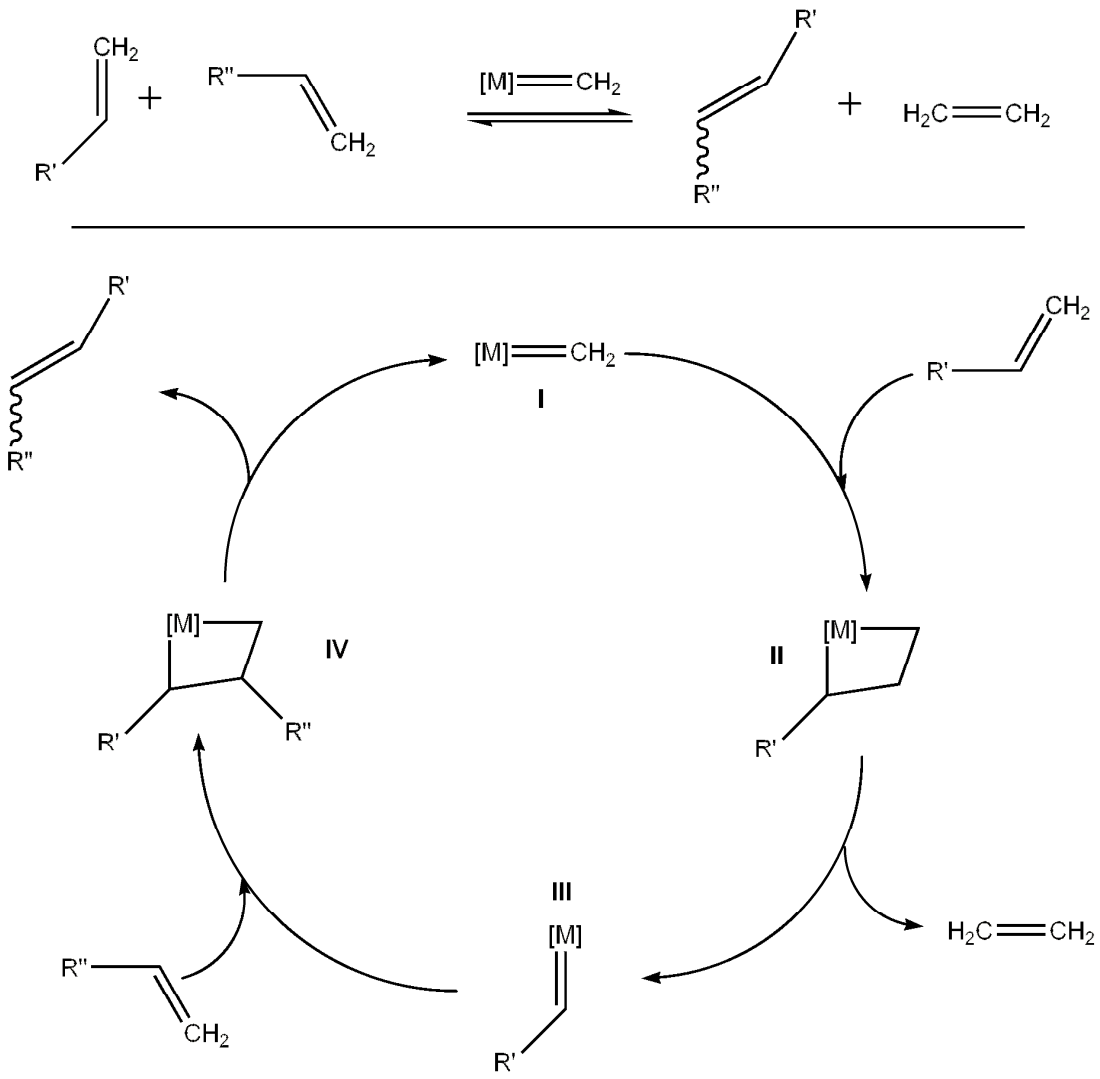

There are three types of transformations in olefin metathesis. The transformation showed in Scheme 1.1 is categorized as cross metathesis (CM). The other two are ring-opening metathesis polymerization (ROMP) and ring-closing metathesis (RCM).[4] The three transformations are shown in Scheme 1.2. Cross metathesis can difficult, because it is a challenge to obtain pure products. A CM between A and B can in principle give 6 different products: *E/Z*-AA, *E/Z*-AB, *E/Z*-BB. As well, it has the disadvantage of missing the entropic driving force, when ethylene is not formed. This often leads to low yields of desired product,[4] and sometimes really complex product mixtures.[3] A ring-closing metathesis will always have the entropy on its side, and thus the closing of the ring will be favoured. This reaction is often more troublesome for larger ring systems.[10] Ring opening metathesis polymerization is driven by ring-strain release,[8] and can also be a difficult metathesis when the benefit of steric strain is lacking.[11]

Scheme 1.2: The main types of olefin transformations in olefin metathesis.

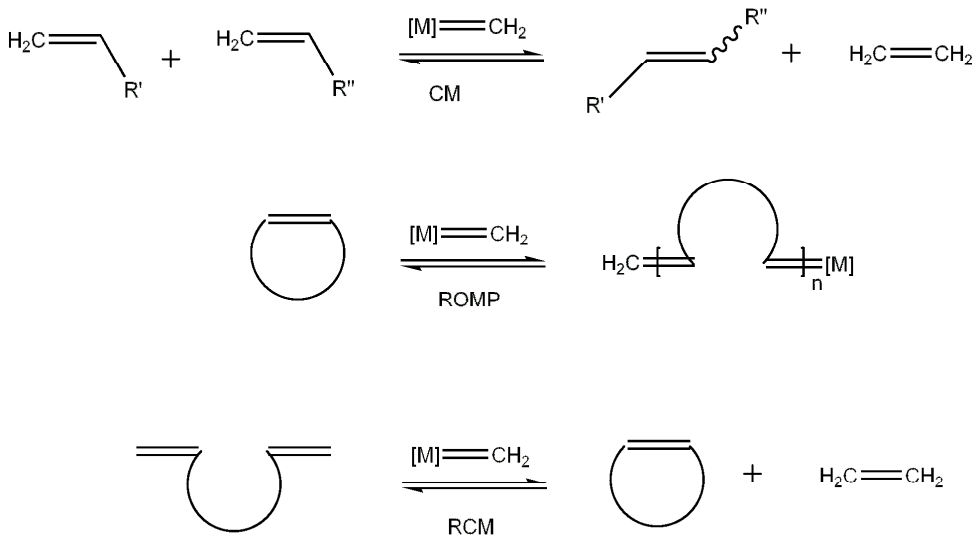

The two scientists who shared the Nobel price in Chemistry with Yves Chauvin in 2005 were Robert Howard Grubbs and Richard Royce Schrock.[5] Grubbs and Schrock and their co-workers have synthesized numerous of important olefin metathesis catalysts. Schrock and his co-workers managed to make well-defined molybdenum alkylidene complexes, which promotes olefin metathesis.[12] Grubbs and his co-workers were able to make the first well-defined olefin metathesis catalyst based on ruthenium in 1992.[13] In 1995 they completed the synthesis of a catalyst which is now known as the first generation Grubbs catalyst (**G1**).[14,15] The ruthenium based catalysts were shown to be more stable towards oxygen and moisture than the molybdenum catalysts made by Schrock.[16,17] In addition the Grubbs type catalysts had a higher tolerance towards functional groups, such as alcohols, aldehydes and acids.[17]

The most important ruthenium based catalysts in olefin metathesis are shown in Figure 1.1. In 1999 Grubbs and co-workers synthesized the first example of the second generation Grubbs catalyst (**G2**).[18] This catalyst was more active than the first generation, while retaining its stability.[18] In fact **G2** is more stable than **G1**. In the end of 1998 Hoveyda and co-workers synthesized an adjusted version of 1. gen. Grubbs by varying the structure of the alkylidene, by using an alkylidene that were substituted with a chelating ether group that functioned as a dative ligand trans to the phosphine (**H1**).[19] The Hoveyda analogue of the second generation Grubbs catalyst was published in 2000 (**H2**).[20] The structures of the mentioned ruthenium-based catalysts mentioned are shown in Figure 1.1.

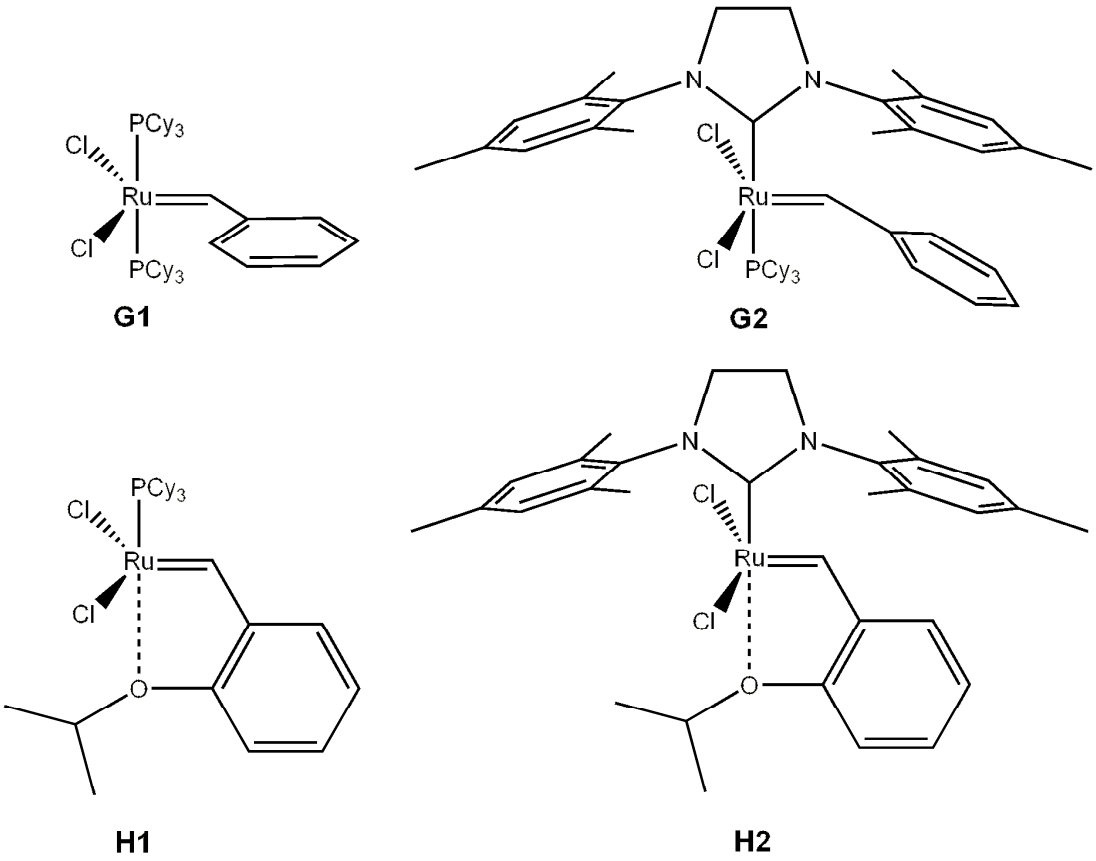

Figure 1.1: The most important ruthenium based olefin metathesis catalyst.

In biological sciences, organic synthesis is thought to be the major stumbling block.[21] This motivates further development of chemical synthesis. In chemical synthesis alkenes are important in numerous reactions, because of their ability to function as precursors for lots of functionalized molecules.[22] The improvement of catalytic olefin metathesis has been of great help for solving a lot of synthetically challenges,[4,23-33] and the second generation Grubbs catalyst class has proved to be among the most economically important catalysts invented in the two last decades.[34]

The need to develop new catalysts with both increased reactivity (metathesis of difficult substrates) and activity (metathesis rate) will always be present, and it can even be useful with some less active catalysts; latent catalysts.[35] This is especially of interest since there are a clear variation in the product mixtures, yields and conversions according to the catalyst used. Blechert and co-workers tested both the **G2** and **H2** under the same conditions. Their results show that these seemingly similar catalysts are showing different catalytic behaviour.[36] There is therefore a need to tune the catalysts to make them handle different classes of substrates.[37] A lot of modifications have been done

on **G2** to try to tune the reactivity and activity.[38] These catalysts are separated into different classes of catalysts according to their structure and properties.

In the last ten years there have been extensive computational studies to rationalize how different factors influence the activity of different catalysts.[34,39] The studies have also extended the knowledge of the mechanism in olefin metathesis in a more detailed manner than projected by Chauvin.[40-43] The development of new catalysts can therefore be aided by quantum and computational chemistry. In 2006 Occhipinti et al. published a large screening of existing and potential olefin metathesis catalysts.[44] Their goal was to contribute to a more cost-efficient optimization of the Grubbs family of catalysts. The work was focusing on the thermodynamics from calculations and treating the variation of the structures in a multivariate manner and they came out with predictions for new and more active catalysts, compared to the ones existing at the time. One example which was similar to the suggested active complex, was synthesized by Grubbs and co-workers in 2008 and later patented.[45,46] In 2007 Fournier et al. followed the suggested strategy to increase the activity of the catalyst by substituting the backbone of the N-heterocyclic carbene ligand, in this case with *tert*-butyl groups.[47] This catalyst was stated to have an intriguing reactivity profile.[47]

In the later stages in olefin metathesis the ability to handle bulky alkenes has become the most appreciated activity,[45,46] since there exists many well-known catalysts which are performing very well for RCM of simple alkenes.[45,48]

Even 18 years after the first well-defined ruthenium based olefin metathesis catalysts was characterized,[13] there are still some major challenges in olefin metathesis. Ring-closing to make macrocycles[49] and selective catalysis was a problem ten years ago,[17,50] and still is.[51] The most interesting and probably most difficult is to obtain a stereoselective catalyst. The most interesting would be to make a *Z*-stereoselective catalyst, since the Z-isomer is usually thermodynamically disfavoured, but even an *E*-stereoselective catalyst would be interesting. This is because one usually obtains a mixture of both isomers (*E* and *Z*) in CM and RCM.[4,52,53] Civetone[53] is a macrocyclic musk, shown in Figure 1.2, and could be purely obtained by a *Z*-stereoselective olefin metathesis catalyst. By conventional olefin metathesis catalyst this is not possible. Another approach has to be used to obtain this nice smelling fragrance.

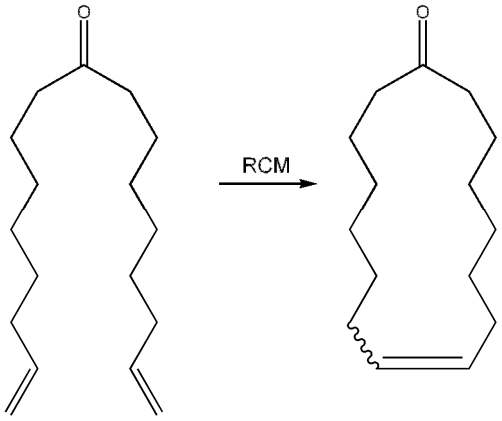

Figure 1.2: Ring closing to form civetone.

Fürstner and co-workers published a method to obtain the *Z*-isomer of some macrocyclic systems by doing *alkyne* metathesis and then do a selective hydrogenation to obtain the *Z*-isomer of the ring.[52,53] By this approach they managed to make civetone selectively.[53] Even though the synthesis is obtainable by alkyne metathesis, it would be preferable to make an olefin metathesis catalyst that could do this transformation. To do the same transformation by RCM one would reduce the number of steps needed to do the ring closing, and it would also be easier to make the needed substrate. In the last years there have been published some catalyst which gives a relative high yield of the *Z*-isomer,[54] but not in RCM which is known to be more challenging.

1.2 Scope

I will continue the work done previously in our group. In 2007 the group synthesized a chelating tertiary amino-benzyloxy ligands which were reacted with second generation Grubbs catalyst to yield new catalysts **A1**,[55] shown in Figure 1.3. Attempts to make the corresponding first generation analogue was not sucessful.[56]

The catalyst was at that time a new class of olefin metathesis catalysts, but during the time the group was working on the publication, Grubbs and co-workers published some similar complexes: **5,6**.[57,58] The motivation to explore these type of catalysts was that the ruthenium amine bond showed a similarity to the ruthenium imine bond.[56] The catalyst class with ruthenium imine bond has been thoroughly explored by Verpoort and co-workers.[35,59,60] These catalysts have been proven as decent catalysts and some are commercial available.[61] This type of catalyst is interesting in the point of view that one can control the activity to a certain extent. The catalytic activity is temperature dependent,

almost not active at room temperature and active at elevated temperatures. In a chemoselective point of view such latent catalysts can be very interesting.

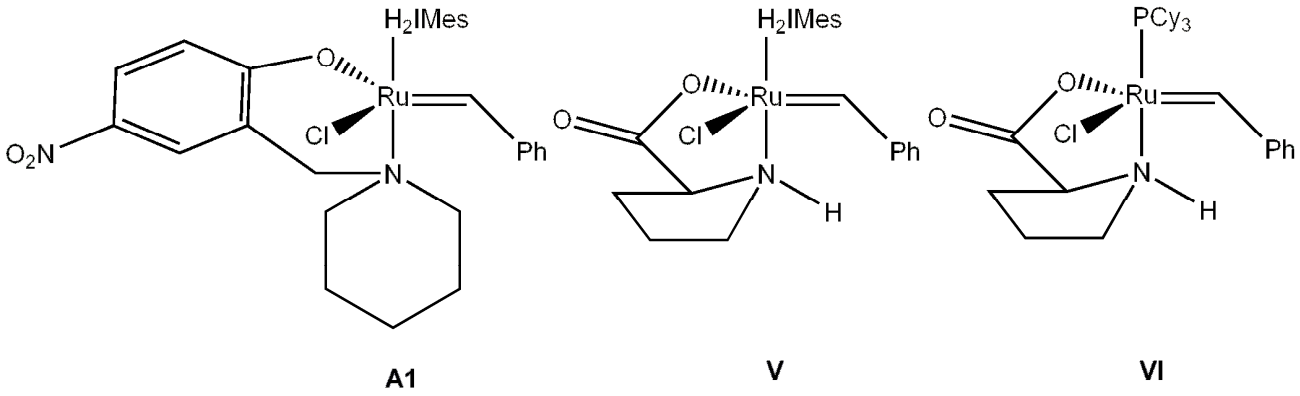

Figure 1.3: The existing catalysts with chelating amine ligands.

The structures in Figure 1.3 are the basis for making new Grubbs type second generation catalysts bearing a chelating tertiary amine-carbooxy ligand. If Grubbs type of catalysts should give any stereoselectivity we need to break the symmetry of the active complex. There are two main strategies of doing this, and both of these have been explored in our group. One approach is to make a catalyst with a ligand containing the decoordinating moiety, here an amine. The other strategy is to make a chelating usymmetrical bidentate non-labile NHC ligand. This approach has been explored by Hoveyda and co-workers and shown potential for enantioselective olefin metathesis.[62] Our group has also followed this approach, but we were unable to make a new catalyst containing the ligand.[63] Unsymmetrical catalysts have potential of being stereoselective, because one of the two possible metallo-cyclobutanes can be favoured relative to the other.

The synthesis of new amine complexes will be followed by a computational study of the main reaction path of the catalysts in the catalytic cycle. The motivation is to understand how the new class of catalysts behaves in the catalytic cycle, and to give information about how to tune them to increase the activity. Hopefully the calculations can reveal some information about their potential for stereoselective catalysis.

In the meantime there will be some work on designing a bidentate N-heterocyclic carbene ligand to obtain a potentially *Z*-stereoselective catalyst. The ligand will be a bulky chelating NHC-phenoxy ligand, forming a six-membered chelate, inspired from the previous work in the group. This ligand is very interesting in a stereoselective point of view.

The main scope of my master degree is to develop some new catalysts for olefin metathesis with the underlying goal to obtain a *Z*-stereoselective catalyst. In this process I will do both computational and experimental chemistry.

2 Theory

In this chapter I will write about the theory behind the most important and used methods during my master degree. The main focus will be on our everyday analytical tool NMR. X-ray diffraction is a rather complicated method that makes it possible to know the arrangement of the complex, and is therefore of great importance to organometallic chemistry. Its main aspects will be described to a certain extent. Chromatography is the most important technique for purifying the ligand precursors and at last there will be a section about computational and quantum chemistry as an introduction to density functional theory (DFT).

2.1 Nuclear Magnetic Resonance

Nuclear magnetic resonance; NMR; spectroscopy was developed in the 1950s. Its main purpose is to determine the molecular structure. For most scientists working with synthesis it is the most important technique. The Nobel Prices in Chemistry in 1991, 2002 and 2003 can reflect its appreciation.[64]

The analysis is based on measuring the relaxation of nuclear spin of one isotope at the time. The nuclei of the isotope has to have an odd number of protons or neutrons to have a nuclear spin; *I*.[65] A nuclear spin is required for an isotope to be NMR-active, since it then will generate a local magnetic field.[64] The most common isotopes measured in NMR is ^{1}H, ^{13}C and ^{31}P. All of these three have nuclear spin ½. Such nuclei are called dipolar nuclei.[65] It makes them seem spherical and is influencing the magnetic field equally in all directions. Because of this characteristic they have strong and sharp NMR signals. Other nuclei with I>½ are called quadrapolar nuclei and have more complicated NMR signals. They are therefore harder to use analytically.[65]

The assumption behind the technique is that nuclei with a nuclear spin will interact with a magnetic field. If placed in a magnetic field a nucleus with nuclear spin will orient along the magnetic field.[64] This is of course a simplification of the actual situation. It is favoured to be oriented along the magnetic field and the population of spin along the magnetic field will be higher than the population with spin against. The reason for this distributuion is that the energy difference is quite small compared to thermical energy.[66] The distribution follows a Boltzmann distribution, a thermical

distribution of the possible states, which is related to the strength of the magnetic field.[64] The stronger the magnetic field, the more spin of the nuclei will be oriented along the magnetic field.

During a NMR-experiment the Boltzmann distribution of the nuclei is manipulated by sending a radio frequency pulse that interacts with the magnetic momentum of the nuclei. The signal is measured when the system is relaxing back to the equilibrium state in the magnetic field.[67]

The location of the peaks is influenced by the environment around the nuclei.[66] This environment is made up of electrons and other atoms, which are affecting the magnetic field. The magnetic field around the nuclei will, because of the environment, always be smaller than the applied magnetic field. The effect, which is called shielding, is small, but it is measurable.[64] It can be expressed by the following equation:

$$B_{eff} = B_0 - \sigma B_0 = (1-\sigma)B_0 \qquad (2\text{-}1)$$

The effect of the outer magnetic field B_0 on the nuclei will be reduced by the shielding (σ) and hence B_{eff} will be smaller than B_0. The shielding is mainly a function of the electron density around the nuclei, but there is also other effects which are influencing the local magnetic field around the nuclei; magnetic anisotropy of neighbouring groups, ring current effects in arenes, electronic field effect, effects of intermolecular interatctions.[64] All these effects make the local magnetic field different for most of the nuclei, unless they are chemically equivalent. The mentioned differences are the foundation of the reference scale in NMR. A nucleus with a certain environment will have a fixed resonance condition which can be expressed by the following equation:[64]

$$\nu_1 = \frac{\gamma}{2\pi}(1-\sigma_1)B_0 \qquad (2\text{-}2)$$

γ is a isotope specific constant and is named the magnetogyric ratio.[68] Tetramethylsilane; TMS; has been used as a reference compound in NMR for a long time and the reference values called *chemical shift* is related to its reference frequency.

$$\delta_{sample} = \frac{\nu_{sample} - \nu_{reference}}{\nu_{reference}} \qquad (2\text{-}3)$$

Equation 2-3 can be rewritten by inserting (2-2) into it and hence the effect of the outer magnetic field on the chemical shift will be cancelled out:

$$\delta_{sample} = \frac{\sigma_{TMS} - \sigma_{sample}}{1 - \sigma_{TMS}} \qquad (2\text{-}4)$$

The fact that the chemical shift; expressed in ppm; is independent on the strength of the magnetic field has one great advantage. It makes all the results expressed in chemical shifts comparable between all the different NMR-instruments.[68] By the formulas above it is straightforward to see that TMS will have chemical shift of 0 ppm (the numerator will be zero).

Spin-spin coupling is an important phenomenon in NMR. This effect is caused by neighbouring magnetic dipoles in a molecule that is interacting with each other.[64] The spin orientation of neighbouring non-equivalent nuclei will influence the local magnetic field around a measured nucleus and therefore change the resonance condition of the measured nucleus.[64] This splits the resonance frequency according to how many neighbouring nuclei it couples to. It usually follows the multiplicity rule which is M=n+1 when I=½. [64]

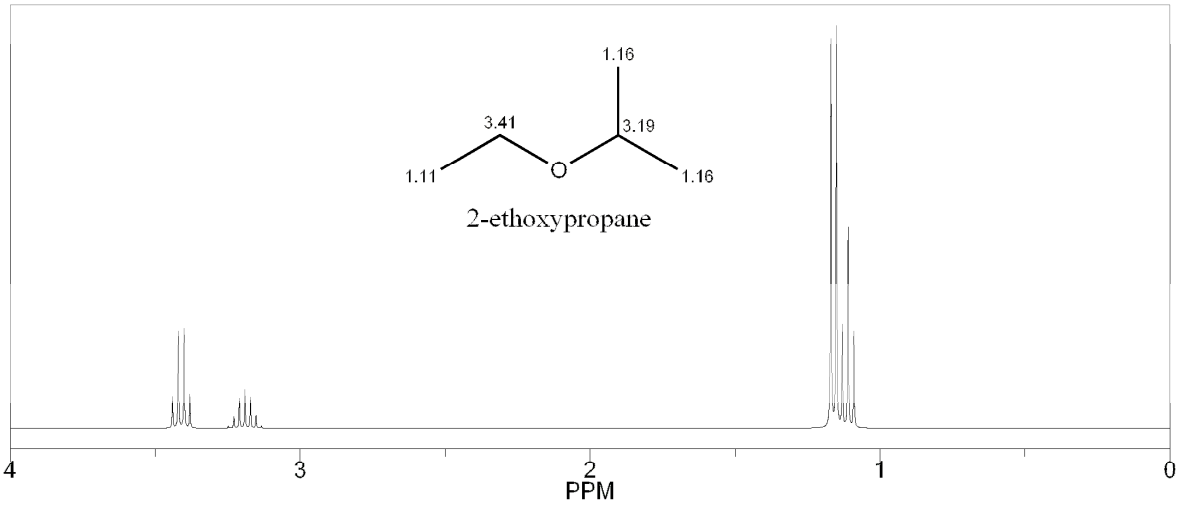

Figure 2.1: Simulated proton spectra of 2-ethoxypropane.[69]

In Figure 2.1 a simulated ^{1}H-NMR spectra shows the extent of coupling for a rather small and simple molecule; 2-ethoxypropane. Without the coupling, it would have been rather difficult to assign the peaks in the spectra, since we had to rely on the shielding alone. The methyl groups at the end of the propane-chain give two identical signals, a doublet at 1.16 ppm, because they are both chemical and

magnetically equivalent. They couple with a proton at the neighbouring carbon and therefore the signal will be split into a doublet. The proton at position 2 gives a septet at 3.41 ppm, since it is coupled to 6 neighbouring protons. The five protons on the ethoxy-group give two signals; a triplet at 1.11 ppm and a quartet at 3.41 ppm. The triplet comes from the 3 protons on the end of the group since these couple with the two protons nearest the oxygen atom. These protons then give a quartet due to their coupling with the 3 protons on the end of the ethoxy-group.

The previous example was rather straightforward. Usually it is more difficult to assign the peaks. It gets more complicated when an aliphatic ring system is involved in the coupling and when the molecule contains double bonds. In the prior example the only significant coupling was proton coupling over three bonds, called vinical coupling. These kind of couplings usually have a coupling constant at around 7Hz in aliphatic systems, written as $^{3}J(H,H)=7Hz$.[64] In more complex compounds the couplings get more advanced. For alkenes one has to take into account the coupling over two and four bonds. In Figure 2.2 the calculated spectra of vinylcyclohexane is shown. Here protons bound to the same carbon is no longer chemical equivalent; prochiral;[64] and will therefore show a more complex coupling pattern. One may be able to solve the coupling pattern, but to be certain we need information from the integration of the peaks to be certain.

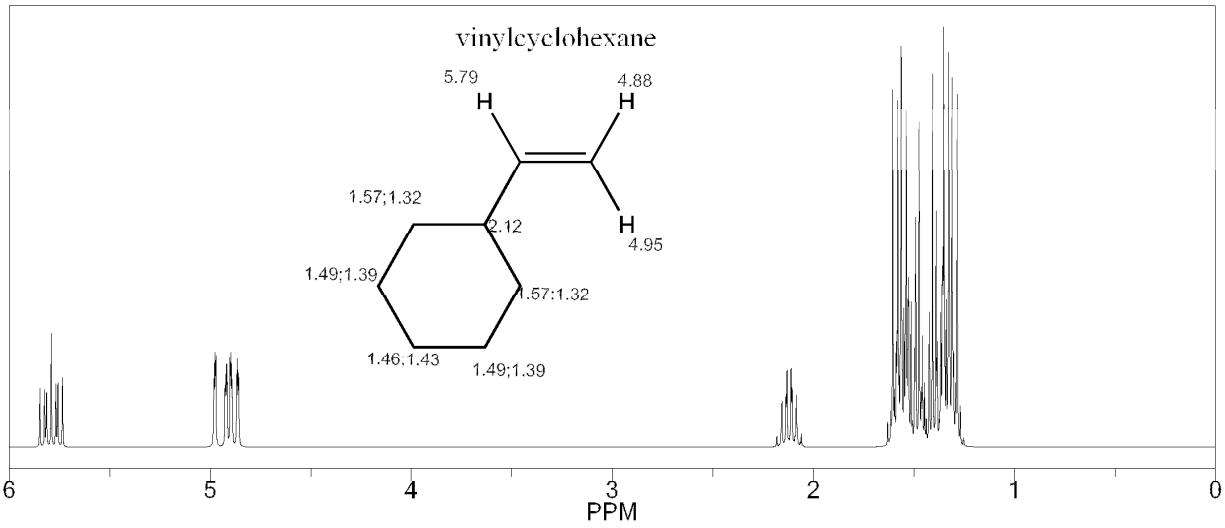

Figure 2.2: Simulated proton spectra of vinylcyclohexane.[69]

Nowadays the integration of the area beneath the peaks is done by the computer and the area gives a relative number of nuclei. Under optimal conditions the septet at 2.12 ppm will have the same integration value as the multiplet at 5.79 ppm.

In the AB_3 coupling system shown in Figure 2.3, the coupling and the intensities follow the Pascal triangle.[66] When the nature of one of the couplings is changed and an AB_2C coupling system is observed, a triplet of a doublet arises. This happens when the coupling between AB and AC is different. Often the coupling is so complex that no logical coupling system can easily be established, as is the case for the peaks around 1.5 ppm in Figure 2.2. The two protons with the peak at 1.39 would is part of an ABCDEF coupling system, because it has five different protons bound in its vicinity (2-3 bonds away).

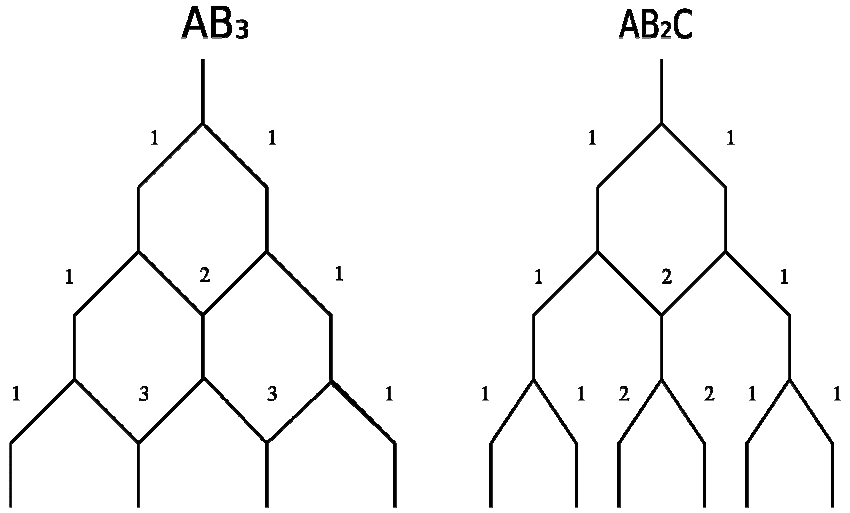

Figure 2.3: Coupling pattern for two similar systems.

2.1.1 ^{1}H-NMR

^{1}H-NMR, often called proton-NMR, is the most used method in NMR-spectroscopy. The main advantage of the technique is that the coupling patterns are simple to solve (shown in Figure 2.1), because the coupling patterns are predominated by homonuclear coupling.[67] This can sometimes be more helpful than the chemical shift of the peaks. Integration of the peaks in proton-NMR is quite useful, but still one should be a bit careful while integrating. As a rule of the tomb one can say that the accuracy of everyday proton-NMR has an error up to about 10%.[67,70-72] But by adjusting the relaxation time; longer delay time; it is possible to obtain more accurate integration.[71] This is done to be certain that the system is relaxing back to a state as close to the equilibrated state as possible.

The proton is very sensitive and the measured isotope has a high natural abundance,[68] which makes it the most analysed isotope in NMR; especially in organic and organometallic chemistry.[66,73] It is

quick, and a standard spectrum can usually be obtained in 5 minutes, even if the sample as dilute as one 1 μmol/mL.

2.1.2 ^{13}C-NMR

^{13}C, on the other hand, is less sensitive than ^{1}H and has a lower natural abundance,[68] which makes it more time-consuming and less informative than ^{1}H-NMR. In total they are about 6000 times weaker than the proton resonances.[67] The coupling pattern, which is dominated by heteronuclear coupling,[67] is much more complex, since one often has couplings over one, two and three bonds; ^{1,2,3}J(C,H).[64] Usually this makes the coupling systems too complex to be solved easily, and therefore carbon spectra are usually obtained in a decoupled manner, and therefore gives one singlet peak for every chemical equivalent nucluei.[64] Normally the range of chemical shifts is from 0-220 ppm, with TMS at 0 ppm and the carbonyl in acetone at around 216 ppm in D_2O.[74]

Usually the integration of standard ^{13}C-spectra can not be trusted, especially not when it is decoupled, since the nuclear overhauser effect then will increase the signal of the peaks relative to the number of protons bound to the carbon.[64,67] The ^{13}C-nuclei need longer time to reach their original Boltzmann distribution, and longer delay times are needed to collect quantitative data.[67]

One advantage with ^{13}C-NMR is that the signals are spread over a larger interval in chemical shift, which can be helpful in determining the different types of carbon in a molecule. This makes the chemical shifts more informative in ^{13}C -NMR than in ^{1}H -NMR.

2.1.3 ^{31}P-NMR

^{31}P is a NMR-active isotope with nuclear spin ½ and has a ~100% relative abundance among the phosphorous isotopes.[68] It couples with both ^{1}H and ^{13}C as well with as all other nuclei with spin different from zero, but the coupling with carbon is only observed in the carbon-spectra. Coupling to ^{1}H is usually eliminated by proton broadband decoupling.[65] The range of chemical shift is around 2000 ppm. 85 % H_3PO_4 in an ampoule submerged in D_2O; 0 ppm; is used as the reference compound in ^{31}P-NMR.[75]

^{31}P-NMR is important in coordination chemistry and is useful when working with organometallic compounds containing phosphines.[73]

2.2 X-ray diffraction

For a chemist working with complexes the main goal is to obtain a crystal with a sufficient quality that it can be analysed by X-ray diffraction. In that case the whole three dimensional structure of the complex can be determined.[73] The roots of the technique goes back to Laue's experiment in 1912, which showed that a single crystal of cupper sulphate diffracted X-rays in a systematic manner.[76] For this work he won the Nobel Price in Physics in 1914.[77]

Diffraction is a result of two or more waves having a certain phase relation; which means that their electric field vectors have the same magnitude and direction at the same instant at any point along the direction the waves are moving.[76] When two waves are moving with a phase relation and one of the waves has to move along a longer path than the other, it leads to a phase difference. This causes a change in amplitude relative to the other.[76] These differences in path ways are important while analysing the diffraction of X-rays in a crystal.

Essentially the diffraction is a scattering phenomenon where lots of atoms cooperate.[76] The X-rays are scattered by the electrons around the atoms.[78] The electromagnetic X-ray radiation makes the electrons in its path oscillate at the same frequency as the radiation, and the electrons will in turn emit radiation in all directions at the same wavelength as the incoming x-ray.[78] When a X-ray with a fixed wavelength impinges a crystal packed structure, the diffraction phenomenon is observed.[79] If the atoms are arranged in a periodical lattice, the scattered rays will have a phase relation. In the directions where there are a constructive interference because of the phase relations the diffracted beams are formed.[76] This constructive interference happens because the wave motion is capable of interference; the X-ray; and because of the atom centres in the periodically arranged lattice.[76] The diffraction will only be observed when the scattered x-rays satisfies the geometrical condition given by Braggs law.[78] The diffraction will occur when the difference in path length of for example two parallel waves equals a whole number of incoming waves wavelength. Bragg's law is given in Equation 2-5. Where n is an integer, λ the wavelength, θ the scattering angle and d the interplanar distance. The interplanar distance is the distance between the crystal layers.

$$n\lambda = 2d \sin\theta \qquad (2\text{-}5)$$

The maximum value of λ is possible when n=1. Then λ must be less or equal to 2d. These are highly energetic. According to Bragg's law the diffraction takes place when n is an integer and at a certain θ the path difference between the diffracted waves will be d. In this case the waves will be in phase with each other and the diffracted X-ray can be measured; constructive interference.[79] When n is a half-integer, destructive interference will occur and no diffracted beams can be measured. In general for a large lattice there will only be diffraction when n is an integer.[79] This is illustrated in Figure 2.4.

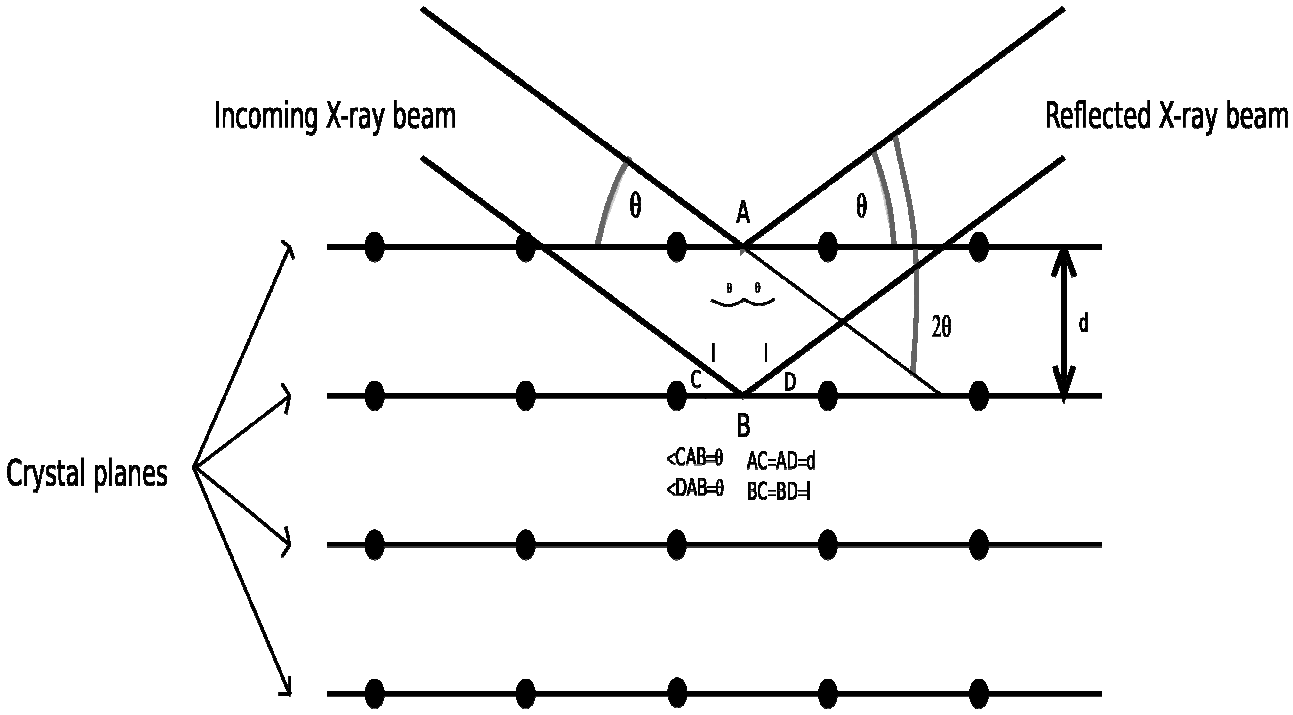

Figure 2.4: Diffraction in crystal planes.

To grow crystals with sufficient quality for X-ray diffraction analysis is difficult. The crystals can not be bigger than 0.5 mm in any direction, since the X-ray beam can not be regarded as uniform in a bigger region.[79]

In modern X-ray diffractometers θ is varied with a fixed λ, and d as a vector is calculated in three dimensions. The intensities of the diffractions are measured and treated by a Fourier transform to solve the phase problem of the crystal structure, which in the end will give a structural model of the

molecule.[79] During the analysis of a single crystal by monochromatic X-rays, the size and content of the unit cell is determined. When the monochromatic X-ray meets the electron cloud around an atom it is diffracted. In an organometallic complex the diffraction pattern will be dominated by the metal, since it has the highest number of electrons,[73] in accordance to this, hydrogen atoms are difficult to locate precisely, since they only have one electron.

The result from X-ray diffraction analysis is usually presented as a diagram showing the atoms position in space.[73] One must be careful with X-ray results, because a by product can crystallize and then be found as the solved structure. It is therefore important to have other analytical results to compare the result with. That is why it is important to have ^{1}H, ^{13}C and ^{31}P-NMR of the crystallized compound prior to X-ray analysis.

2.3 Chromatography

Chromatography is the name of a collection of methods used to separate different substances from each other by their partitioning in two phases, where one of the phases is mobile and the other stationary.[80] If the mobile phase is a gas it is called gas-chromatography (GC). If it is liquid it is called liquid-chromatography (LC).[80] The substances are separated due to their different adsorbility on the stationary phase and solubility in the mobile phase.[81] There are different types of chromatography based on the mechanism of the interaction between the solute and the stationary phase: adsorption, partition, ion-exchange, molecular exclusion and affinity.[81]

Adsorption chromatography is a very important technique in synthetical chemistry, especially in organic chemistry.[82] It is used to purify reactants, products and to isolate a wanted product from a reaction mixture.[82] Before one starts using a column to purify a product mixture one should know how the different compounds would separate in the system set-up that is going to be used. This is done by *thin layer chromatography; TLC*.[82] TLC is usually used in an analytical manner to get analytical knowledge about a mixture or reaction mixture[82].

Thin layer chromatography is performed on metal/glass plate coated by a thin layer of silica or alumina. This makes out the stationary phase.[82] It is an advantage to use TLC plates with a UV-active indicator, because it helps spotting colourless and UV-inactive substances.[80] A small sample of the mixture is placed on the plate about 1 cm from the bottom of the plate. The plate is then placed

in a closed chamber filled with about 0.5 cm of the solvent mixture. The substances in the mixture will start eluating upwards on the TLC plate and spread on the plate perpendicularly according to their interaction with the stationary phase. The solvent mixture often has to be tuned to give a good separation. If the goal of the TLC analysis is to prepare a system to do preparative adsorption chromatography one needs to measure the retention factor; R_f.[82]

$$R_f = \frac{d_{solute}}{d_{solvent}} \qquad (2\text{-}6)$$

The retention factor is the distance the substance is eluated; d_{solute}; and distance the solvent has moved; $d_{solvent}$. The difference in R_f values, between two compounds that are going to be separated, should be 0.15 or more. The R_f of the target substance should be around 0.35.[83] The distance is measured from the point the sample is placed, both for the eluent and the substances. When a proper solvent mixture has been found a preparative adsorption column chromatography can be done.

In the preparative column, the substance mixture will be separate in the same order as on the TLC.[83] One must be careful while packing the column if one wants a good separation, it has to uniformly packed to give a good separation.[83] It is smart to collect the eluate; the solvent out from the column; in small glasses and monitor the column by TLC to be sure in which glasses the different substances are.[83]

2.4 Quantum and computational chemistry

The aid given by quantum and computational chemistry is important to understand how a catalyst interacts with the substrates and how the products are formed. By analysing the assumed elementary steps of a chemical process, one could suggest a mechanism for the process by mapping the minimum energy path (MEP) from the reactants via the intermediate and transition states to the product.[84]

The foundation of modern quantum chemistry is the Schrödinger equation constructed by Erwin Schrödinger, who won the Nobel prize in physics for this work in 1933.[85]

$$\hat{H}\,\Psi = E\,\Psi \qquad (2\text{-}7)$$

In the Schrödinger equation (Equation 2-7), Ψ is the wave function, which is dependent on the electronic and nuclear coordinates of the studied system, $\hat{H}$ is the quantum mechanical Hamiltonian of the system and E the energy of the system. The Hamiltonian contains all the information about the system. By considering the motion of the electron as much faster than the motion of the nuclei, it is possible to simplify the Schrödinger equation by fixing the nuclei's positions in space; the Born Oppenheimer approximation.[86] This is because the electron is 1800 times lighter than a proton; in carbon the nucleus weights about 20 000 times more than the twelve electrons and the nuclei is therefore regarded as fixed in space relative to the electron. The Schrödinger equation is then simplified and rewritten as expressed in Equation 2-8.

$$\hat{H}_{el}\,\Psi = E_{el}\Psi \qquad (2\text{-}8)$$

The kinetic energy of the nuclei is then omitted according to the Born Oppenheimer approximation and the repulsion between the nuclei is reduced to a constant, $\boldsymbol{V_{ext}}$.[87] Equation 2-8 is much simpler than Equation 2-7 since electron nuclear correlation is removed, but the electron-electron correlation is still remaining. Solving Equation 2-8 will give all the wanted information about a system, but sadly it is only analytically soluble for some trivial examples.[87] The wave function in Equation 2-8 is a multiple electron equation and is usually expressed as a linear combination of one electron wave functions.[88] This is called the linear combination of atomic orbitals approach; LCAO. The

Hamiltonian; $\hat{H}_{el}$; is in general only dependent on the number of electrons in the system and to build the Hamiltonian one in addition needs to know the external potential V_{ext}.[87] V_{ext} is fully determined by the positions and charges of the nuclei in the system.[87]

The *variational principle* states that the energy computed by a trial wave function; Ψ_{trial}; and the $\hat{H}$ will be an upper-bound estimate to the ground state energy.[87]

$$\left\langle \Psi_{trial} \middle| \hat{H} \middle| \Psi_{trial} \right\rangle = E_{trial} \geq E_0 = \left\langle \Psi_0 \middle| \hat{H} \middle| \Psi_0 \right\rangle \qquad (2\text{-}9)$$

By applying different Ψ_{trial} to Equation 2-9 by searching for acceptable N-electron wave functions the one with the lowest energy will be the best estimate to the ground state; Equation 2-10.

$$E_0 = \min_{\Psi \to N} E[\Psi] = \min_{\Psi \to N} \left\langle \Psi \middle| \hat{T} + \hat{V}_{Ne} + \hat{V}_{ee} \middle| \Psi \right\rangle \qquad (2\text{-}10)$$

In Equation 2-10 $\hat{T}$ is the kinetic energy operator, $\hat{V}_{Ne}$ is the nuclei electron attraction operator, and $\hat{V}_{ee}$ is the electron electron repulsion operator. The conclusion from Equation 2-10 is that by knowing N and V_{ext} one may construct the Hamiltonian operator and then obtain the ground state wave function.[87] This will enable us to find the ground state energy; Equation 2-11; and all the other properties of the system.

$$\{N, Z_A, R_A\} = \{N, V_{ext}\} \Rightarrow \hat{H} \Rightarrow \Psi_0 \Rightarrow E_0 \qquad (2\text{-}11)$$

The *electron density* can be calculated from the wave function.[86] The wave function can not be observed, but the electron density can be observed to a certain extent by X-ray diffraction.[87]

$$p(\bar{r}) = N \int \Psi^2 d\bar{r} \qquad (2\text{-}12)$$

Equation 2-12 states the probability of finding an arbitrary electron of the N electrons in the volume element $d\bar{r}$.

$$p(\bar{r} \to \infty) = 0 \tag{2-13}$$

$$\int_0^\infty p(\bar{r})d\bar{r} = N \tag{2-14}$$

From these equation it is possible to find a ground state energy that is decided by V_{ext} and N. Hohenberg and Khon laid the foundation for what was later know as Density Functional Theory in 1964.[89] They stated that the ground state energy; E; of a system is determined by the electron densisty. The electron density is again related to the V_{ext}. By a reductive absurdum they showed that a system with a defined E_0 can only have one and only one clearly defined V_{ext}. Therefore the ground state electron density is defined by V_{ext}. In relation with Equation 2-11 this gives a new relation shown in Equation 2-15.

$$p_0 \Rightarrow \{N, Z_A, R_A\} \Rightarrow \hat{H} \Rightarrow \Psi_0 \Rightarrow E_0 \tag{2-15}$$

The main result from Hohenberg and Kohn is that the ground state energy is a functional of the ground state electron density.[87]

$$E_0[p_0] = T[p_0] + E_{ee}[p_0] + E_{ext}[p_0] \tag{2-16}$$

By separating Equation 2-16 into the system dependent parts and universal parts; independent on N, R_A and Z_A; the following expression arises:

$$E_0[p_0] = \int_{system\_dependent} p_0(\bar{r})V_{ext}d\bar{r} + \underbrace{T[p_0] + E_{ee}[p_0]}_{universally\_valid} \tag{2-17}$$

The universally part of Equation 2-17 is usually expressed as a *Hohenberg-Kohn functional;* $F_{HK}[p_0]$.[87]

$$F_{HK}[p] = T[p] + E_{ee}[p] = \left\langle \Psi \middle| \hat{T} + \hat{V}_{ee} \middle| \Psi \right\rangle \tag{2-18}$$

If *Hohenberg-Kohn functional* had been known exactly, one could have solved the Schrödinger equation exactly, independent of system size.[87] Sadly this is not the case! The functional; $F_{HK}[p]$;

contains the kinetic energy; $T[p]$; and the electron-electron interaction; $E_{ee}[p]$. Neither of these is known explicitly. The last term can be further separated and one can find some known terms.

$$E_{ee}[p] = \frac{1}{2}\iint \frac{p(\bar{r}_1)p(\bar{r}_2)}{r_{12}} d\bar{r}_1 d\bar{r}_2 + E_{ncl}[p] = J[p] + E_{ncl}[p] \quad (2\text{-}19)$$

The $J[p]$ functional in Equation 2-19 represents the classical columbic interaction, which is known.[87] $E_{ncl}[p]$ represents the non classical contribution to the electron-electron interaction, is not known. The major challenge in relation to the *Hohenberg-Kohn functional* is to find the explicit expressions for $E_{ncl}[p]$ and $T[p]$. This will open up the possibility of solving the Schrödinger equation; equation 2-8; completely.[87] This way of solving the Schrödinger equation laid the foundation for what today is know as the *Density Functional Theory; DFT*.

There exist no systematic way to improve the approximate *Hohenberg-Kohn functional.*[34] But over the years some useful approximations have arisen. The most important one is the spin polarized approach by Kohn and Sham.[90] They suggested an approximate method for treating an inhomogeneous system of interacting electrons. A generalized theory from the Kohn-Sham approximation is the hybrid-DFT. This method contains a combination of Hartree-Fock exchange with explicit local densities functions and their gradients.[34]

In the 1980s the methods described above became of significant importance in computational chemistry,[91] then called DFT chemistry. Over the last three decades its use has developed a lot and the method research is still ongoing with probably the last major development is the inclusion of dispersion correction in the DFT-functionals.[34] The functionals can be classed in a Jacob's ladder[92].[84] The lowest step on this ladder is the local density approximation suggested by Kohn in 1965.[90] The next step is the generalized gradient approximation (GGA) where the functionals contains an energy correction related to the derivative of the electron density; $p(\bar{r})$; with respect to $\bar{r}$.[84] BP86[93], BLYP[94] and PBE[95] are some well known and tested GGA functionals.[84] Better functionals can be created by including higher order terms of the derivatives. These functionals make out the third step on the Jacob's ladder and are referred to as meta-GGA functionals. One example of such a functional is TPSS.[96] In 1993 Becke laid the fourth step of the ladder by combining BLYP with the HF energy expression in the well known and much used B3LYP functional.[97] Such functionals are known as hybrid functionals. In the last five years a new family of functionals has come from Minnesota; often referred to as the Minnesota density functionals.[98-100] Whether these are the fifth step on the ladder is

too early to state. At the top of the ladder, with an exact solution of the Schrödinger equation, the quantum chemical heaven looms.

3 Computational work

The aim of this theoretical study is to understand how the amine catalysts behaves in the catalytic cycle (Scheme 1.1) and to do a pre-screening of what might effect the activity of this class of catalysts. All the catalysts being synthesized are included in the study, as well as the catalyst synthesized earlier in our group; **A1**[55] (Introduction). This will be done with the aid of quantum and computational chemistry described in Section 2.4, more precisely DFT. The following work can be used to design a method of predicting new catalysts in the same class of catalysts. The study will give us some structural information of how to construct new chelating amine based olefin metathesis catalysts, and lay the foundation of a large screening of amine based olefin metathesis catalysts at a later stage.

Regarding the use of polarization functions there are one general guideline: *On second period atoms bound to ruthenium an additional d-function shall be used, and on the atoms bound to the Ru-bonded atoms. Second period elements involved in a chelate shall also have an additional d-function. Hydrogens bounded to elements bounded to ruthenium shall have an additional p-function.*

Access to the super computers was done through the Notur-program.[101] Chemcraft Linux version 1.6 e87 was used as the graphical interface.[102] The calculations were done in Gaussian09[103] and in NwChem.[104] Programming was done in Python (when needed).[105]

Computational details are given in the Appendix in section A.1.

3.1 Functional benchmarking

Prior to any calculation one has to decide which method should be used to obtain results with the sufficient accuracy. How the calculations are performed is of great importance for the accuracy in the obtained result. If the wrong procedure is used, one could obtain an imprecise result or in the worst case a flawed result.

In this project the geometry of the intermediates are of great importance, because it is a novel study of a relatively new class of Grubbs type catalyst containing a chelating ligand with a decoordinating

amine moiety. The decoordination of the amine results in the active complex. These new catalysts should have reasonable 16 electron structures with the amine coordinated; equilibrium structure. These equilibrium structures should resemble the X-ray structure to a certain extent, and hence it would be reasonable to find out which DFT functional that gives geometries of the equilibrium structure most similar to the X-ray structure. MP2 and such methods gives the wanted accuracy,[106] but is regarded too costly to study systems of this size; 50-120 atoms.[107]

A literature search was done to see if there was reported any superior DFT functional for this purpose. The literature search focused on geometry optimizations for X-ray structures of transition metal complexes and ruthenium based olefin metathesis catalysts complexes.

The impression in our group was that M06-L was the best functional for reproducing geometries. We did some in preliminary tests with the functionals M06-L and B3LYP for **A1**. The results showed that M06L gave the most X-ray like equilibrium structure of the compound; GIOAMIN[55]. This was the opposite of what Grubbs and co-workers had described in an article about conformations of NHC ligands related to olefin metathesis.[108] Their result has also been followed up by Cramer and Truhlar and been cited in a review about DFT for transition metals and transition metal chemistry.[34] In their conclusion they claim: *"We show that the B3LYP flavor of DFT predicts geometries for Ru metathesis relevant complexes in better agreement with experiment than M06-L.".*[108] Since their conclusion contrast our view and the results from the preliminary test, we decided to look into their work and how they had gotten their results to make such a conclusion. Their conclusion was based on one structure and unfortunately they did not report any quantitative data. Therefore the crystal structure described in their article was re-analysed using our approach, and from our results it was not obvious that B3LYP performed better than M06-L. Their performances were comparable.

The literature contains different conclusions regarding which functional gives the equilibrium structure of the DFT functional most similar to the X-ray structure. For example; Grubbs and co-workers stating that B3LYP is better than M06-L,[108] Scneider et al. documented that BP86 has a good reliability,[109] Huang et al. reported that TPSS shows a good performance,[110] Machuare et al. reported reasonable performance of B3LYP,[111,112] Sieffert et al. reported poor performance for B3LYP and reasonable performance for BP86 and B97-D.[113] Rydberg and Larsen recommended in a paper about porhpyrin complexes not to use B3LYP, and instead to use BP86, PBE, PBE1PBE, TPSS, TPSSh and B97-D which reproduced reasonable geometries.[114]

Due to this inconsistency in the literature, we decided to look more deeply into this problem and to find out which functional that gives the equilibrium structure of the complexes most similar to the X-ray structures. This motivated screening of 18 relevant X-ray structures of olefin metathesis relevant complexes with eight different functionals: B3LYP, BP86, B97D, wB97XD, TSSPTSS, M06, M06-L and PBEPBE.

The following structures were calculated: ABEJUM01[115], BIBREK[116], CAZVEE[19], GALGOQ[117], GALGUW[117], GAQGAH[118], GIOAMIN(**A1**)[55], JOFREC[45], KIJFIT[119], LEMRAX[120], NALTIE[121], ROHHAY[122], STEWART[108], TIHLIF[10], XACYOQ[123], YIQWUQ[124], ZETLOZ[14] and ZIPLEP[125]. The structures for these complexes are shown on Chart 3.1.

Chart 3.1: The structures analyzed in the benchmark study.

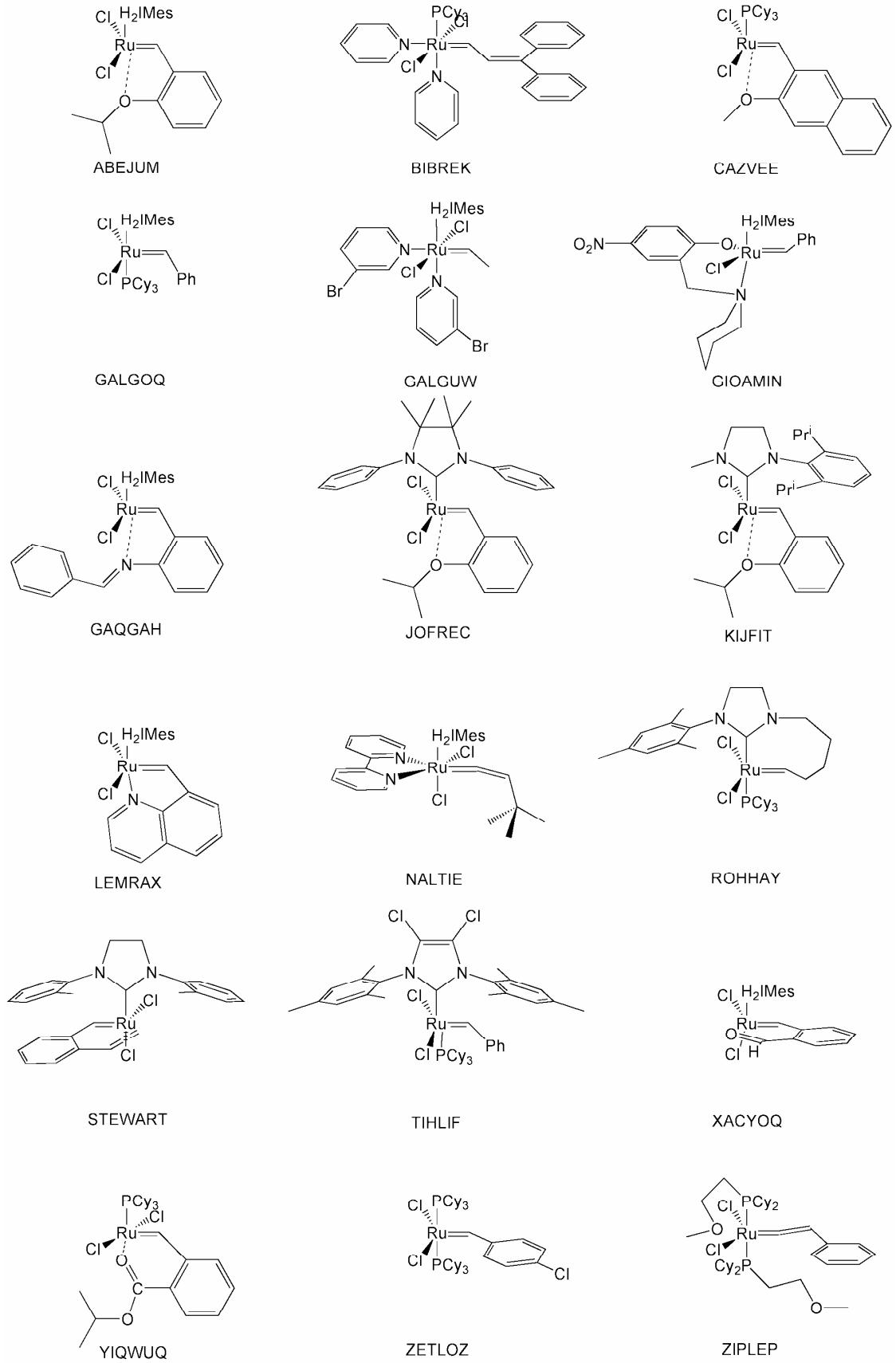

3.1.1 Selection of functionals

The functionals used by Grubbs and co-workers; M06-L[99] and B3LYP[97]; was the natural starting point.[108] In the group there was some knowledge that BP86 was known to have a good reproduction of x-ray structures, although the amount of supporting data was small.[126] BP86[93] was therefore included in the study. M06[100] and PBEPBE[95,127] were also included since they are related to M06L. TPSSTPSS[96], B97D[128] and wB97XD[129] were also chosen. We also decided to test the basis set effect by doing in total 36 additional calculations with M06 and PBE with a triple zeta quality basis set.

3.1.2 Benchmarking

Pre-optimizations of equilibrium structures were performed in NWChem. When the pre-optimizations were finished, the results were transferred to Gaussian09. All calculations were finalized in Gaussian09 and all conclusions were made from these results. The results were analysed by Quatfit[130] and the script final_geometry_12.py[131].

To estimate the time required for the different functionals 12 single-point calculations were computed. These computations included two extra calculations using an ultrafine integration grid.[132] The motivation for this was a publication stating that ulfrafine integration grid should be used for the M06-family of DFT functionals to obtain reliable data.[133]

3.1.3 Results and discussion

The results in this project were obtained in collaboration with PhD. student Y. Minenkov.[134] The focus in this section is to motivate the functional chosen for the amine project, where the focus in the coming paper is on which functional that gives the most similar equilibrium structures to the X-ray structures. Since the hydrogens position is not well defined from X-ray diffraction, the hydrogens are omitted in the further analysis.[79]

Figure 3.1 shows the results from Quatfit with equal weighting for all atoms. Quatfit superimposes the calculated structure onto the X-ray structure and calculates the distance between the same nuclei in the two structures; example goes: Ru1-Ru1, Cl1-Cl1, Cl2-Cl2 and so forth. There is no typical winner in Figure 3.1, but if we ignore the trippel zeta; TZ; the results can be divided into two bulks: B3LYP, BP86, B97D and TPSS in the worst performing and wB97XD, PBE, M06 and M06L in the best performing.

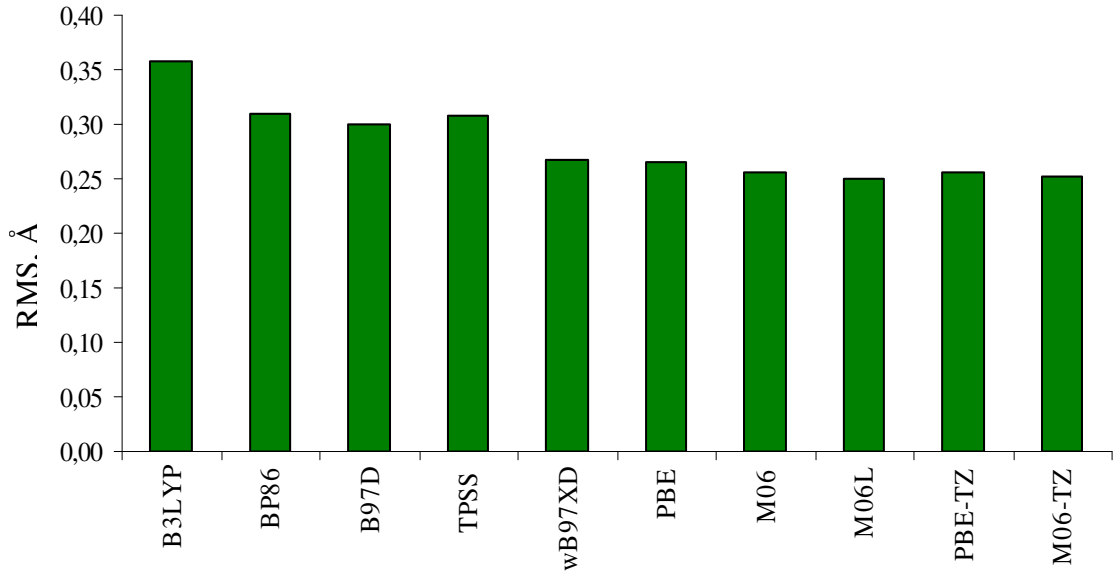

Figure 3.1: Results from Quatfit.

During our work we made our own test to evaluate the performance. This test calculates all inter nuclear distances in the X-ray structures and compares them with same value in the calculated structure. The results from this test will implicitly contain all information (distances, angles and torsions). This test is called Mean All Internuclear Distance Error (MAINDE) and is one of the outputs from the script final_geometry_12.py.[131] The main advantage with MAINDE is that its result

implicitly contains information about angles (similarity measure). It produces root mean squared error, mean unsigned error and mean signed error. In the coming figures mean unsigned error (MUE) and mean signed error (MSE) for the different functionals will be compared. The results from MAINDE for the complexes are shown in Figure 3.2. The results here are somewhat different from the results in Figure 3.1. The grouping here is related to if the functionals contain the dispersion correction or not. B97D, wB97XD, M06 and M06-L performs the best. This is most likely due to the dispersion correction in these functionals. This result is not revealed by Quatfit due to the different type of comparison.

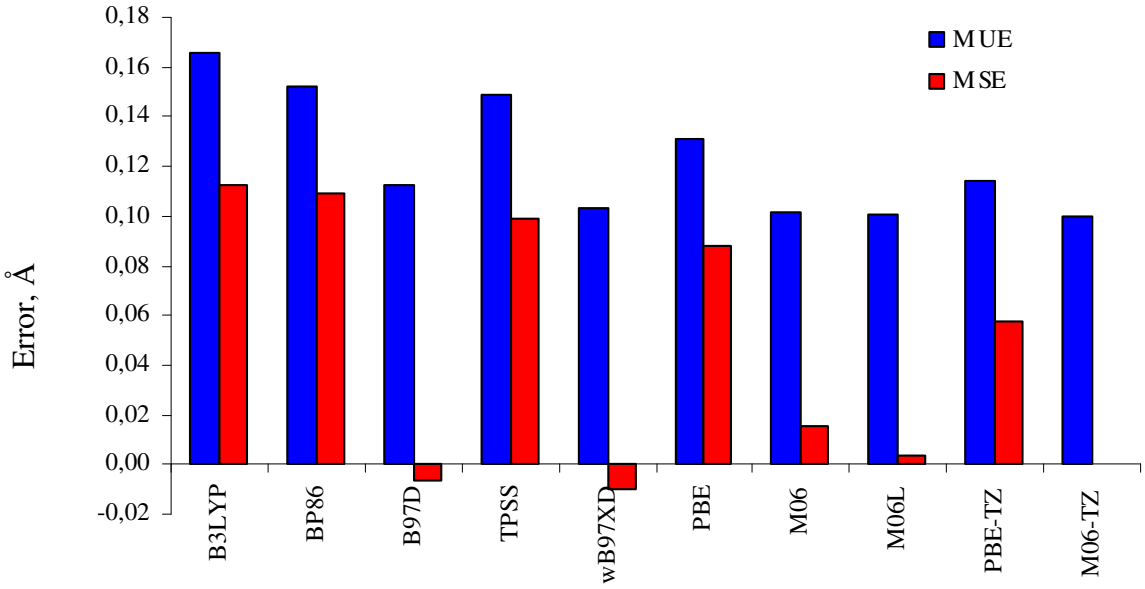

Figure 3.2: Results from MAINDE for the whole complex.

The graphs in the previous figures show how the functionals perform for the whole complexes. Most of the structure is organic fragments. However, we are more interested in the coordination centre and therefore our main focus is on the performance around the metal centre, since these geometries are the most important in the catalytic cycle. Figure 3.3 shows the results from MAINDE for the coordination centre. It is hard to group the functionals in this graph, but the most obvious conclusion is that B3LYP does not perform any good, and that PBE and wB97XD are among the best. If we take the functionals with the triple zeta basis into account PBE-TZ is the best performer for the coordination centre in total.

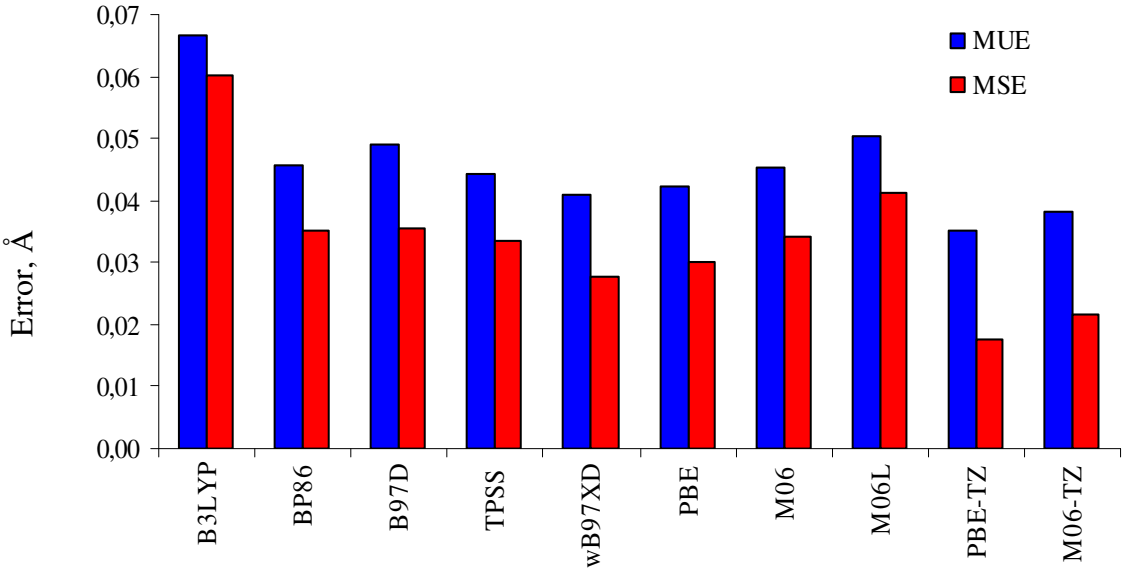

Figure 3.3: Mean errors for coordination centre.

For ruthenium based olefin metathesis catalyst the initiation of the catalysts involves a decoordination of a datively bound ligand to form the 14 electron complex. Therefore the bonded distances of the dative ligands are of significant interest in our work. The results for the analysis of dative bond are given in Figure 3.4. Here again B3LYP stands out as the poorest functional, while the rest are more similar in their performance. TPSS stands out as the best, followed by wB97XD, PBE-TZ, M06-TZ and PBE.

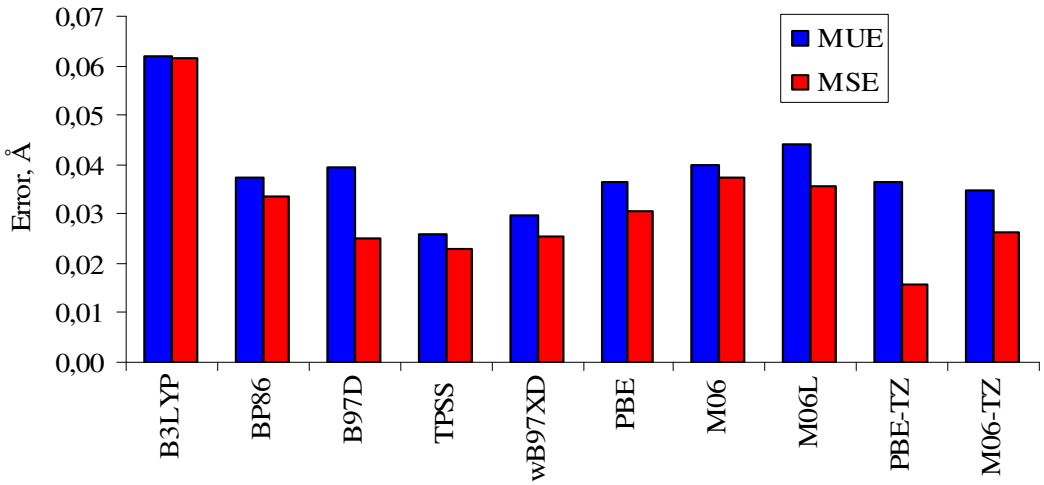

Figure 3.4: Mean errors for dative bonds.

In the amine project the dative ruthenium nitrogen bond is the most important parameter to describe precisely. The mean errors for this bond are given in Figure 3.5. Again B3LYP stands out as poor, while TPSS, is the best (that is if the functionals are competing with the same basis sets) and is followed by PBE.

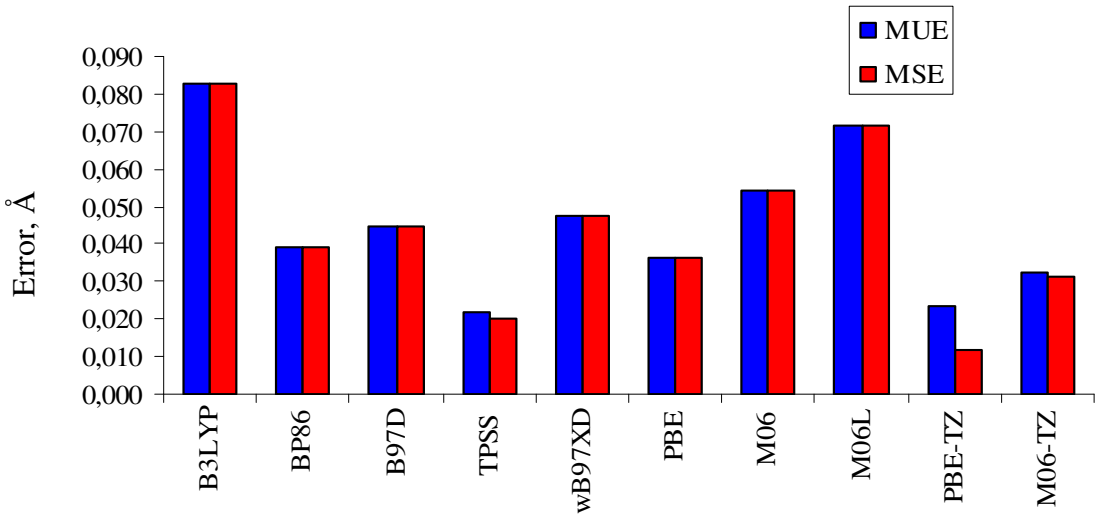

Figure 3.5: Mean errors dative Ru-N bond.

In Figure 3.5, we can see that if we want to describe the dative ruthenium nitrogen really precise, the best choice would be to choose PBE with tiple zeta basis set. It is therefore interesting to take the time needed to do the calculations into account. The time needed for a single-point calculation is given in Table 3.1. These calculations were done on the supercomputer Stallo[135]. The absolute computer time given in Table 3.1 is the cpu-time needed to perform a single-point calculation of ZETLOZ, with one node and eight cores. The cores have a clock frequency of 2.66GHz and each node have 16 GB ram.[136] The functionals are sorted with the fastest at the top and the slowest at the bottom. The relative time is given with PBE's time set to 1. The total impression before the cpu-time was taken into account was that TPSS and PBE stand out as the most obvious choices, because we expect the needed cpu-time for the functionals with triple zeta quality basis set to be significantly higher.

Table 3.1: Cpu-time for singlepoint jobs

Functional	**Time**	**Relative time**
PBE	3 h 47 min 52.3 sec	1 (3.79786)
B97D	3 h 48 min 13.9 sec	1.00
BP86	4 h 3 min 16.6 sec	1.05
B3LYP	5 h 10 min 6.8 sec	1.36
TPSS	5 h 38 min 7.3 sec	1.48
M06-L	5 h 43 min 18.0 sec	1.51
wB97XD	6 h 1 min 17.4 sec	1.59
PBE ulfrafine grid	6 h 2 min 56.0 sec	1.59
M06	7 h 1 min 26.8 sec	1.85
PBE trippel zeta	9 h 19 min 1.7 sec	2.45
M06 ultrafine grid	12 h 4 min 38.0 sec	3.18
M06 trippel zeta	27 h 43 min 51.7 sec	7.30

3.1.4 The chosen functional

For the coordination centre, the most accurate of the benchmarked funcionals is PBE with the triple zeta quality basis set. However, it is almost 2.5 times as expensive in computer resources as the PBE with our standard basis set (in this project). If we exclude PBE-TZ, the two best functionals that stand out as the best choice for the coordination centre with a weighting on dative and ruthenium nitrogen bonds are TPSS and PBE. For the total picture PBE is superior to TPSS and in computer resources it has a discount of almost 50%. This motivates the use of PBE as the functional for geometry optimizations in the following amine project.

3.2 Amine based metathesis catalysts

To obtain better knowledge about amine-oxy ligands and their complexes deriving from the reaction with the second generation Grubbs catalyst (**G2**) it would be useful to know something about the thermodynamics and the kinetics of the propagation phase of the catalysts. By doing calculations, we are able to find an estimated overall barrier and do some qualitative comparisons. Earlier, our group did a large screening of olefin metathesis catalyst to predict new active catalysts.[40,44] The work described in this section can be seen as a first step in a direction of a larger screening of the class of amine based olefin metathesis catalysts. There have been some other studies trying to explore the minimal free energy surface for olefin metathesis catalysts,[39,41,42] but not for a system involving the decoordination of a hemilabile dative bidentate ligand. For this reason, this work is novel. The knowledge of the whole catalytic cycle will be helpful for designing new catalysts at a later stage; to do predictive calculations.

It is generally accepted that catalytic ruthenium-based olefin metathesis follows the Chauvin mechanism, which involves an *active complex* (AC) formed from the *pre-catalyst* (PC) and a *metallo-cyclobutane* (MCB).[6] In addition, there is another stationary state. This state is called the *π-complex* (πC) and is formed prior to the metallo-cyclobutane, when the olefin is coordinated.[39,40,137] A complex chemical reaction can in general be divided into elementary steps. In each elementary step there is a reactant state and a product state. According to transition state theory there should be a transition state between these states.[138] The guesstimated minimal free energy surface is shown in Figure 3.6 as an illustration of the states going to be calculated. It contains three elementary steps (PC→AC, AC→πC, πC→MCB). The graph to the left includes only minima and the one to the right includes all the suggested transition-states (barriers) as well. The highest barrier will decide the overall rate, and can be called effective barrier or rate limiting step.

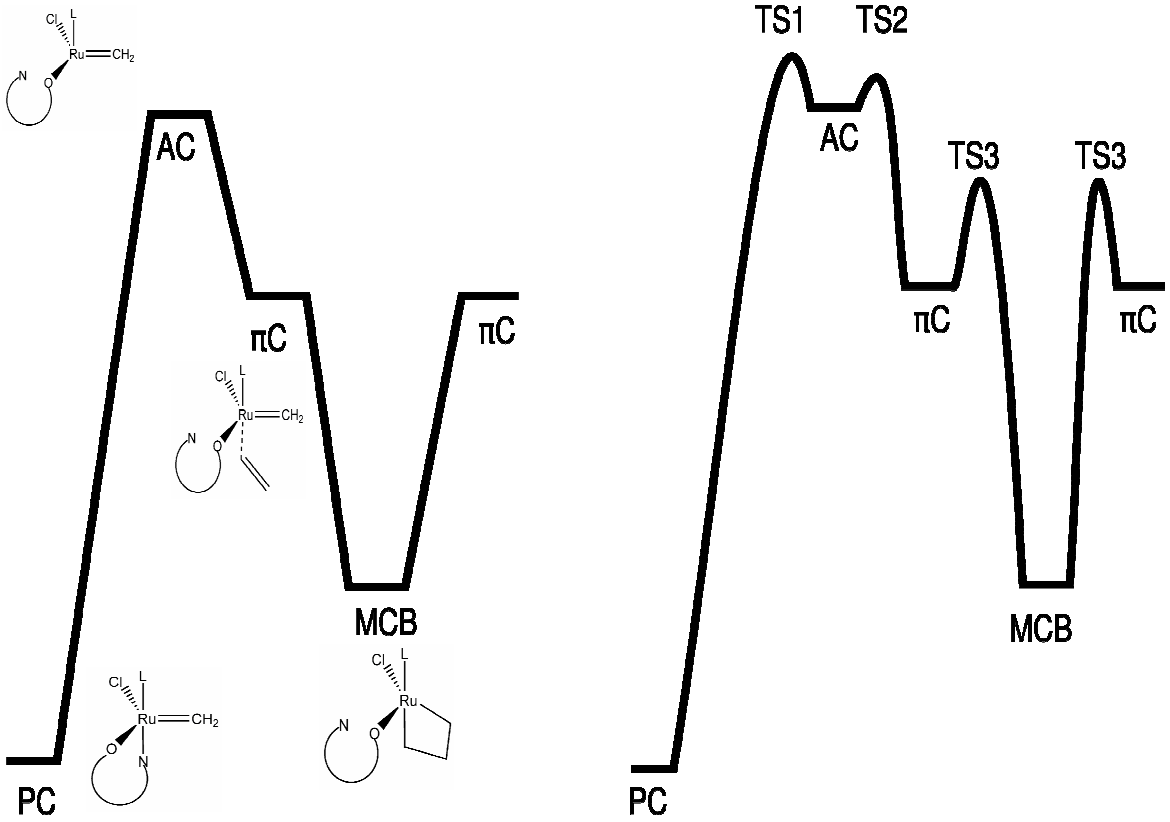

Figure 3.6: Suggested minimal Gibbs free energy surface.

The results described in the previous section, motivated to the use of PBE as the functional for the geometry optimizations and for the single-points M06-L are used. M06-L energies are used since this family of functionals is known to produce a good overall performance predicting bond energies,[43,113,139,140] and barrier heights in catalysis.[141] All the calculations were done in Gaussian09.[103] The polarizable continuum model (PCM)[84] was the used as the solvation model and the solvation energy was calculated in Gaussian03[142].

The catalyst **A1** and potential catalysts **A2** and **A3** shown in Figure 3.7 were investigated. The results were compared with the results obtained in the laboratory.

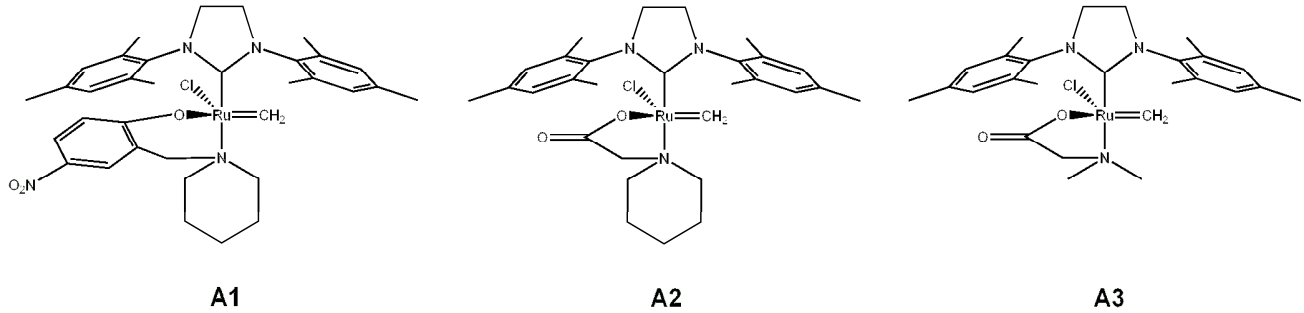

Figure 3.7: Studied catalysts **A1, A2** *and* **A3.**

The main results in this section are discussed in relation with the experimental results in Section 5.3.

3.2.1 Computational procedure

The geometry of the minima is fairly well known in the literature. However, it is very challenging to locate all these 12 minima accurately, because the position of the decoordinated amine moiety is unknown. The most difficult and the most important of these are the active complex, since both the πC and MCB are related to the AC. The guesstimated geometry for the minima is presented simplistically in Figure 3.8.

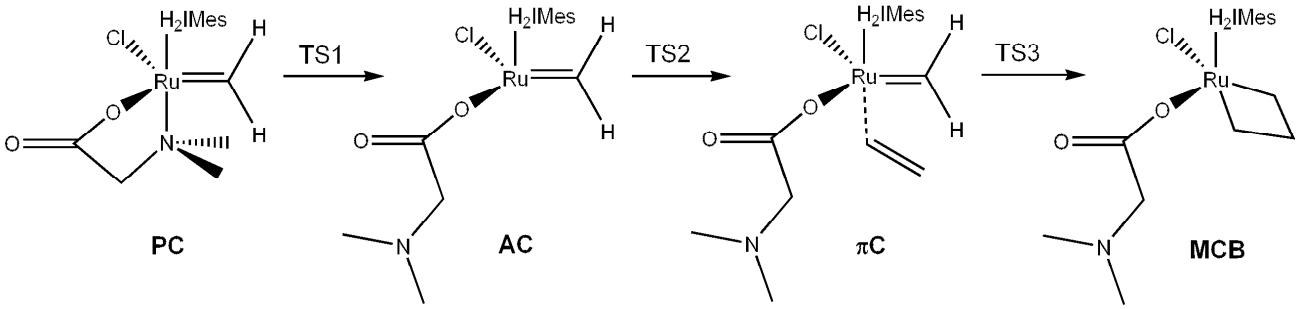

Figure 3.8: Suggested structures for stationary states.

To simplify an already complicated and challenging calculation and to obtain the most general insight possible, the pre-catalyst contains the simplest possible alkylidene; the methylidene; in the calculations and the incoming olefin is also the simplest possible; ethylene. This approach and similar approaches have been successfully applied in several other theoretical studies.[39,44,137,143,144] The simplifications will create a symmetric energy surface and therefore the transitions involved in the decoordination of the olefin will then be the same as the coordination of the olefin. That will also be the case for the πC.

All the *pre-catalysts* and ethylene were calculated at the start of the calculations. From the optimized pre-catalysts a linear transit scan of the potential energy surface was carried out. This "scan-job" scanned the distance between ruthenium and the datively bound nitrogen from the distance in the optimized pre-catalysts (about 2.2 Å) and to a distance of 5 Å. From this scan-job good guesses for the involved *active complexes* and *TS1* were found and optimized.

From the active complexes a new "scan-job" was started; the olefin coordination. Ethylene was coordinated to the active complex to form the *π-complex*. In the literature there is reported some different conformations of the π-complexes.[39,137] To find the lowest energy conformation, the four suggested π-complexes were optimized. The structures of these are shown in Figure 3.9. The conclusion from these optimizations was that the suggested structure in the middle **πC** was the most stable *π-complex*. The optimization of the two conformations to the left; **π1** and **π2**; converged to the one in the middle (**πC**). The conformation to the right; **π3**; converged to the *MCB*, which means that it had passed the barrier between the π-complex and the metallo-cyclobutane.

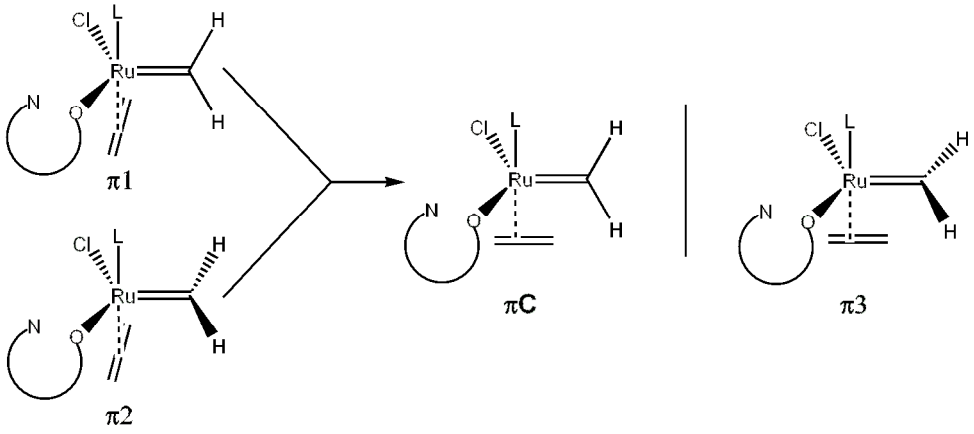

Figure 3.9: Different types of π-complexes suggested in the literature.

From the π-complexes the distance from the carbon-methylidene and carbon-ethylene was scanned towards forming the *metallo-cyclobutane*. The distance between ruthenium and the other carbon on the ethylene was scanned increasing from πC distance to 6 Å (this scan should contain *TS2*). Prior to the formation of the metallo-cyclobutane there should be a transition-state *TS3*.[140]

Any found TS must have one and only one imaginary frequency and the motion of this frequency must conquer with the suggested reaction coordinate for the reaction path.[84] Suggested *reaction coordinates* before the calculations were assumed to be along the following distance interatomic distances: PC to AC: Ru-N(amine), AC to πC and πC to MCB Ru-C1(ethylene). The reaction coordinate for the transition from πC to MCB was later found to be along the distance between *C(methylidene)-C2(ethylene).*

Other competing stationary states were evaluated when found. This involved a bidentate acetate function and the acetate interacting with the methylidene. When the geometry of all the mentioned states were found the energy of solvation and single point calculations were done.

The *Gibbs free energy correction* (298.15K) was computed within the ideal-gas, rigid-rotor, and harmonic oscillator approximations following standard procedures, *electronic energy* from the single point calculations and *energy of solvation* in toluene from the polarizable continuum model; PCM;[145-147] calculations in Gaussian03.

3.2.2 Results and discussion

TS1 was clearly defined on the potential energy surface, and from this state the active-complexes could relatively easily be located. The formation of the *π-complex* was straight forward in all cases. However, the *TS2* was difficult to locate. It did not appear to be a maximum on the potential energy surface. In polymerization of ethylene the coordination of ethylene is known to be barrierless on the potential energy surface.[148] This changes when the entropy is included and the barrier to form the π-complex is dominated by the entropy.[84] For ethylene polymerization there has been reported that there is a transition state around 3 Å for a Ni(II)-catalyst.[148] Several calculations were done around this distance to approximate the *TS2*. The Ru-ethylene distance for TS2 was expected to be larger, due to the larger ruthenium radius. The distance for the found TS2 in this project was varying from catalyst to catalyst with A1 at 3.2 Å, A2 at 3.5 Å and A3 at 3.5 Å. The formation of the *metallo-cyclobutane* involved rotating the methylidene group 90°, which proved to be the transition-state; *TS3*; in all cases. This observation agrees with the result obtained by Straub in 2007.[39]

From the calculations, the minimum free energy surface for the catalytic cycle of the catalysts; **A1-A3**; was calculated and plotted. The free energy along the reaction coordinate for catalyst **A1** is shown in Figure 3.10.

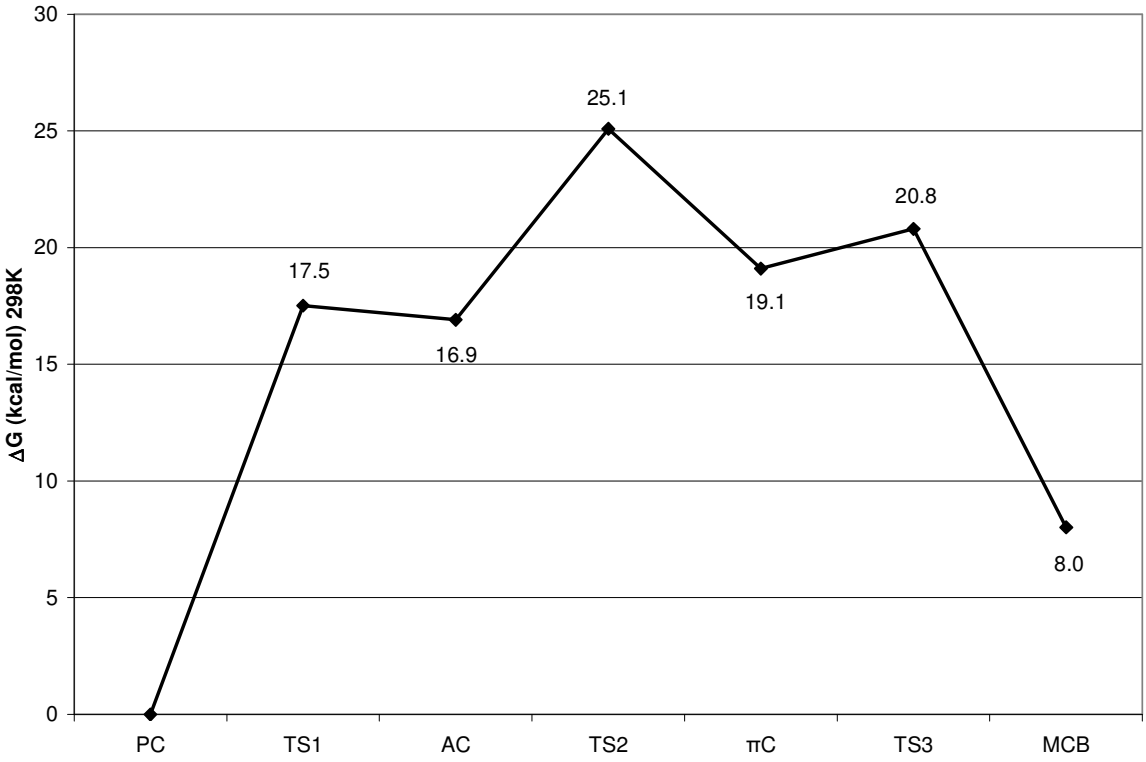

Figure 3.10: Calculated minimal free energy surface for **A1.**

The effective barrier in Figure 3.10 is 25.1 kcal/mol and is related to the coordination of the olefin. All reported energies are relative to that of the pre-catalyst which has been set to zero The experimental activation energy for disassociation of the triocyclohexylphosphine (PCy_3) of second generation Grubbs catalyst (**G2**) is reported to be 23.0±0.4 kcal/mol.[149]

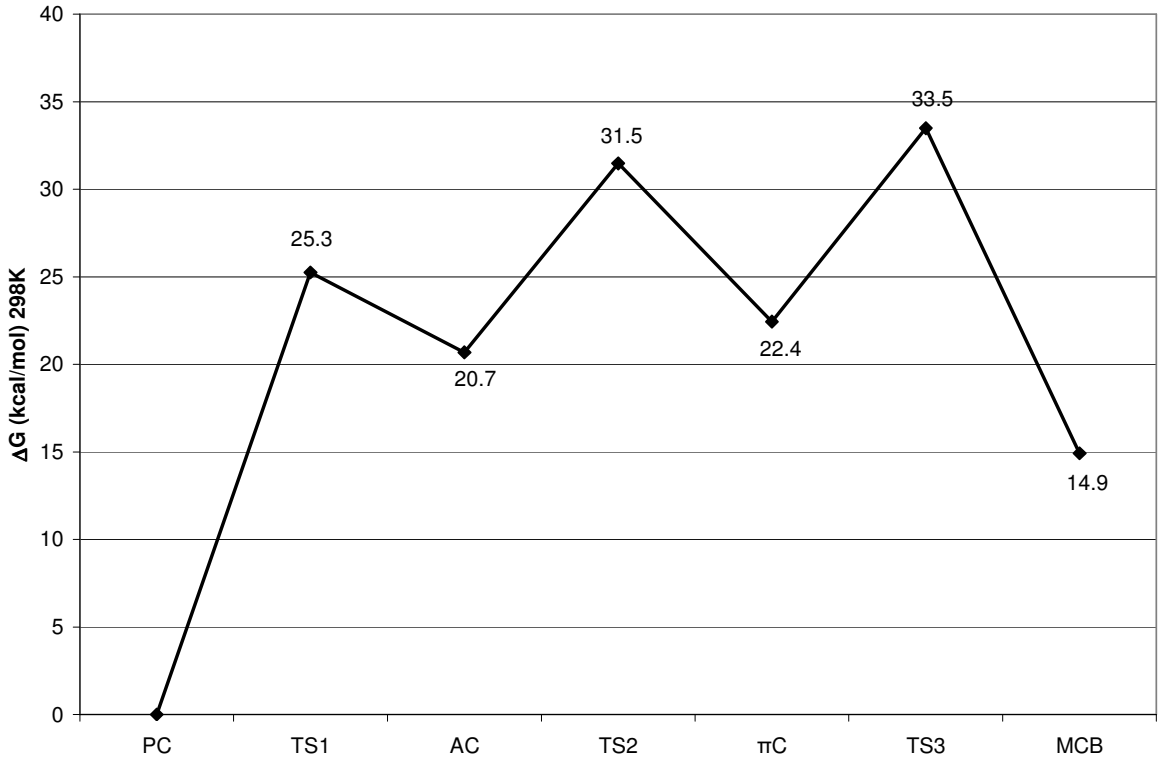

Figure 3.11: Calculated minimal free energy surface for **A2.**

The free energy along the reaction coordinate for catalyst **A2** can be seen on Figure 3.11. The total barrier of this catalyst is 33.5 kcal/mol and it is related to the formation of the metallo-cyclobutane. The barrier is 10 kcal/mol higher than the one experimentally obtained for the **G2**. Compared to **G2** it does not appear to be a very active catalyst.

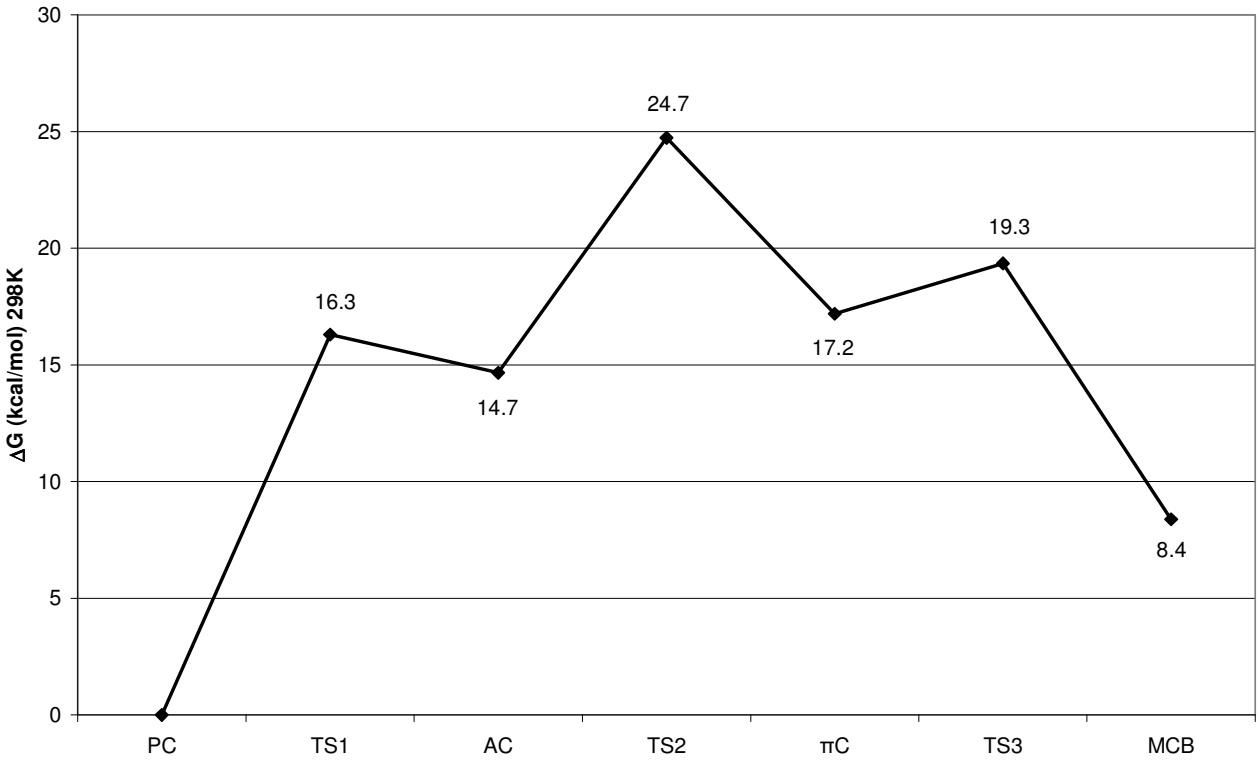

Figure 3.12: Calculated minimal free energy surface for **A3.**

The free energy along the reaction coordinate for catalyst **A3** can be seen on Figure 3.12. The energetic profile appears to be very similar to that of catalyst **A1.** For catalyst **A3** as well as for catalyst **A1**, the second transition state corresponding to the olefin coordination is the highest barrier and makes the effective barrier 24.7 kcal/mol, which is 1.7 kcal/mol higher than for the second generation Grubbs catalyst (**G2**). The main results from the calculated minimal free energy surface for catalysts **A1-A3** are given in Table 3.2 and their effective barrier compared with **G2** to give a relative rate in toluene at 25°C. However, one should not read too much into these relative rates since **G2** has a much higher barrier of recoordinating the phosphine than is the case for the amine catalyst.

Table 3.2: Summary of results

Catalyst	**Highest barrier**	**Effective barrier** (25°C,toluene)	**Rate relative to G2*** (25°C,toluene)
A1	TS2	25.1 kcal/mol	0.03
A2	TS3	31.5 kcal/mol	0.6×10^{-7}
A3	TS2	24.7 kcal/mol	0.06

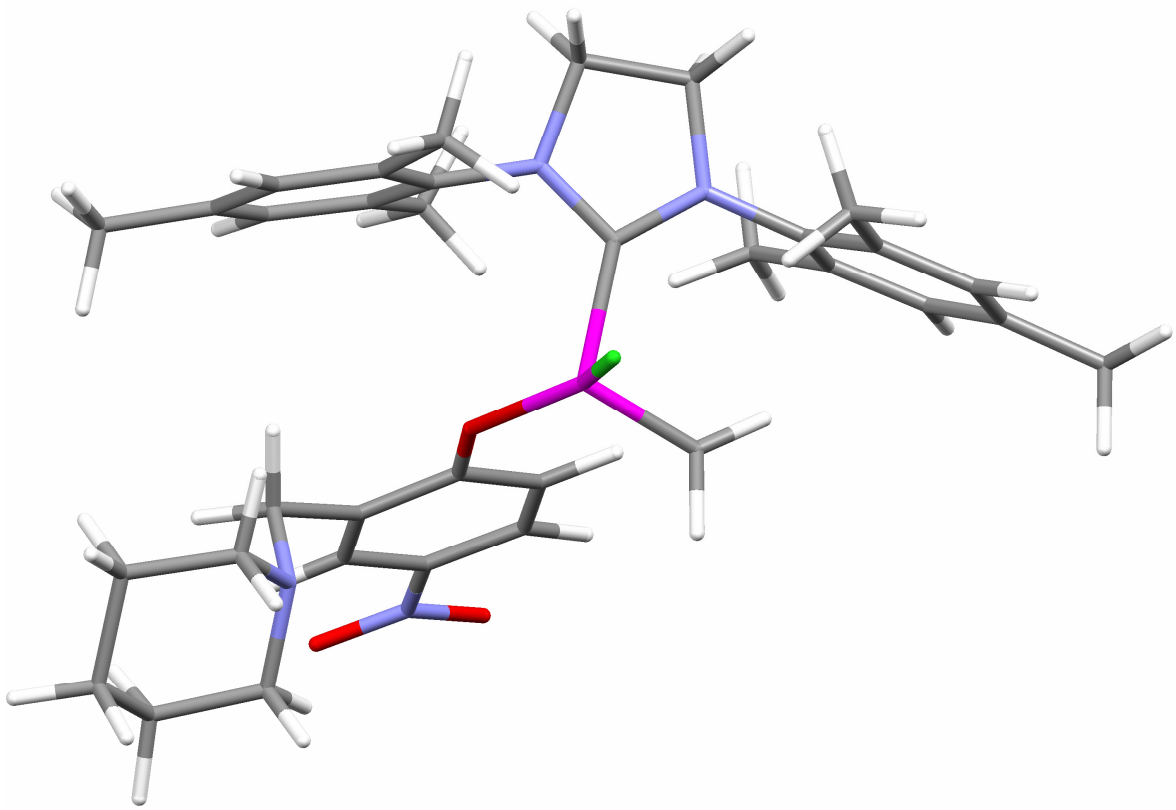

Figure: 3.13: Calculated active complex of **A1**.

In Figure 3.13 the active complex of **A1** is shown. There is a clear vacant site, coordinate site for the incoming olefin, trans to the NHC ligand. The methylidene has the perpendicular configuration as mentioned earlier.

From the minimal free energy surfaces in Figures 3.10 and 3.11, we can conclude that **A1** and **A3** will be more active than **A2**. Still, it can be hard to distinguish the activity between **A1** and **A3** because they have similar minimal free energy paths.

The highest barrier is the coordination of the ethylene, which means that the coordination of the olefin is the rate-determining step in the catalytic cycle. The barrier is heightened for larger olefins.[150]

When designing new ligands, it has to be taken into account that the decoordinated amine gives space for the acetate function to act as a bidentate group. This may cause problems in the catalytic cycle, since it has the possibility of forming a 16 electron intermediate without a vacant site to

coordinate the olefin. Another problem with this type of design is the possibility of the carbonyl group interacting with the alkylidene, an interaction which will decrease the activity and possibly decompose the catalyst. Hydrogen atoms on the chelate can also have an agostic interaction with the metal centre. These agostic interactions can stabilize unreactive resting states of the catalyst.

4 Laboratory routines

This chapter is a summary of the most important laboratory routines relevant to the following experimental work. The experimental work is described in Chapter 5 and 6 with detailed laboratory description given in the Appendix.

4.1 Inert atmosphere

All work with organometallic compounds was done under inert atmosphere and with dry and degassed solvents.

Schlenk manifolds and traps were made by Mellum; Friedel.[151] Inert atmosphere was secured by Argon 4.6 was delivered by Yara.[152] The vacuum pump had a maximum vacuum of 2×10^{-3} mBar measured by Gauges from VWR. [153]

Filtrations were done with celite over a glass frit under argon. This glassware was bought from Normag[154] in Germany.

Solvents and solutions were transferred by syringes and canulla. All solids were dried under dynamic vacuum.

A glovebox was available for use. All air-sensitive compounds were stored in the glovebox and these compounds were brought in and out from the glovebox in schlenk flasks.

4.2 Purification of solvents

Pentane was dried over a sodium-potassium alloy; NaK; and distilled. NaK was made by taking equal amounts of sodium and potassium, washing them with hexane to remove the mineral oil, and cutting them to remove the oxide-layer on the surface to have shiny surfaces. They were then put under argon in a 500 mL round bottom flask and heated to the melting point with a heating gun under vigorous stirring. The alloy was then formed. The alloy is a liquid at room temperature and is therefore a superior drying agent compared to solid sodium or potassium.[155] NaK is a strong reducing agent and also scavenges any oxygen in the solvent. One has to take care while handling NaK, since

it can catch fire in air and reacts violently with water and chlorinated solvents. It is safe to handle in pentane, hexane and mineral oil, and can be destructed with isopropanol.

Dichloromethane was dried over CaH_2 and distilled and degassed under vacuum.

The *deuturated solvents,* $CDCl_3$ and CD_2Cl_2, were dried with CaH_2, vacuum-distilled and degassed. C_6D_6 was dried over NaK, vacuum-distilled and degassed. CD_3OD was stored over activated 3Å molecular sieves.

Hexane, toluene, dichloromethane, ether and THF were in general collected from MBraum 800 SPS Solvent Purifier.

All solvents were degassed by cooling the solvents to the freezing point on liquid nitrogen under static vacuum shaken, and opened to dynamic vacuum to remove gasses from the solvent. This was done several times until a clear "bing" was heard during the shaking under static vacuum. This is called freeze-pump-thaw degassing.[155]

4.3 Characterization

In the characterization of known compounds it was relied on ^{1}H-NMR-anlysis which gave the same NMR-spectra as reported in the literature.

Characterizations of unknown compounds were done by ^{1}H-NMR, ^{13}C-NMR and HR-MS(DART) or elemental analysis (Vario EL *III*). Melting point, IR, ^{31}P-NMR and X-ray characterization was done when applicable and possible. Youngs-NMR tubes were used for air sensitive compounds. The NMR analysis was done on the following instruments: Bruker Avance DRX 600 and Avance DMX 400.

Different used NMR experiments were CAPT, HSQC and COSY.[156] CAPT is a ^{13}C experiment which will phase quaternary positive, tertiary negative, secondary positive and primary negative. This is somewhat opposite of standard phasing in APT; attached proton test.[156]

4.4 Chemicals

In general all the chemicals that could be bought were bought unless it was more reasonable to synthesize it; time and cost considerations.

Suppliers:	Sigma Aldrich[157]	organic compounds, **G1** and **G2**.
	Strem[61]	Metal compounds and complexes.

5 Synthesis of catalysts with amine ligands.

Until recently, amines have been regarded as a catalyst poiseners, and olefin metathesis catalysts have not been able to handle substrates containing amines.[17] The use of amines as ligand for an olefin metathesis catalyst might seem a bit strange, but the theoretical work in our group has shown that olefin metathesis catalysts containing a dative amine might be as good a olefin metathesis catalyst as one containing an imine or a phosphine.[44] This theoretical work was followed by an experimental project to synthesize some amine based olefin metathesis catalysts.[56]

Olefin metathesis catalysts containing a bidentate ligand with imine decoordinating moiety were first introduced by Grubbs and co-workers,[158] and has been studied in a great detail by Verpoort and co-workers.[159-164] Verpoort's group has focused on different Schiff bases,[165] and by tuning their electronic and steric environment they have obtained a series of olefin metathesis catalysts.[163] Some of these catalysts are commercial available[61] and are used as latent catalysts.[35] They show low or no activity at room temperature and high activity at elevated temperatures in polar solvents.[163] Some of the imine based catalysts are shown in Figure 5.1.

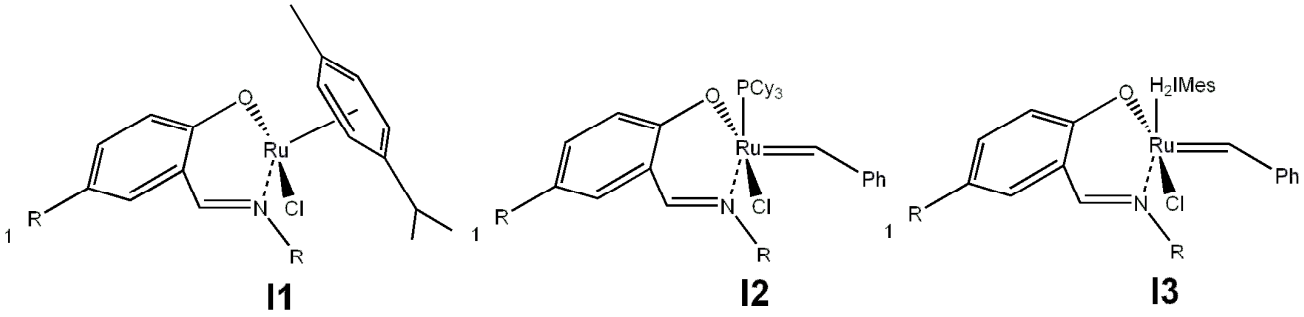

Figure 5.1: Imine based olefin metathesis catalysts.

Amines have steric and electronic differences compared to imines. The nitrogens have different hybridization; the imine has a sp^2-hybridization, while the amine has a sp^3-hybridization. And where the amine is an almost pure σ-donator the imine is more of a symbiotic σ-donator and π-acceptor ligand. In general, imines are regarded as softer[166,167], more nucleophilic and less basic than amines. In addition, the geometry of amines and imines are quite different; where amines are tetrahedral when coordinated, imines are planar. These differences might open the door to some interesting catalytic activity and might also show some new interesting chemoselectivity.

The experimental work in this part is concentrated on synthesizing some new amine based olefin metathesis catalysts, and thereafter compare them with the theoretical studies described earlier. The chelating amine ligands were made as simple as possible to not use too much time obtaining these results. By studying the already existing amine based olefin metathesis catalysts and their chelating amine ligand, some new accessible ligands were suggested as potential ligands in this project.[55-58] The suggested potential ligands are shown in Chart 5.1. They contain a tertiary amine and a potential carboxy or phenoxy moiety. The full structure of the H_2IMes;1,3-dimesityl-4,5-dihydro-imidazol carbene; is not shown fully in the chart for the simplicity of it. Three of the potential ligands were commercial available from Sigma Aldrich: **L0, L3** and **L4.** The others can easily be synthesized in a two step synthesis[56,168,169].

We limited our work to the second generation Grubbs catalyst analogues in this project. The amine catalysts based on the second generation are more robust, easier to prepare and more active.[55,56] In addition, the catalysts were tested and compared with GIOAMIN; **A1**;[55] that was made previously in the group. The first generation analogue of **A1** was not stable, where as **A1** showed a good stability.

The ligand corresponding to **A1** should have been **L1** but is not shown in the chart.

Chart 5.1: Potential chelating tertiary amine-oxy ligands.

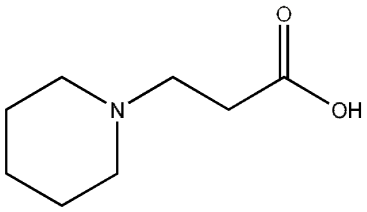

L0

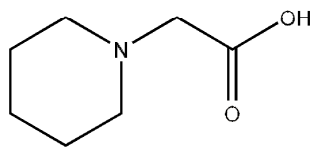

L2

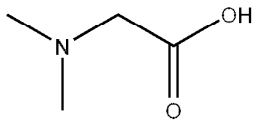

L3

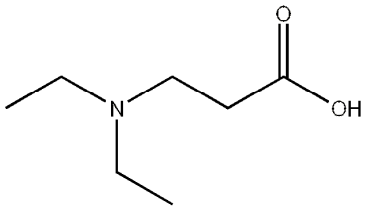

L4

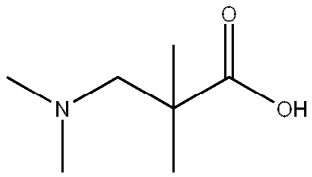

L5

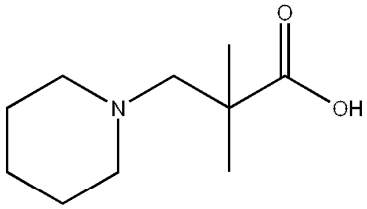

L6

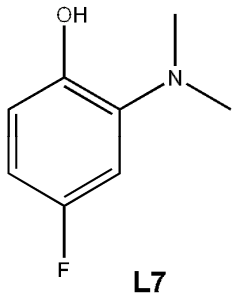

L7

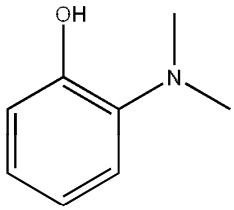

L8

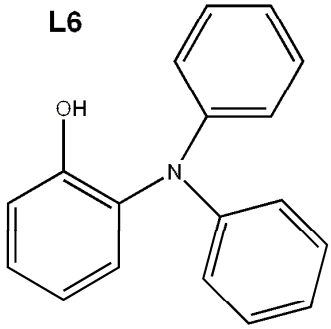

L9

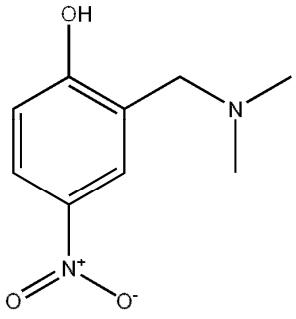

L10

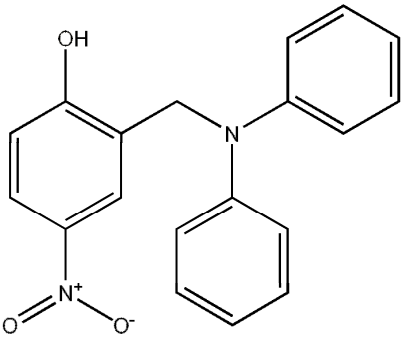

L11

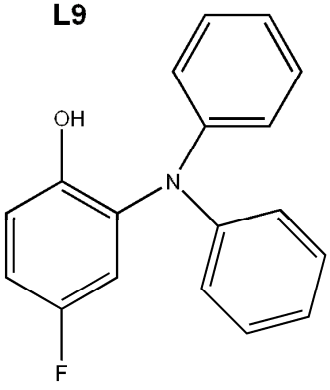

L12

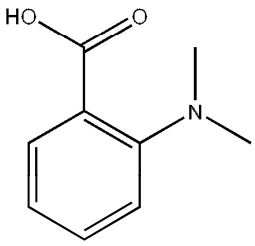

L13

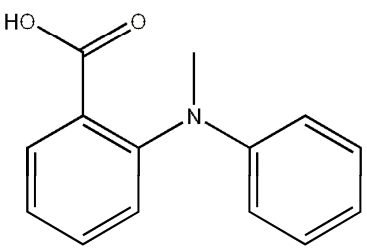

L14

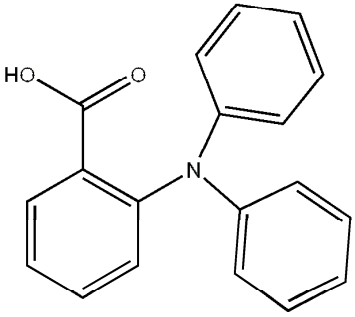

L15

5.1 Experimental

Our goal was to make two or three new catalyst corresponding to the new class of olefin metathesis catalysts made in our group in 2007. The first approach was to buy some commercial available potential ligands and react them with Grubbs second generation catalyst (**G2**). Secondary amines have been shown to be problematic as ligands for ruthenium based olefin metathesis catalysts because they can be oxidised to imines by the ruthenium metal centre.[170] As shown of Chart 5.1 all proposed ligands contain a tertiary amine and a potential anionic oxygen; either a carboxylate or a phenolate. Alkoxy ligands have been reported to degrade the catalyst from a ruthenium-alkylidene into a ruthenium-hydride and were for this reason avoided. This problem has been reported for the first generation Grubbs catalyst,[171] and has also been experienced in our group for the second generation Grubbs catalyst.

5.1.1 Ligand synthesis

L0, L3 and **L4**, which are classed as two potential alkyl based ligands, were bought from Sigma Aldrich. The potential ligands were deprotonated by a base before reacted them with **G2**; 2-(dimethylamino)acetate and 3-(piperidin-1-yl)propanoate.

One ligand was synthesized in the lab; 2-(piperidin-1-yl)acetic acid; according to the procedure reported by Brimble and co-workers.[169] The synthesis is shown in Figure 5.2.

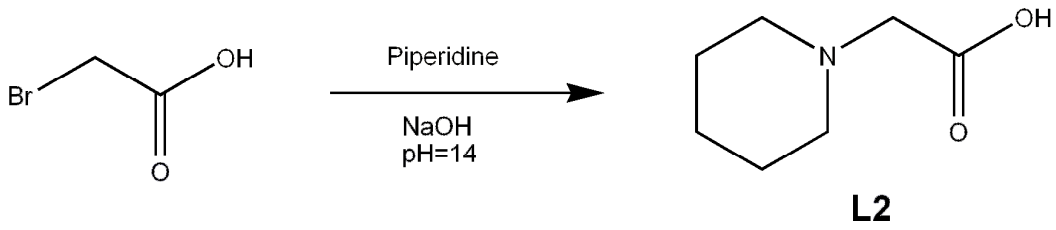

Figure 5.2: The synthesis of 2-(piperidin-1-yl)acetic acid; **L2**.

Prior to the complexation reactions the amino acids were treated with potassium *tert*-butoxide to form the corresponding potassium salt. This was done following a general method inspired by previous work done in our group.[55,56] The reactions are described in detail in the Appendix; A.3.

5.1.2 Complex synthesis

There has been reported a couple of methods of how to prepare the complexes shown in Figure 5.3.[56,57] One strategy published by Grubbs and co-workers was first tried. At first, the reaction was concluded to be a failure, but this was a mistake, since it was at a later stage concluded as a success by ^{1}H-NMR. Nevertheless, this method was reported with low yields (40 %)[57] and therefore the method used previously in the group was preferred.[56] Both of these methods prepare the needed amount of the salt just prior to the reaction.

The target complexes are shown Figure 5.3. These complexes were made in the lab from the ligand made earlier; described in Section 5.1.1; and **L3,** which was bought. In ^{1}H-NMR the alkylidene peak at 19.14 ppm in $CDCl_3$ of **G2** was used as an indication of a successful reaction. A new alkylidene peak would arise in the area 17.5 ppm to 21.0 ppm if the reaction had been successful.

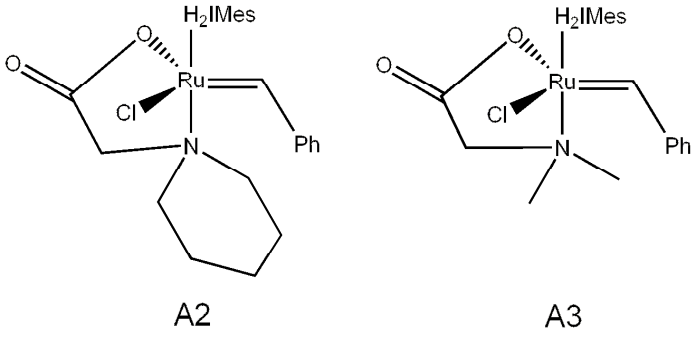

Figure 5.3: Target complexes.

Prior to the complexations a large scale preparation of the potassium salt of **L2** and **L3** were prepared by mixing **L2** and **L3** with 1.5 equiv of potassium *tert*-butoxide. The potassium salt was reacted with **G2** in the presence of AgCl, which was used as a phosphine scavenger.

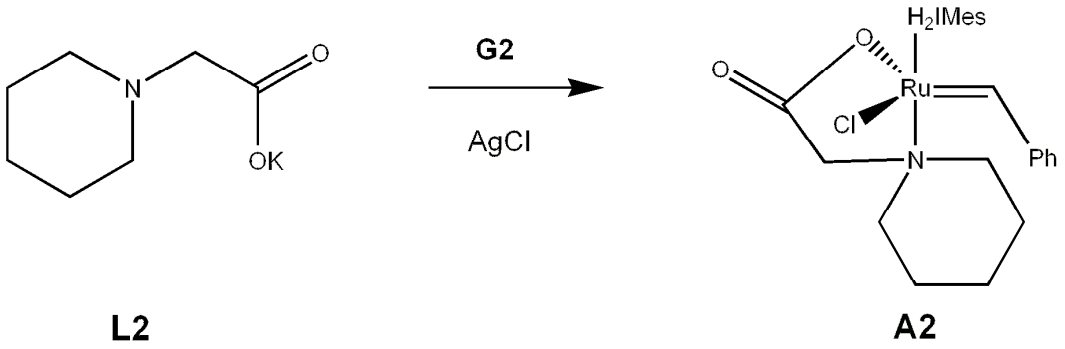

L2 **A2**

*Figure 5.4: Synthesis of **A2** from **G2**.*

The synthesis described in Figure 5.4 was successfully done twice and the product mixture purified by column chromatography. After this purification the yield was 51 %. For the reaction to go to completion, 3 equivalents of potassium salt of **L2** had to be used. At one stage we thought that this complex contained two equivalents of **L2**, but that was disproven by the integration of a purified ^{1}H-NMR sample and the results from high resolution mass spectroscopy.

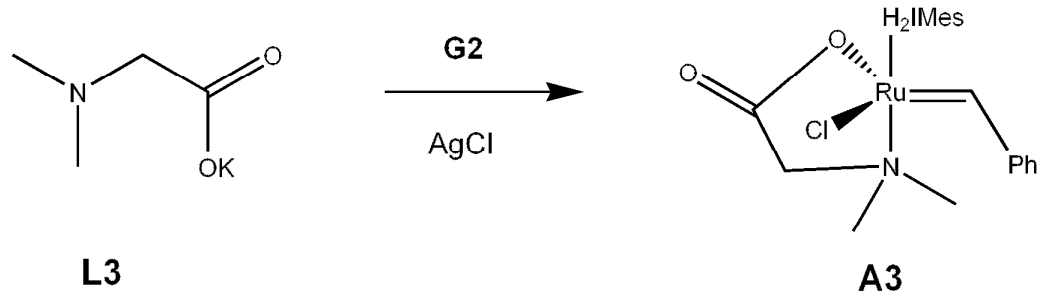

L3 **A3**

*Figure 5.5: Synthesis of **A3**.*

The reaction described in Figure 5.5 went to completion. The product mixture was purified by column chromatography. The target complex was then tried crystallized from a concentrated hexane solution in the freezer, but this attempt was not successful. At a later stage we managed to crystallize **A3** by diffusion of pentane into a concentrated fluorobenzene solution at room temperature. The yield was 68 % after column chromatography.

Complexation reactions with **L0** and **L4** did not result in any new stable alkylidene, although a significant amount of a new ruthenium alkylidene complex most likely containing **L0** was observed in ^{1}H-NMR with an alkylidene peak at 19.09 ppm in small scale reactions. However, this compound was not stable in silica and attempts to purify and characterize it was not successful.

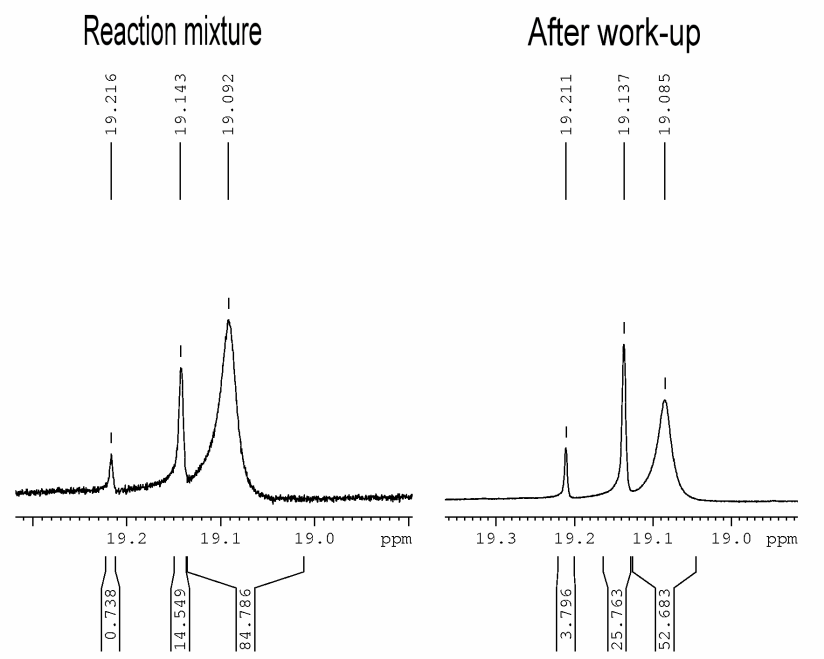

Figure 5.6: ^{1}H-NMR-*peaks in the alkylidene area for complexation with* **L0** and **G2**.

The complex with **L0** was tried isolated by a precipitation from a solvent mixture and then filtered. From Figure 5.6 it is possible to see the two new alkylidene peaks one at 19.09 ppm and another at 19.21 ppm. The peak at 19.09 ppm is decreasing relative to the starting material (19.14 ppm) during the work-up, which points to a low stability of the product compared to the starting material. Such an unstable complex or potential catalyst is not of much interest in this project.

5.2 Results and discussion

Two additional amine based olefin metathesis catalysts have been successfully synthesized and characterized. The new catalysts will be tested in ring closing metathesis of diethyl 2,2-diallylmalonate.

The full structure of **A3** was characterized by X-ray diffraction. It was crystallized in an NMR-tube by diffusion of pentane into a concentrated fluorobenzene solution of the complex. A suitable crystal was selected and analysed by X-ray diffraction. The crystal structure is shown in Figure 5.7. It is shown with centroids of a 50% probability level. The white balls are hydrogen atoms, the grey

centroids are carbon, blue nitrogen, red oxygen, green chloride and pink ruthenium. Figure 5.7 confirms the structure of the target molecule **A3**. The crystal packing contains half an equivalent of fluorobenzene, which has two antiparallel orientations in the ratio 72:28. The fluorobenzene molecule has been removed to obtain a better clarity.

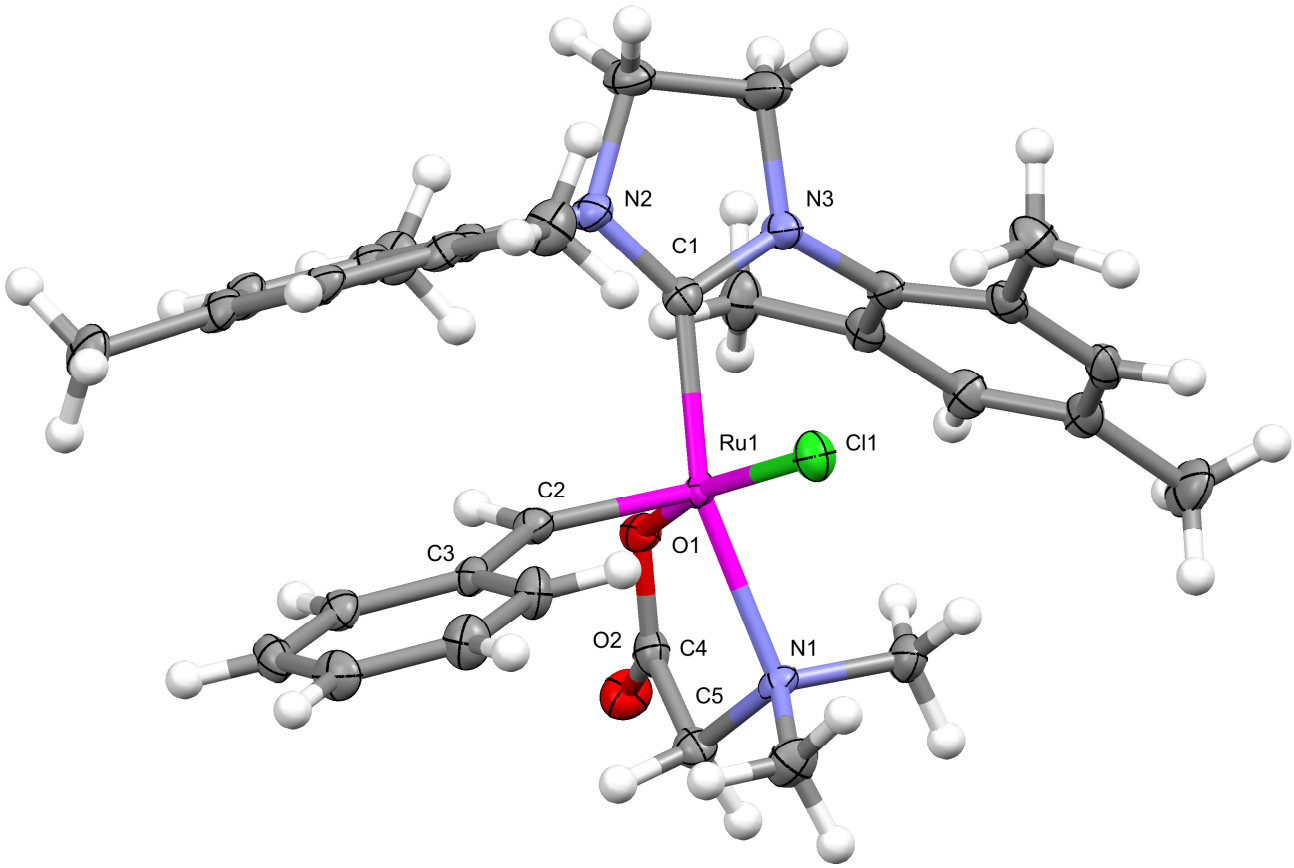

*Figure 5.7: Crystal structure of **A3**.*

The crystal structure of **A3** shown in Figure 5.7 was compared with the crystal structure obtained previously in our group in Table 5.1. The numbers for **A1**, given in parenthesis, is the corresponding numbers from the benchmark study in Chapter 3; functional PBEPBE. The most significant difference of the catalysts are the orientation of the alkylidene, in **A1** the hydrogen on C2 is on the opposite side as O1, while the corresponding hydrogen in **A3** it is one the same side.

Table 5.1: Comparison of **A1** and **A3.**

	Atoms	**A1**		**A3**
Bonds(Å)	Ru1-C1	2.020	(2.011)	2.015
	Ru1-C2	1.840	(1.846)	1.834
	Ru1-O1	2.075	(2.108)	2.099
	Ru1-N1	2.186	(2.263)	2.162
	Ru1-Cl1	2.405	(2.423)	2.395
Angles(°)	C1-Ru1-C2	97.34	(97.48)	98.15
	O1-Ru1-Cl1	174.89	(174.40)	167.00
	O1-Ru1-N1	87.21	(86.32)	79.68
Torsions(°)	N1-Ru1-O1-C24	28.08	(28.92)	13.03
	C1-Ru1-C2-C3	-104.30	(-113.53)	-113.47
	O1-Ru1-C2-C3	-12.35	(-13.10)	150.65

5.2.1 Catalytic activity

All catalytic tests were done with *dry solvents* in closed Youngs NMR-tubes. This enables us to use temperatures slightly above the boiling point. The ring closing of diethyl 2,2-diallylmalonate is among the most tested olefin metathesis transformations,[4] and it is common to test new olefin metathesis catalysts' activity in this reaction; as shown in Figure 5.8. The reference peaks for the ring closing was the substrate ^{1}H-NMR peak which is a doublet at 2.61 ppm (J = 7.4Hz), and the product which gives a singlet at 2.98 ppm in CD_2Cl_2.[172] The peaks were found at similar chemical shifts in all the solvents; $CDCl_3$, C_6D_6 and CD_3OD. Both the peaks correspond to the four protons allylic methylene protons.

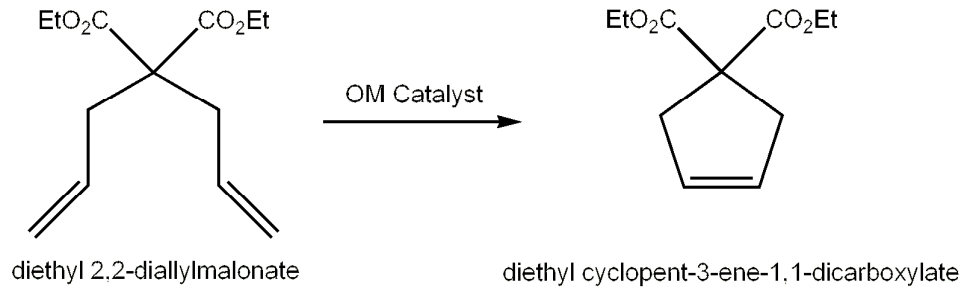

Figure 5.8: Ring closing metathesis of diethyl 2,2,-diallylmalonate.

The first catalytic test was done in accordance with the method published by Grubbs and co-workers in 2008.[58] This test was done in **C_6D_6** with 1 mol% catalyst with a substrate concentration of 0.3 M. The result of the test is shown in Table 5.3. A sub-goal behind this test was to evaluate the latency of the catalyst. Therefore, the temperature was increased during the experiment to improve the conversion. TON was estimated to ~200 from this catalytic test and at the end of the catalytic test the concentration of catalyst was approximately 0.8 mol%.

Table 5.3: RCM with **A3** *in C_6D_6.*

Time	Interval	Temperature	Conversion	
1 hour	0-1 hour	50°C	0.8 %	0.8 %/hour
2 hours	1-2 hours	60°C	1.4 %	0.6 %/hour
3 hours	2-3 hours	80°C	6 %	4.6 %/hour
5 hours	3-5 hours	90°C	50 %	22 %/hour

Some imine containing catalysts synthesised by Verpoort and co-workers are shown in Figure 5.9. **I4**[159] has been reported to give 90 % yield after 72h in dry C_6D_6 at 55°C with 5 mol% catalyst and a concentration of 0.1 M substrate,[173] and 100 % after four hours under the same condition with a "undried" solvent (this might be due to an increase in the polarity of the "solvent-mixture").[159]

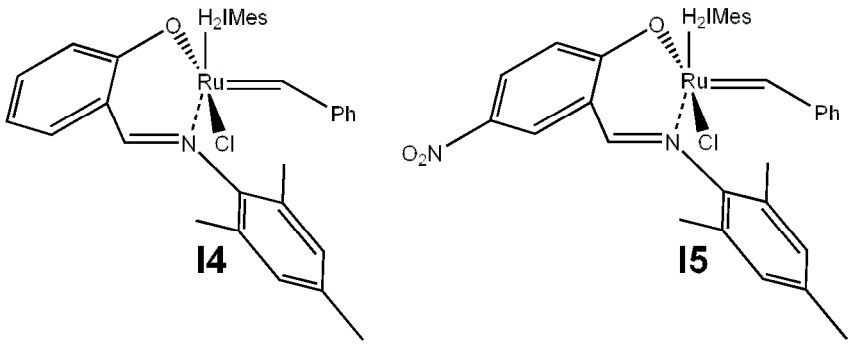

Figure 5.9: Imine containing catalysts with comparable activity.[159]

In CD_2Cl_2, 2 mol% of catalyst **A2** and **A3** were used at a substrate concentration of 0.3M. The conversion was only approximately 2 % after 2 hours at 35°C. In comparison, **G2** is reported to give 99 % conversion after 90 min at 20°C.[174]

Due to the low activity in both C_6D_6 and CD_2Cl_2 the main testing for comparing the catalysts was done in $CDCl_3$. These tests were done with a catalyst concentration of 1 mol% and a substrate concentration of 0.3 M. The results of the tests of **A1**, **A2** and **A3** are given with second generation Grubbs catalyst as reference in Table 5.4.

Table 5.4: RCM catalytic activity of A1, A2 and A3 in $CDCl_3$.

Time	**Temperature**	**Conversion**			
		G2	**A1**	**A2**	**A3**
15 min	50°C	>99%	-	-	-
1.5 hours	50°C	-	5%	4%	22%
20 hours	50°C	-	74%	18%	91%
25 hours	50°C	-	98%	20%	94%
50 hours	50°C	-	>99%	35%	>99%

To compare the catalysts with some catalysts tuned for protic solvents,[173] some additional RCM tests were done in CD_3OD for **A1**, **A2** and **A3**. The tests done in CD_3OD, 3 mol% catalyst and 0.3 M concentration of substrate at 60°C, did not show any activity. Second generation Grubbs catalyst is not soluble in methanol and therefore no activity can be reported for this catalyst. **I5**[159] gave a conversion of 95 % after 23 hours in methanol at 55°C with a 5 mol% catalyst loading and a substrate concentration 0.025 M. **I4** is not reported under these conditions, possibly because of no activity.

All synthesized new catalysts were tested for potential *E/Z* stereoselectivity. Both **A2** and **A3** were been tested for self-metathesis of styrene in $CDCl_3$, with a catalyst loading of 2 mol%, and a substrate concentration of 0.5 M. This was done to see if this design showed any potential for *Z*-stereoselectivity. Self-metathesis of styrene has been reported as *E*-stereoselective for Schrock-type catalysts.[175] Only the *E*-isomer is observed when using styrene in cross-metathesis with Grubbs-type catlyst.[176,177] The potential products from the self-metathesis are given in Figure 5.10.

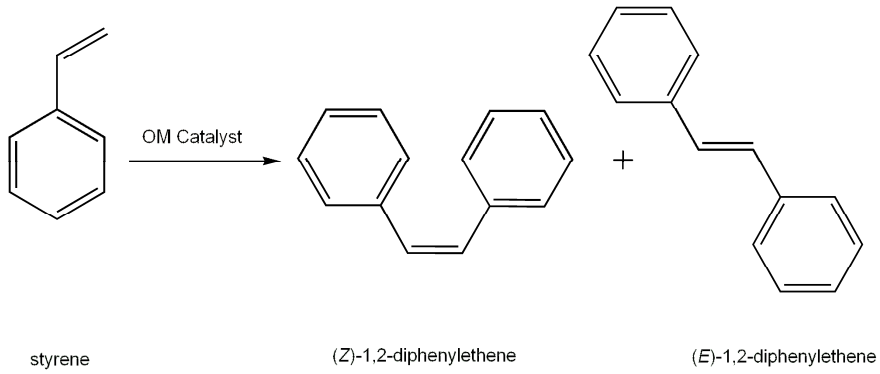

Figure 5.10: Self-metathesis of styrene.

The results for self-metathesis of styrene are given in Table 5.5. The test was observed on ^{1}H-NMR and there was no sign of any *Z*-isomer. The reference peaks in the ^{1}H-NMR were the substrate with a doublet at 6.69 ppm, the *E*-isomer with a singlet at 7.15 ppm and the *Z*-isomer with a singlet at 6.57 ppm.[178] The peaks correspond to the proton on the second position in the double bond for the styrene. The peaks were integrated and normalized to 100 % to give the conversion, since two molecules of styrene are needed for one self-metathesis.

Table 5.5: Self-metathesis of styrene.

Time	**Temperature**	**Conversion**			
		A2		**A3**	
		E	**Z**	**E**	**Z**
1.5 hours	50°C	26%	0%	23%	0%
20 hours	50°C	36%	0%	74%	0%
25 hours	50°C	49%	0%	77%	0%
50 hours	50°C	65%	0%	82%	0%

Based on the catalytic test RCM of diethyl 2,2-diallylmalonate in $CDCl_3$ (shown in Table 5.4), an attempt of estimating the stability of the catalysts was made. This was done by measuring the degradation of the catalysts from the 1.5 h to 25 h. The integral of the alkylidene peak in ^{1}H-NMR was measured relative to the substrate and product peaks, which should sum to 100 due to the normalization. The results are shown in Table 5.6.

Table 5.6: Stability ranking of the catalysts.

Catalyst	**Integral 1.5 h**	**Integral 25 h**	**Degradation**	**Rank**	**Conversion/ Degradation***	**Rank**
A1	0.14	0.02	85%	2	1.09	1
A2	0.11	0.08	27%	1	0.59	3
A3	0.15	0.01	93%	3	0.77	2

** A scalar of the TON.*

5.3 Comparison of theoretical and experimental results

By combining the theoretical and experimental work, one can obtain a better knowledge about the amine based second generation olefin metathesis catalysts. As described previously in this chapter two new catalysts were synthesized and characterized, **A2** and **A3.** In addition to these two **A1** has been synthesized and characterized at an earlier stage.[55] The catalytic activity of the all three catalysts was measured and compared. Parallel with the experimental work, a novel theoretical study of the catalytic cycle for bidentate amine based olefin metathesis catalysts was performed. The main motivation back this additional work is to provide deeper insight in the factors responsible for the observed experimental catalytic activities.

The first experimental work showed a low stability of alkyl based six-membered amine carboxy chelates (**L0** and **L4**). We were able to synthesize it and observe it on ^{1}H-NMR, but we decided to leave these instable chelates and instead focus on the seemingly more stable catalysts with five-membered chelates. This instability may be due to a more flexible ring system, when six bonds are involved. Such chelates have a higher number of possible conformations and it is therefore often harder to form the chelate. The broad peaks in Figure 5.6 might signal of the existence of many different conformations of the chelate, or of the piperidine ring moiety, at room temperature. This may suggest that these ligands are in fact too flexible to provide stable complexes. These systems would probably show a good activity even at room temperature if they were isolated.

From the experimental work and catalytic testing we ended up with the following ranking regarding to the activity: **A3, A1** and **A2**. An estimation of the degradation from ^{1}H-NMR gives the opposite with the regard to stability. By dividing the conversion on the degradation the following ranking comes out **A1, A3** and **A2**, estimation of the turn over number (TON).

The computational studies present the following ranking **A3**, **A1** and **A2**. This resembles the ranking observed in the laboratory. It is interesting to figure out what causes these differences in the activity. The structures are shown again in Figure 5.11.

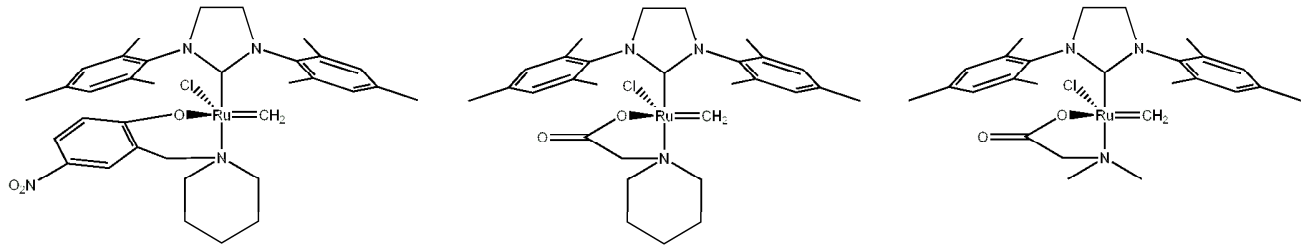

A1 A2 A3

Figure 5.11: Structure of the catalysts.

The only difference between **A2** and **A3** is the amine. In **A2** it is substituted by ring forming the piperidine in addition to the acetate, and in **A3** it is substituted by two methyl groups. This difference leads first of all to a significant difference in the energy needed to decoordinate the amine. The most important parameters and results are listed in Table 5.7.

Table 5.7: Most significant parameters and results

Catalyst	**Chelate**	**Amine**	**O-type**	**Decoordination of amine (Ru-N)**	**Effective barrier**	**Conversion 20 hours**	**Stability**
A0*	6-ring	piperidine	carboxy	-	-	-	4
A1	6-ring	piperidine	phenoxy	16.9	25.1	74%	2
A2	5-ring	piperidine	carboxy	20.7	33.5	18%	**1**
A3	5-ring	dimethyl	carboxy	**14.7**	**24.7**	**91%**	3

* Not isolated.

The results show that replacing a piperidine with a dimethyl amine in this class of catalysts it will increase the activity significantly. Going from **A2** to **A1** involves changing the anionic oxygen from a carboxy group into a phenoxy and a larger chelate. This change increases the activity as well. It is most probably due to the larger chelate, which makes it easier to decoordinate and more difficult to recoordinate the amine group. Going from **A2** to **A3** involves changing the amine from a piperidine analogue to a dimethylamine analogue. This also increases the activity significantly since it is easier to decoordinate the less basic amine. In other words; a six-membered ring seems to be more active than the corresponding five-membered ring, and the dimethylamine analogue is more active than the piperidine analogue.

The difference in activity between **A2** and **A3** can to a certain extent be explained by the basicity of the corresponding amine. By comparing the pKa of trimethylamine with N-methyl-piperidine's pKa value 9.76 and 10.08[179] one could expect the increase activity of **A2** compared to **A3** due to the decreased strength in the ruthenium amine bond.

Based on these arguments, one can conclude that three new potentially more active catalysts could be synthesized from the ligands **L10** and **L13** and from a new ligand. The corresponding catalysts are shown in Figure 5.12.

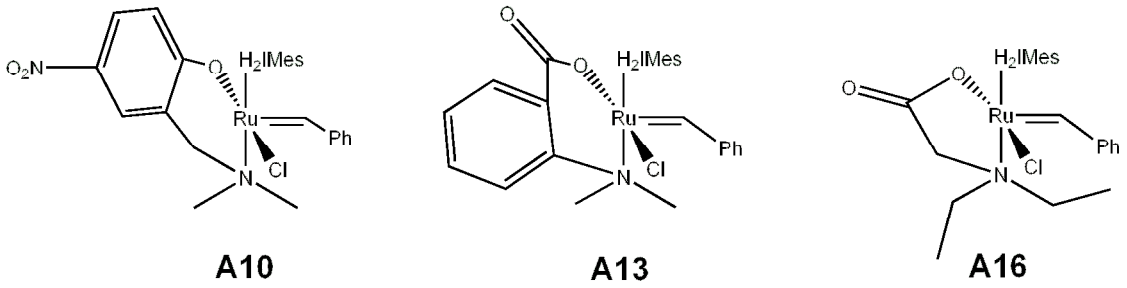

Figure 5.12: Suggested new catalysts based on results.

If our assumptions are correct, **A10** should be more active than **A1**. The activity of **A13** is harder to predict, but probably a better catalyst than **A3**. **A16** could also be an interesting catalyst if it is possible to synthesize it. Due to the larger on the amine substituents (ethyl groups are fairly large compared to methyl groups; e.g. tolman cone angle of $PMe_3$118° and Pet_3 132°)[166], this ligand is expected to decoordinate more easily, and therefore result in a more active catalyst than **A3**. A contradiction to this is to use the pKa value to predict the activity. The corresponding methyldiethyl amine has a pKa of 10.29.[179] This would result in a less active catalyst than **A3**, but probably the sterical hindrance of the amine will make the ruthenium amine bond weaker and then again result in a more active catalyst than **A3**. After all the pKa might no be the best parameter to use to optimize ligands. It is of larger value to calculate the energy needed to decoordinate the amine in **A16** by doing a small computational study.

In general these catalysts have a fairly low activity compared to the second generation Grubbs catalyst. In RCM of diethyl 2,2-diallylmalonate second generation Grubbs gives 99% conversion after 90 min at 20°C in CD_2Cl_2.[174] But it might not be fair to the amine based catalyst to compare them with Grubbs second generation catalyst. From the catalytic test in benzene even the most active

catalyst shows low activity even at 50°C. This is a sign that the catalysts should be classed as latent olefin metathesis catalysts instead.[35] Latent olefin metathesis catalysts are not showing any activity at room temperature, but a good catalytic activity at higher temperatures, example goes **A3** in C_6D_6 at 90°C. The most latent of them all is **A2** which shows a fairly low activity even in chloroform at 50°C. It would probably show none at room temperature. In the future it might be interesting to design and synthesize a more latent catalyst based on **A2** to explore the latency of this class of catalysts.

Latent amine catalysts might have some interesting applications in reactions where catalysts active at room temperature fail to produce the wanted product. One example is ring opening polymerization metathesis. Here it is necessary to avoid incorporation of solid catalyst in the polymer.[180] This could be avoided using latent amine catalysts, since their activity can be controlled by the temperature. Indeed, they show no activity at room temperature, thus they have the advantage to be a part of a homogenous mixture (no solids) before the polymerization starts. The good stability of this class of catalysts, even at high temperatures, may suggest other applications as well, for example in the manufacture of large macrocycles through ring closing metathesis. Indeed, the unwished oligomerization side reaction significantly reduces the overall yield of the target molecule.[181] To favour the ring closing metathesis, high temperatures are generally required (entropy favoured). Thus, amine based-catalysts being both stable and highly active at elevated temperatures could be useful for such applications.

Latent catalysts might not be the obvious choice to make a *Z*-stereoselective catalyst where one wants to obtain what is usually the kinetic product. This is because they need be heated to above 50°C to show a significant activity, which in most cases would ruin any concentration of a kinetic product in a mixture. If one for example wants a stereoselective catalyst, a catalyst that has an easy initiation (the ligand dissociation cannot be the rate limiting step) should be the target catalyst. In addition, the height of the catalytic barrier should be sufficiently different for the formation of the two stereoisomers. It is quite intuitive to understand that those catalysts that have a good activity at a relative low temperature are also more suited to exploit the relatively small difference between the two barriers.

Even if some features of amine catalysts may be interesting (e.g. the ligand dissociation is generally much easier than the alkene coordination), the very low activity recorded at room temperature is a

serious drawback. For this reason other classes of catalyst may be much more suitable to design an efficient stereoselective catalyst. The search for such a catalyst continues in the next chapter.

6 A bulky ligand and a potential stereoselective catalyst.

The aim of this project is to make a potentially *Z*-stereoselective catalyst based on a novel sterically demanding bidentate N-heterocyclic carbene (NHC) ligand. In the previous section I have described the synthesis of two novel latent catalysts, containing a bidentate ligand with an amine decoordinating moiety. Despite the fact that these catalysts were asymmetrically substituted they did not show any sign of Z-stereoselectivity in the self-metathesis reaction of styrene. The new strategy will be to use a bidentate non-labile ligand that constantly applies a large steric pressure in one side of the catalyst during the catalytic cycle.

In the field of olefin metathesis there has only been reported a few catalysts containing chelating NHC ligands. Hoveyda and co-workers have synthesized the only known catalysts bearing such ligands.[62,182-184] Their complexes contain eight-membered NHC-phenoxy chelates. Two of these structures, **1**[184] and **2**[62], are shown in Chart 6.1. These catalysts showed a good stability and the chirality makes them interesting with the regard of enantioselectivity in olefin metathesis.[62]

*Chart 6.1: Existing catalysts (***1**-**2***), attempted catalyst (***3***) and suggested catalyst (***4***).*

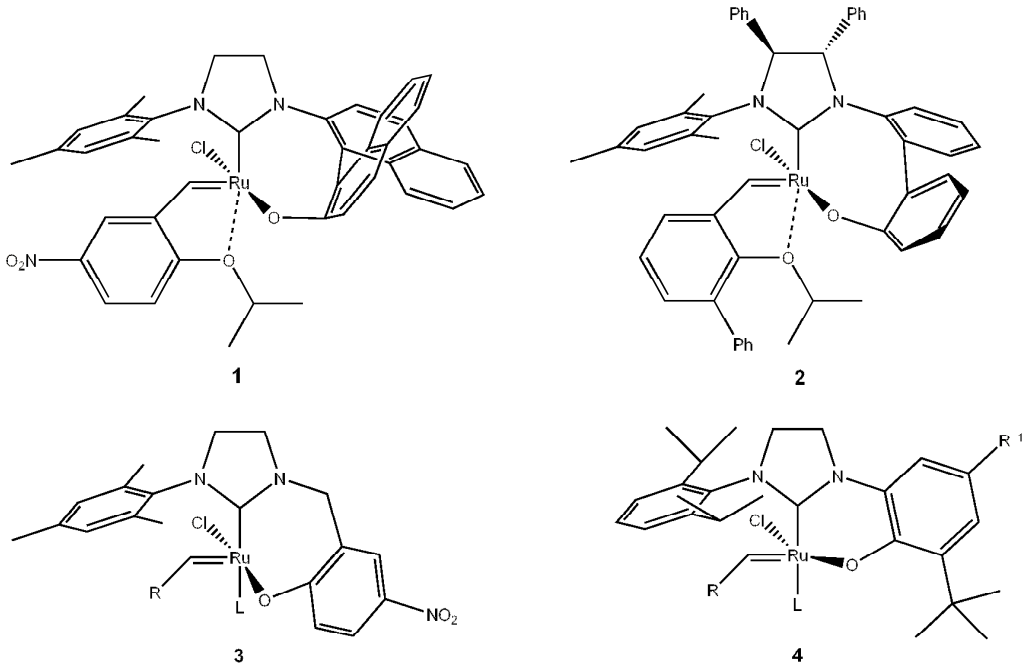

More recently, our group has attempted the synthesis of Ru-based catalysts substituted by a novel chelating NHC ligand.[63] However, instead of the target catalyst **3** two new alkylidene complexes were synthesized and isolated, both substituted by two bidentate ligand NHC-phenoxy ligands. One of these complexes was the first example of an imidazolium-substituted metal alkylidene.[56,63,185] Differently from the ligands used by Hoveyda, the ligand proposed in our group formed a seven-membered chelate instead of an eight-membered chelate when coordinated to the metal centre. Moreover it is also less sterically demanding and hence the possibility of coordinating two bidentate ligands.

The goal of the present project is to investigate the possibility to make a catalyst having a 6-membered NHC-pheonxy chelating ligand (**4**). In order to prevent the bis-coordination to the ruthenium centre, the NHC ligand contains two bulky moieties. When coordinated to the metal the 2,6-diisopropylphenyl moiety should apply a steric pressure to the alkylidene moiety to increase the activity[44], while the tert-butyl group could promote Z-stereoselectivity by applying a strong steric pressure selectively in one the two faces of the metallo-cyclobutane intermediate.

The first suggested ligand was with a hydrogen or a nitro group at the R^1-position in **4;** 3-(3-*tert*-butylphen-2-olate)-1-(2,6-diisopropylphenyl)-4,5-dihydro-imidazol-2-ylidene or 3-(3-*tert*-butyl-5-nitro-phen-2-olate)-1-(2,6-diisopropylphenyl)-4,5-dihydro-imidazol-2-ylidene. We anticipated this ligand too hard to make; from retrosynthesis. Especially the synthesis of the unknown 2-amino-6-*tert*-butylphenol is presumably very challenging, because the formation of the wanted product would have been disfavoured due to the chemistry of arenes.[22] We decided to synthesize 2-amino-6-*tert*-butyl-4-methylphenol, which is much easier to make and that has been successfully made before.[186] That means that the target ligand is then 3-(3-*tert*-butyl-5-methyl-2-olate-phenyl)-1-(2,6-diisopropylphenyl)-4,5-dihydro-imidazol-2-ylidene which makes R^1 a methyl-group. The procedures to make these kind of ligands have been well documented in work done by Grubbs[186-188] and Fürstner[189]. My synthesis will be based on the procedures reported by Grubbs.

6.1 Experimental work

The NHC-phenoxy ligand needed to make **4** involves synthesizing a new NHC ligand that has not been reported before. Similar ligands have been made by Waltman and co-workers and complexated on Pd(II)[186] and Ni(II)[190]. This specific ligands will involve the synthesis of three until know unknown compounds. These are made in the three last steps. When the ligand has been synthesised it will exist as a 4,5-dihydroimidazolium salt. The salt needs to be deprotonated to yield the N-Heterocyclic carbene.[191] The NHC is then introduced to the complex precursor. In the nomenclature these are called 4,5-dihydroimidazol-2-ylidene analogues.

The synthesis and characterization of ligands and complexes is fully described in section A.4.

6.1.1 Ligand synthesis

Scheme 6.1 illustrates the synthesis plan for 3-(3-*tert*-butyl-2-hydroxy-5-metylphenyl)-1-(2,6-diisopropylphenyl)-4,5-dihydroimidazolium chloride (**5**). The first step is a nitration of a phenol, which is followed by a reduction to form the 2-amino-6-*tert*-butyl-4-methylphenol. A bought 2,6-diisopropylaniline is reacted with a acid chloride to for an amide. This amide also contains an ester group which is reacted with the 2-amino-6-*tert*-butyl-4-methylphenol to form a diamide which in turn is reduced to a diaminium followed by a ringclosing reaction to form the 4,5-dihydroimidazolium salt analogue; **5**.

*Scheme 6.1: Synthesis plan for **5**.*

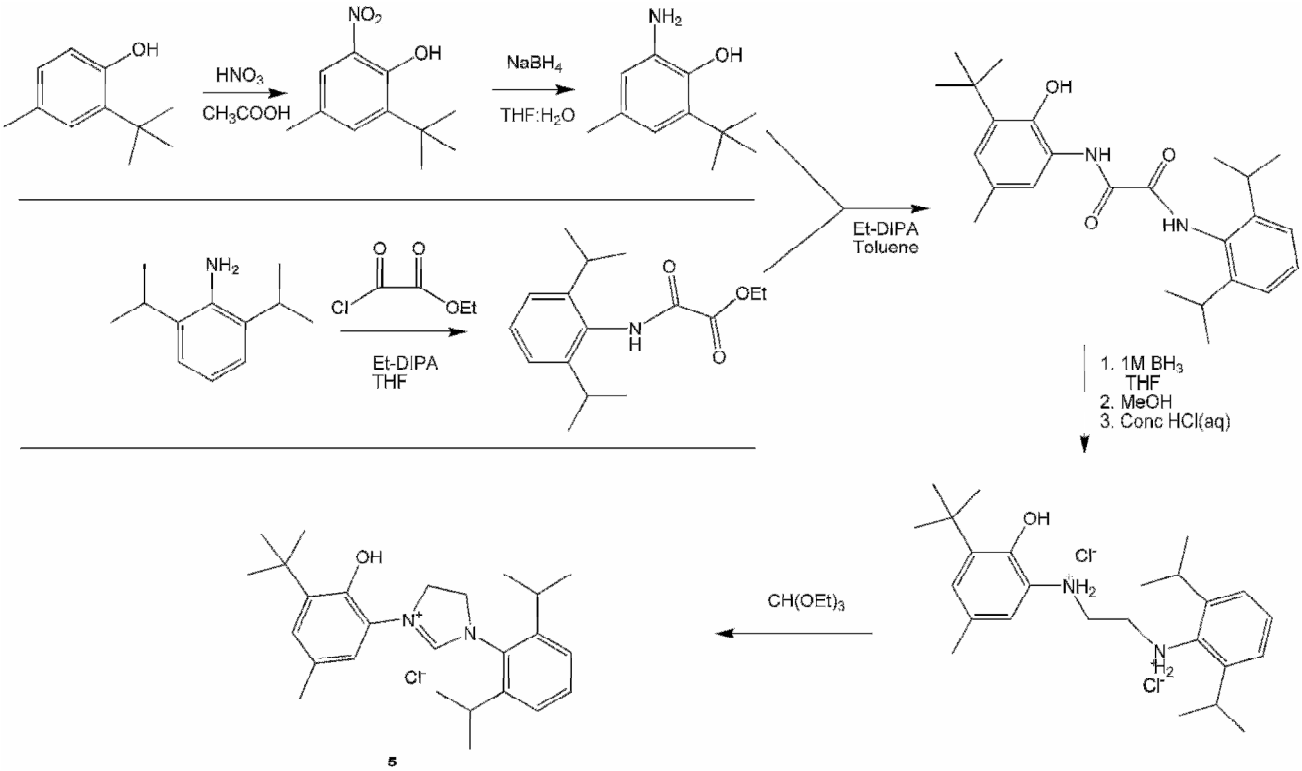

Synthesis of 6-*tert*-butyl-4-methyl-2-nitrophenol.

This synthesis was done according to the procedure Harry E. Albert described in his article about some new amino-alkylphenols in 1953[192]. The reaction is shown on Figure 6.1.

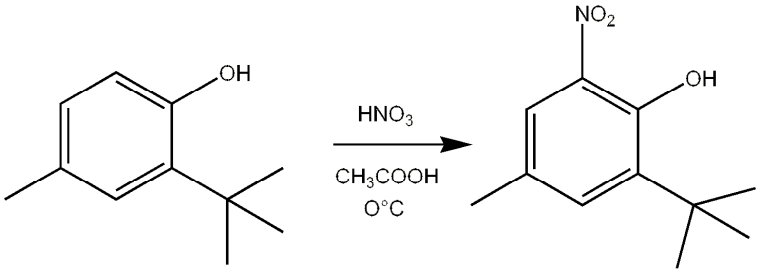

Figure 6.1: Nitration of 2-*tert*-butyl-4-methylphenol.

The reaction was simple and a pure product was crystallized from hot ethanol to yield orange thread like crystals.

Synthesis of Synthesis of 2-amino-6-*tert*-butyl-4-methylphenol.

The compound was synthesized according to a procedure described by Behzad Zeynizadeh and Davood Setamdideh in 2006.[193] The method is mild and a convenient method of reducing nitroarenes. The method gives a fairly high yield (77 %) and we do not have to buy a relatively expensive catalyst.

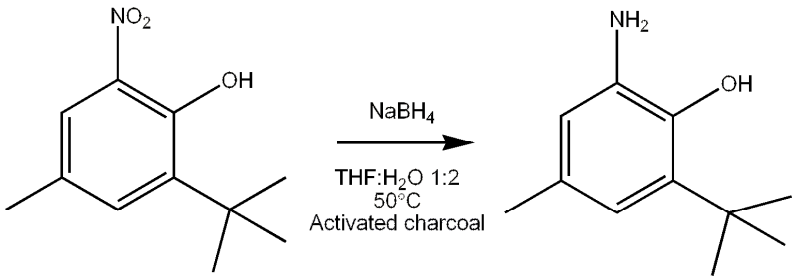

Figure 6.2: Reduction of 6-*tert*-butyl-4-methyl-2-nitrophenol.

The reaction shown in Figure 6.2 was monitored by TLC (disappearance of orange substrate). Sodium borohydride was added until there was nothing left of the substrate in the reaction mixture.

The work-up had to be done fast, because the colourless product gets oxidized to a red unidentified compound in solution, when air (oxygen) is present.

Synthesis of ethyl 2-(2,6-diisopropylphenylamino)-2-oxoacetate.

The reaction was done as described by Grubbs and co-workers[188]. The reaction time was adjusted from 16 hours to 4 hours, because these types of reactions is general known to be fast,[22] and monitoring with TLC showed almost full conversion after 2 hours.

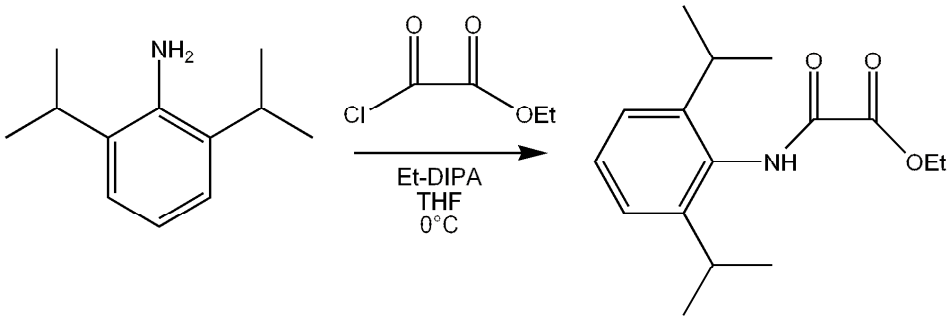

Figure 6.3: Amide formation.

The reaction shown in Figure 6.3 is done by adding the ethyl chlorooxoacetate dropwise and gives quantitative yields. Crystallization from 9:1 Hexane:EtOAc gives colourless thread like crystals.

Synthesis of

N^1-(3-*tert*-butyl-2-hydroxy-5-metylphenyl)-N^2-(2,6-diisopropylphenyl)oxalamide

This reaction was done following the description of the work done by Grubbs and co-workers in 2004.[186] This compound was until then unknown.

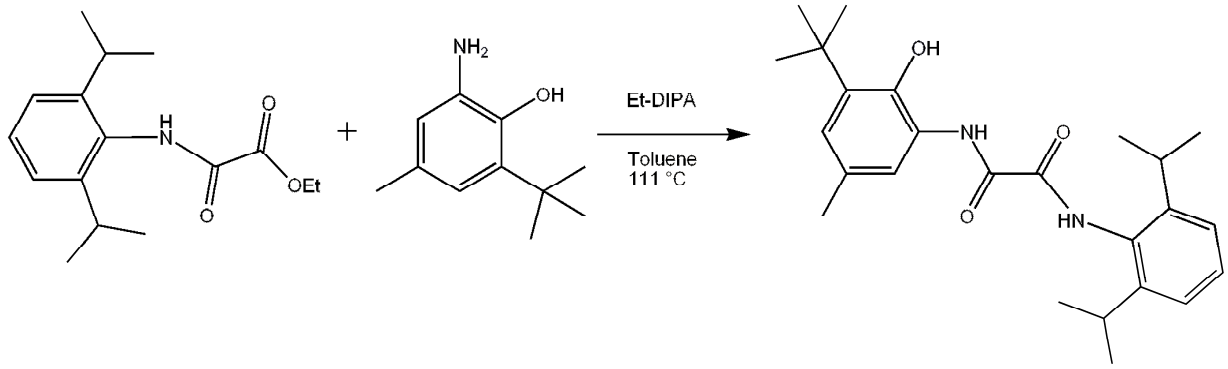

Figure 6.4: Oxalamide analogue.

The product shown in Figure 6.4 has not been crystallized, but a purification with precipitation from a 1:1 diethyl ether:hexane mixture gave a product pure enough to do the next reaction step. This new compound was isolated with 79 % yield.

Synthesis of N^1-(3-*tert*-butyl-2-hydroxy-5-metylphenyl)-N^2-(2,6-diisopropylphenyl)ethane-1,2-diaminium dichloride

This reaction was done as an adjustment to what Grubbs and co-workers did in 2008.[188] This compound was also unknown at the time. The quality of the THF-adduct of the borane is important to be sure that the reaction goes to completion, since there is no reported method to purify this salt. It might be possible to crystallize. During this project the amounts of borane-adduct varied from 8 to 20 equivalents, depending on the freshness/quality of the borane-adduct.

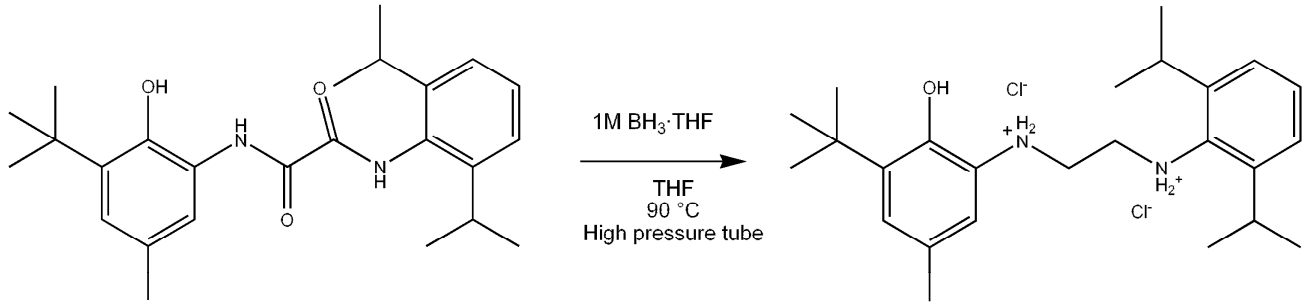

Figure 6.5: Reduction of oxalamide.

Grubbs and co-workers did not isolate their analogue compound, but due to some problems in the next step it was more convenient to isolate and characterize it.[186] The product in Figure 5.6 was hard to characterize because of broad and overlapping NMR-peaks. It was isolated with a yield of 95 %.

Synthesis of 5

The reaction was done several times according to the two articles by Grubbs and co-workers[186,188]. Their reaction strategy did not work out well for this imidazolium salt. Therefore an adjusted approach was used. They had reported that the product precipitated from the solution when the reaction had reached completion, but by just filtering the highest possible yield was around 40 %. This might be due to some structural differences. By adding pentane to the reaction mixture after it had cooled to ambient temperature the yield was increased to 70 %. This method is fully described in A.4.

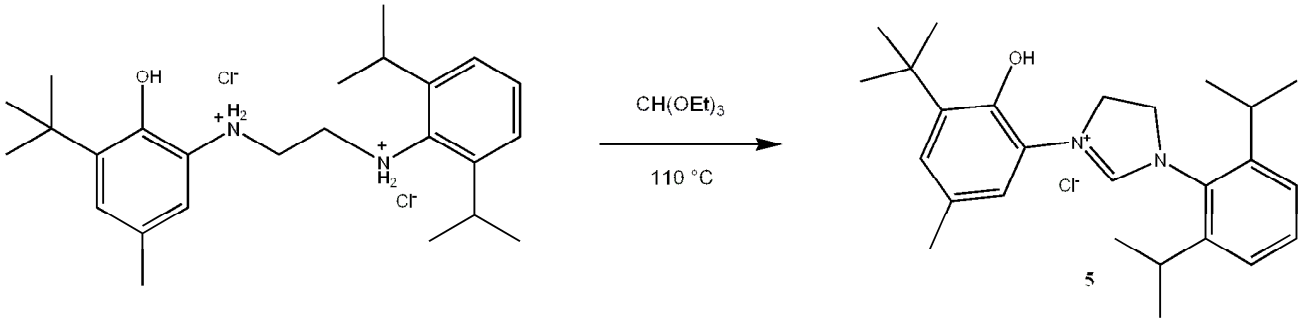

Figure 6.6: Cyclization with triethylorthoformiate.

The product in Figure 6.6 is the target precursor of the ligand. The purity of the previously described precipitate was good enough to use for the complexation. The salt was crystallized from fluorobenzene to yield very thin colourless crystal threads with a good enough quality for X-ray diffraction analysis. The 4,5-dihydroimidazolium salt is very stable and is usually a white fluffy powder.

6.1.2 Attempted Ruthenium complex synthesis

Lots of different approaches were tried to get the **5** to be a ligand for ruthenium. The different approaches are shown in Scheme 6.2.

Scheme 6.2: Suggested reactions with the NHC-ligand with Ruthenium complexes.

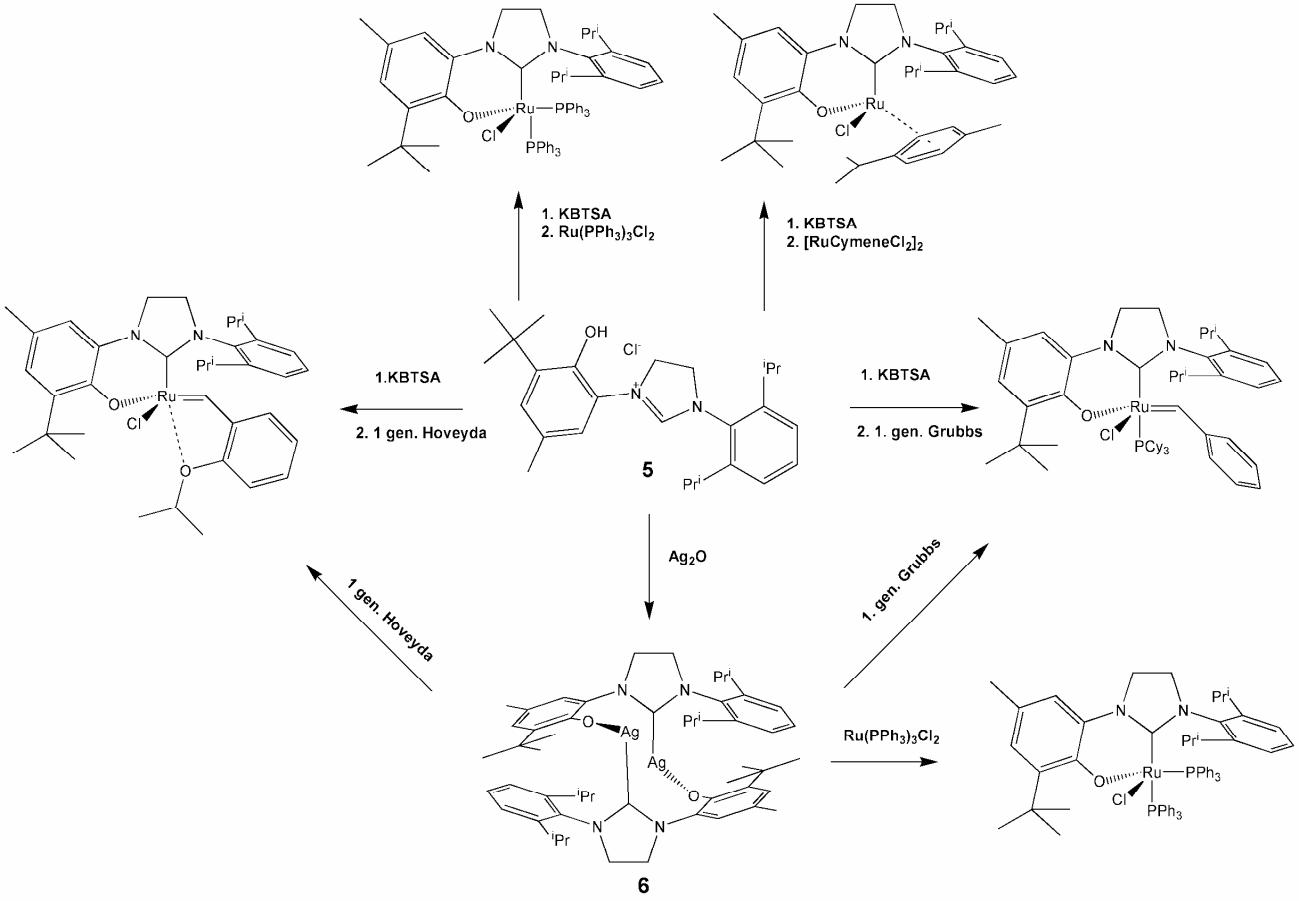

All reactions below are thoroughly described in the appendix; A.5. Following reactions with a crossing line on the arrow in the figures can be regarded as failed reactions. To characterize reactions with **G1** or **H1** as a failure or success the ^{1}H-NMR peak of the alkylidene was used as an indication. Where the starting material contains such a peak the product should contain a corresponding peak at another chemical shift. The reference peaks for the catalysts are shown in Table 6.1. The peaks have been measured in our lab in $CDCl_3$ with the solvent peak at 7.26 ppm as the reference.

Table 6.1: Reference ^{1}H-NMR alkylidene peaks in $CDCl_3$.

Compound	**Peak**	**Multiplicity**
G1	19.99 ppm	Singlet
H1	17.43 ppm	Doublet, J=4.5Hz

In-situ complexation

The first complexation method tried was in-situ inspired by the work of our group in 2007.[194] The reaction was done with **H1** at room temperature with Ag_2O and Ag_2CO_3 as the base in separate experiments. The reactions did not show any new alkylidene peak in ^{1}H-NMR, but their ^{1}H-NMR gave an indication that these bases were strong enough to deprotonate both the acidic positions on **5**. The reaction is shown in Figure 6.7.

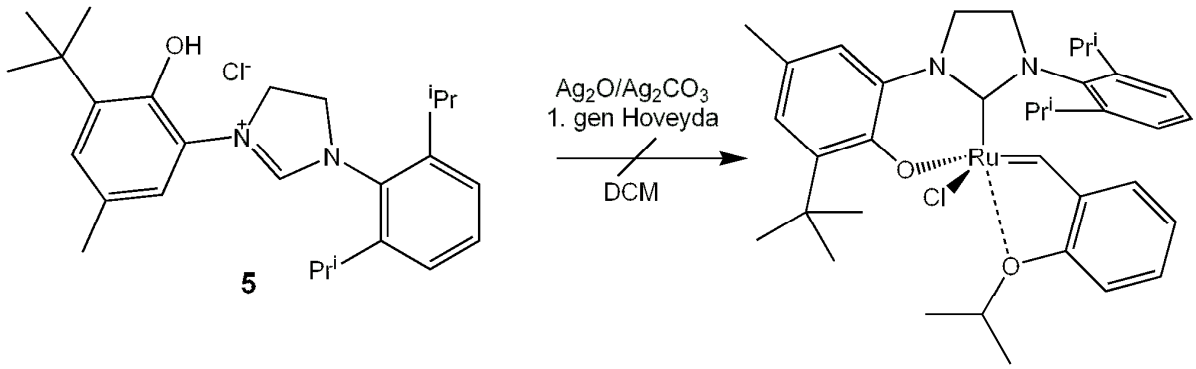

*Figure 6.7: A general procedure for in-situ introduction with **5**.*

Free carbene complexations with 5

We tried to introduce **5** as the corresponding free carbene. The base that was used to make the free carbene was potassium bistrimethylsilylamide; KBTSA. This base was used by Grubbs and co-workers for deprotonation and complexation of similar ligands in 2004.[186] The first reaction was done in THF with **G1**.

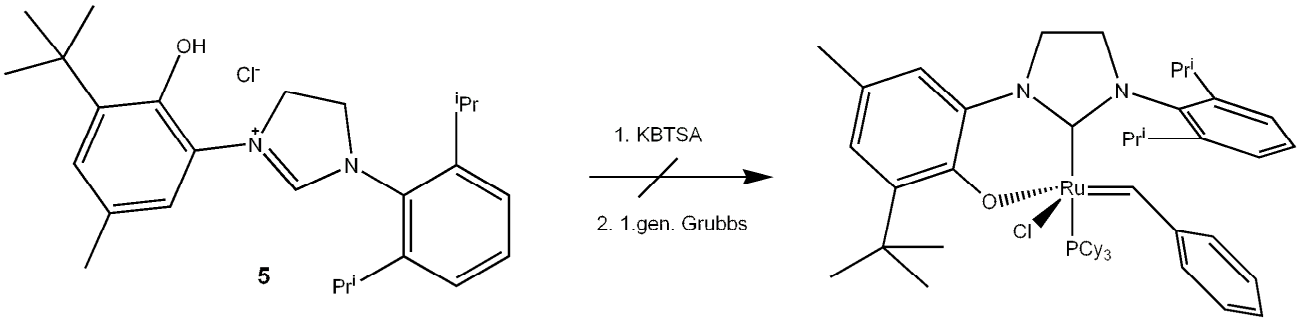

*Figure 6.8: Generalized method of reacting **5** with **G1**.*

The ^{1}H-NMR of the reaction mixture, corresponding to the reaction shown in Figure 6.8, did not show any new alkylidene peak, only that most of the **G1** had decomposed.

The second reaction was done in toluene and the free carbene formed in THF. From this reaction as well, no new ruthenium complex bearing an alkylidene was formed.

The reaction was also tried with **H1**. This reaction was done in toluene at 50°C with silver chloride as a phosphine scavenger and is illustrated in Figure 6.9. It did not yield a product bearing **5** and an alkylidene group.

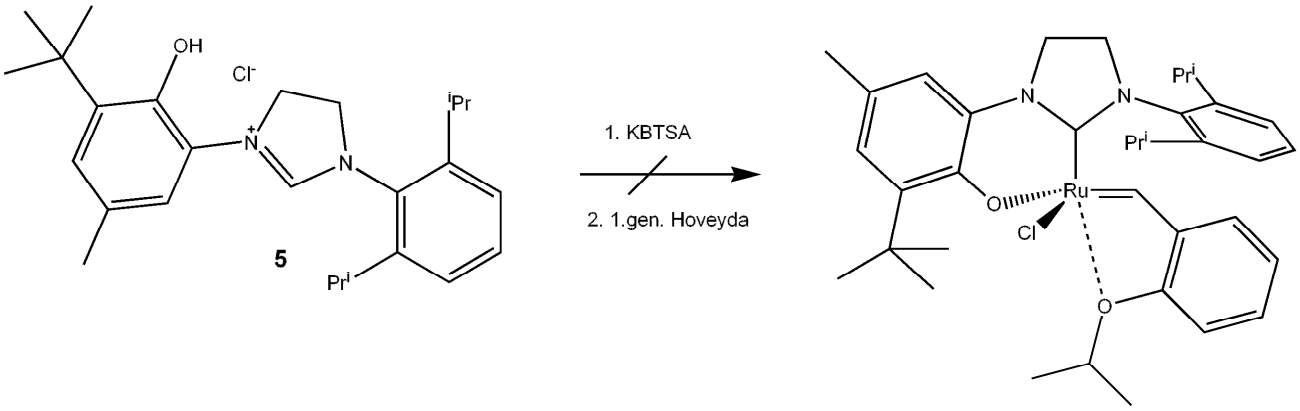

*Figure 6.9: Generalized method of reacting **5** with **H1**.*

Transmetalation

When both in-situ complexation and the introduction of **5** as the free carbene failed the next approach was to try a transmetalation with a silver complex. Silver NHC complexes are easy to synthesize and are useful reagents to prepare other metal NHC complexes by transmetalation.[195,196] Hoveyda and co-workers used transmetalation to make their complexes in 2005.[183] They used a transmetalation approach to introduce their ligand to **H1**. One of the advantages with a transmetallation is the mild reaction conditions needed to introduce a new ligand and the driving force of the precipitation of AgCl or the formation of the stable (μ_2-Chloro)(tricyclohexylphosphine) complex $(PCy_3AgCl)_2$.[194] By these reasons it was tried to synthesize a silver complex with the ligand coordinated; **6**. The reaction was done in dichloromethane at 37°C with a suspension of the imidazolium salt and Ag_2O.

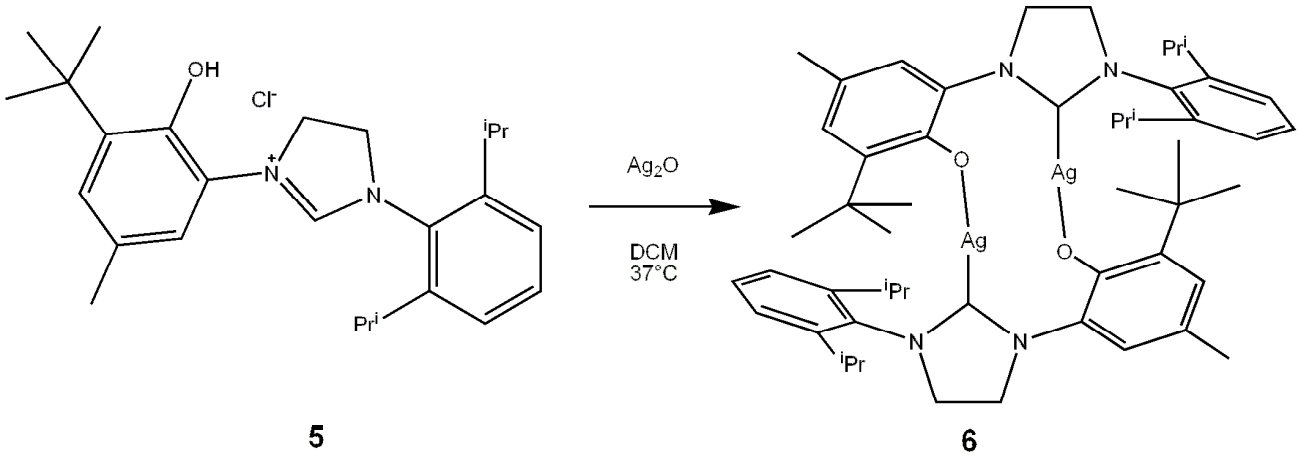

5 **6**

Figure 6.10: Synthesis for the dimeric silver complex.

Results from DART high-resolution mass spectroscopy, peaks at 800-900 m/z, suggest that the product structure formed in the reaction shown in Figure 6.10 also has a dimeric structure. A similar structure has been reported by Hoveyda and co-workers as a dimeric complex,[183] and some other silver NHCs have also been characterized as dimers.[196] None of the several attempts to obtain a crystal of this complex were successful.

Complex **6** was reacted with **G1** and **H1** in separate experiments.

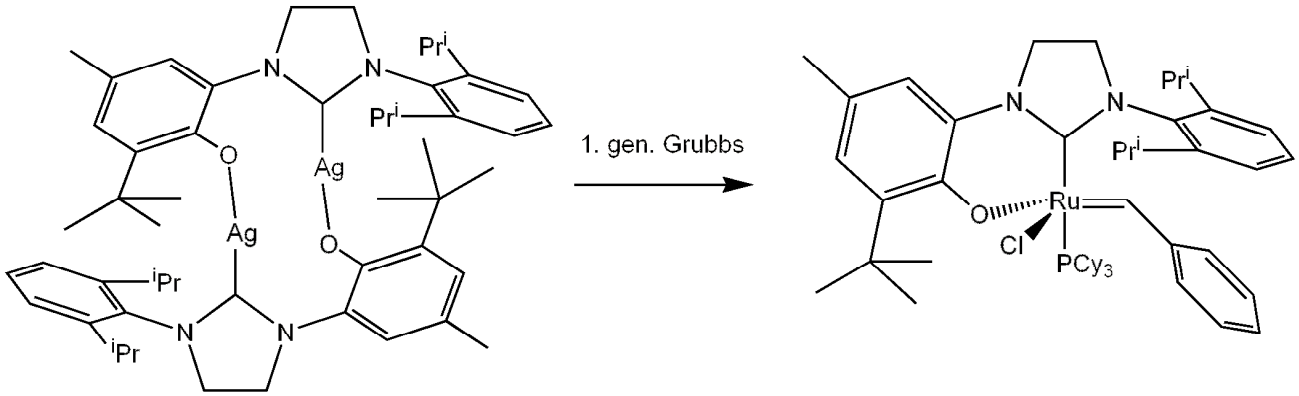

6 **7**

Figure 6.11: Silver complex **6** *with* ***G1***.

One of the reactions with **G1** and **6** shown on Figure 6.11 showed some potential on the ^{1}H-NMR. It suggested the presence a new alkylidene with a doublet at 19.73 ppm (J=9.1Hz). Anyhow the yield was quite low; 6 %; and the compound was decomposing in the NMR-solvent. ^{1}H-NMR of the alkylidene area is shown in Figure 6.12.

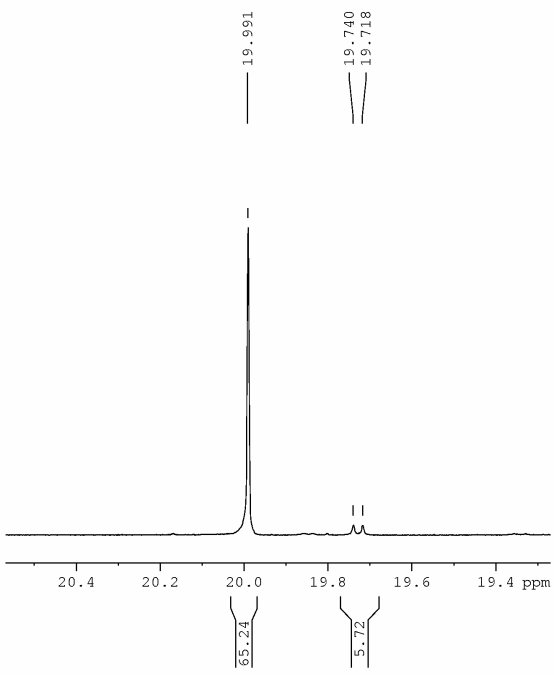

Figure 6.12: ^{1}H-NMR of alkylidene area reaction between ***6*** *and* ***G1***.

This new alkylidene appeared only once when the reaction was done in toluene. The new alkylidene compound and could not be spotted on TLC. It was tried to change the solvent, to increase the yield.

The same reaction in dichloromethane did not yield the new alkylidene. A similar result was obtained in our group when the seven-membered ring NHC silver complex was reacted with **G1**.[185]

After these reactions it was concluded as very difficult to introduce the ligand to **G1** and **H1** directly. It was therefore decided to try to make the catalyst from standard Ru-precursors.

Synthesis of Ru-precursors

After several failed attempts to do a transmetallation, a different approach was chosen. We wanted to try making the catalyst from simple ruthenium precursors. The precursor compound synthesized was the standard starting material for the Ru-based olefin metathesis catalysts; $RuCl_2(PPh_3)_3$, dichlorotristriphenylphosphineruthenium.[183,197] This was synthesized according to the relatively new method reported by Moscatelli and co-workers.[198]

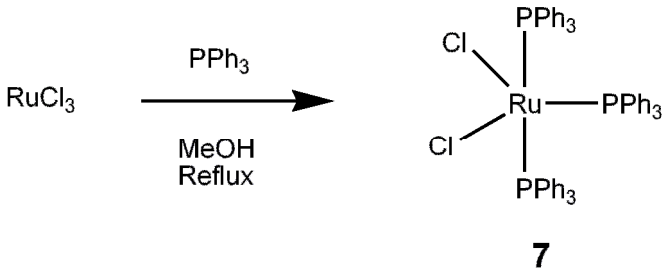

7

Figure 6.13: Synthesis of $RuCl_2(PPh_3)_3$.

The reaction shown in Figure 6.13 was successful and yielded 90% of the pure product. The purity was confirmed by ^{31}P-NMR.

Another starting material $[(\eta^6\text{-p-cymene})RuCl_2]_2$ was synthesized, **8**. This is not a common starting material for ruthenium based olefin metathesis Grubbs type of catalysts, although it has been reported with some NHC ligands and Schiff bases and also shown some activity in olefin metathesis.[162,199]

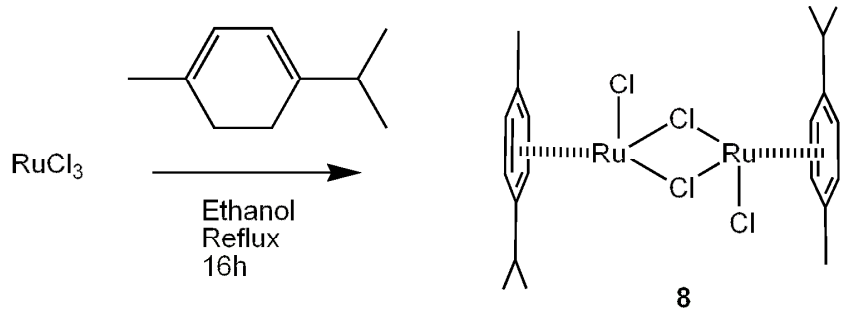

Figure 6.14: Shows the synthesis of $[(\eta^6\text{-}p\text{-cymene})RuCl_2]_2$.

The synthesis shown on Figure 6.14 was done by a method which was a combined procedure from what Spicer and co-workers[200] and Simpson and Hodson[201] had done earlier. The adjustment of the procedure was mainly in the purification of the product.

Introduction of 5 to a Ru-complex

The free carbene of **5** reacted with **7**. The reaction is shown in Figure 6.15 and it was not proven to be successful, because it was impossible to isolate a pure product. There were some new peaks on the ^{31}P-NMR, but I was not able to isolate the compounds resulting in these peaks.

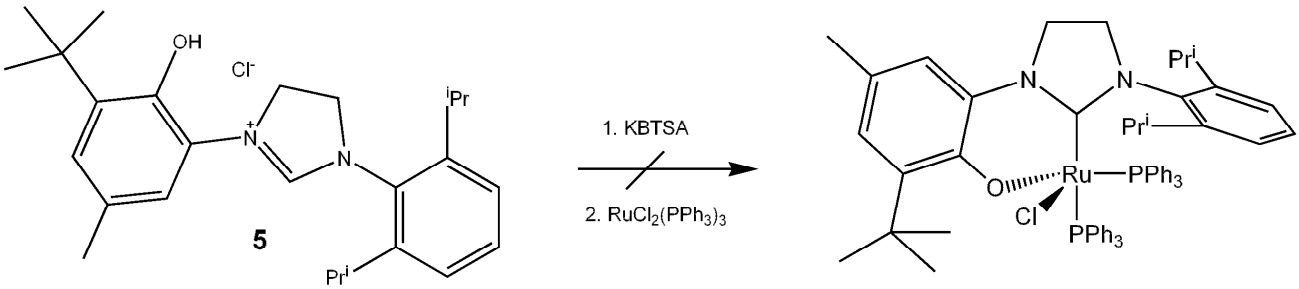

Figure 6.15: Free carbene of **5** *with* **7**.

An attempt shown in Figure 6.16, was to try to introduce the free carbene to $RuHCl(PPh_3)_3$. This attempt was thought possible since it has a less sterical hindrance, and that it has been reported a method to introduce an alkylidene to a ruthenium hydride complex.[202-204]

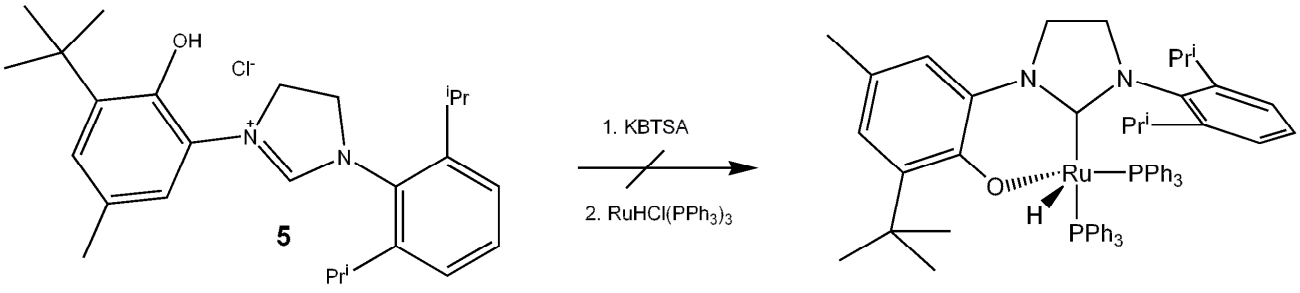

Figure 6.16: Free carbene of **5** *with* $RuHCl(PPh_3)_3$.

The wanted product from the reaction described in Figure 6.16 should contain both **5** as a ligand and a hydride. From the ^{1}H-NMR the reaction mixture did not contain any new hydride species in significant concentrations and the reaction was therefore concluded as a failure.

It was also tried to transmetalate **6** with **7**. The reaction was assumed to be the most promising approach to make a Grubbs type catalyst with this **5** since the reaction is mild and has a entropic drivingforce; the formation of AgCl.

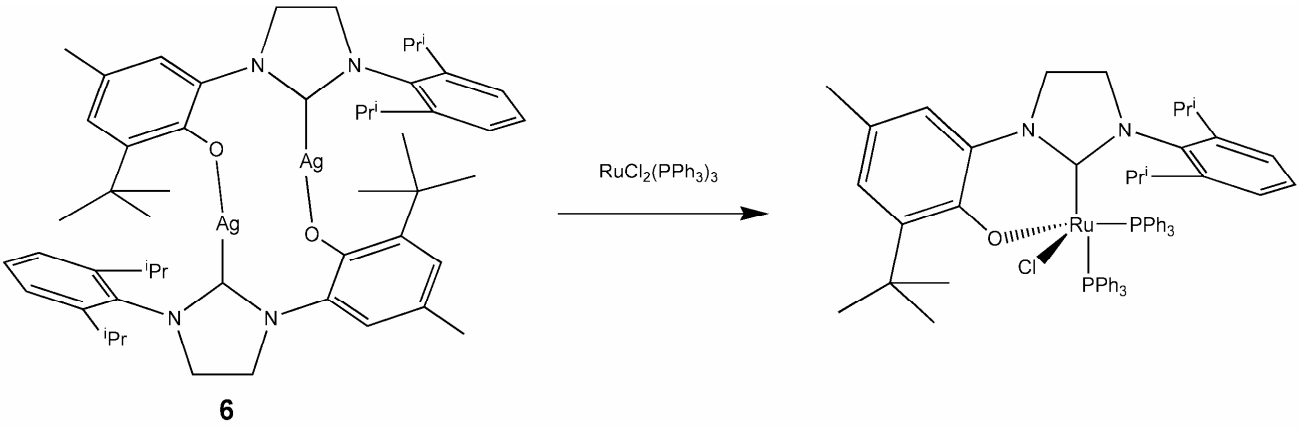

Figure 6.17: Transmetalation of **6** *with* **7**.

The reaction described in Figure 6.17 was repeated several times under different conditions to try to isolate a ruthenium complex with the ligand. The first attempt was done in a small scale in toluene, 2 hours at 50°C. According to ^{31}P-NMR, the reaction gave a new complex; at least there were some new phosphine peaks at 61.3 ppm and 54.1 ppm. By the ^{31}P-NMR of this reaction mixture one could conclude that a new complex had been synthesized. Therefore the reaction was repeated in a larger scale to try to isolate this new complex. The reaction was done at 40°C for 16 hours. ^{31}P-NMR of this reaction mixture showed the same peaks as the small scale reaction, but it proved difficult to

obtain a pure product and the product was unstable in silica as well as air sensitive. The product mixture was cooled on liquid nitrogen with different solvents and solvents mixtures to try to separate some of the compounds, but neither this approach was successful.

The reaction was also done in THF in the presence of AgCl as a phosphine scavenger at 50°C for 4 hours. From this reaction as well it turned out impossible to obtain a pure product. The general impression from several ^{1}H-NMR was that the silver complex never reacted and therefore **5** was not bound to the Ru-metal centre. The conclusion is based on all the peaks from originating from the NHC-phenoxy ligand, which were always consistent with the starting material; **6**. This means that the new peaks found in ^{31}P-NMR were probably due to some decomposition of **7.**

When this reaction was concluded as a failure we decided to try to introduce the ligand to **8** [(η^6-*p*-cymene)$RuCl_2]_2$**.**

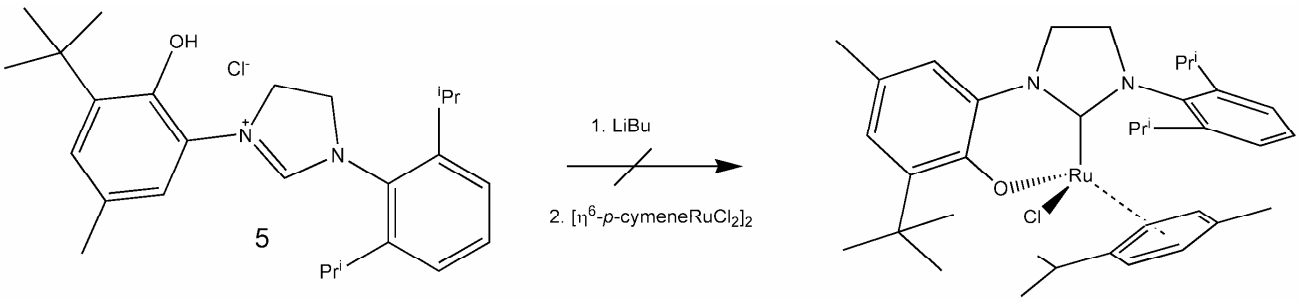

Figure 6.18: **5** *with* ***8***.

The reaction shown in Figure 6.18 did not yield any Ru-complex bearing the NHC-phenoxy ligand. The ^{1}H-NMR showed that the dimer; [(η^6-*p*-cymene)$RuCl_2]_2$; was not even broken.

6.1.3 Iridium complex with the chelating NHC-phenoxy

The experiments described earlier in this chapter showed that it was very difficult to introduce **5** to a ruthenium complex. Therefore the wanted catalytic activity was out of reach. We wanted to investigate if the ligand could be used in another type of complex for a different catalytic application.

Ligands similar to **5** have previously been reported in palladium(II) [186] and nickel(II)[190] complexes, and quite recently in one iridium(I) complex.[205] These complexes are square planar. Similar ligands have been reported in silver complexes,[183] and we have also made a silver complex which we were unable to characterize by X-ray diffraction. The iridium complex has a ligand which is more different to **5**, compared to the ligand in the palladium and nickel complexes. The iridium complex was in fact easy to synthesize. The complex can in addition have some interesting catalytic applications like hydrogenation of alkenes.[205] The starting material $[IrClCOD]_2$ was made by a small adjustment of the method described at in Inorganic syntheses.[206] The adjustment was due to a different starting material.

The complex was made by a adjusted version of the procedure described by Bercaw and co-workers.[205] This reaction is shown on Figure 6.19.

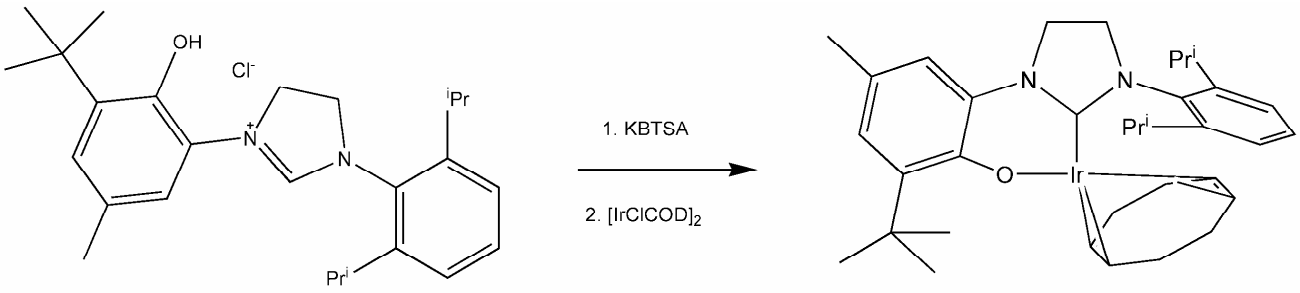

Figure 6.19: Synthesis of IrCOD-(3-(3-tert-butyl-5-methyl-phen-2-olate)-1-(2,6-diisoproylphenyl)-imidazol-2-ylidene).

The precursor $[IrClCOD]_2$ was strongly orange in THF, and when mixed with the free carbene on ice it turned darkly red after an hour. After filtration over celite it was tried to dissolve the crude product in hexane. The product was slightly soluble in hexane and therefore the corresponding red solution was put in the freezer to yield tiny red/pink crystals with a good enough quality to be analysed by X-ray diffraction. The ^{1}H-NMR and ^{13}C-NMR also confirmed a successful reaction.

6.2 Results and discussion

The ligand synthesis was difficult but proved to be successful in the end. The integrity of the ligand was confirmed by X-ray diffraction. The X-ray structure of **5** is shown in Figure 6.20. Two solvent molecules (fluorobenzene) have been removed and hydrogens are not shown for clarity. Carbons are grey centroids, nitrogens blue, oxygens red, and chlorines as green. Centroids are drawn with a 50% probability level.

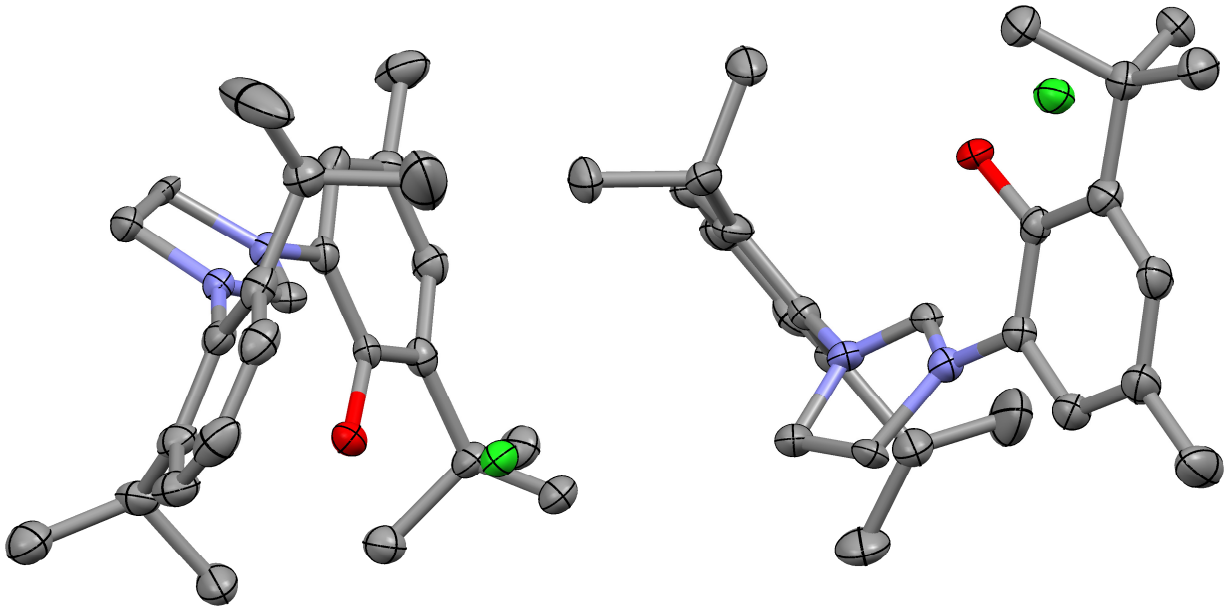

Figure 6.20: Crystal structure of **5.**

Of Figure 6.20 we can see that the crystal contains two conformers of **5** and in addition it contains two molecules of fluorobenzene which has been removed.

The first aim was to introduce the NHC-ligand to a Grubbs type catalyst. After 15 attempts we concluded that this was more or less impossible to do. At that stage it was decided to go for a complex with ruthenium which also turned out to be difficult.

When we started this project we knew that similar ligands was known in square-planar palladium complexes with no reported catalytic activity,[186] a square planar nickel(II) complex[190] which is under

a patent,[207] and that similar silver complexes had been synthesized and successfully characterized.[183,185] The ligand we made is one of the most sterically hindered bidentate NHC ligand made and therefore might have been among the most sterically hindered NHC-ligand used in olefin metathesis if it been successfully complexated. Quite recently D. R. Weinberg et al. reported an iridium(I) complex with another six-membered bidentate NHC ligand. By oxidizing their Ir(I) complex to a Ir(III) they obtained a complex showing catalytic activity in hydrogenation of cyclohexene.[205]

The precursor $[IrClCOD]_2$ is also known to have catalytic activity: ring-opening reactions of *N*-Boc-azabenzonorbornadiene with secondary amine nucleophiles,[208] reductive coupling reaction of secondary amines, aldehydes, and alkynes.

The reaction between the NHC-phenoxy ligand and $[IrClCOD]_2$ was successfully performed. The crystal structure of the complex is shown in Figure 6.21, where the white are hydrogen, grey carbon, blue nitrogen, red oxygen and pink iridium.

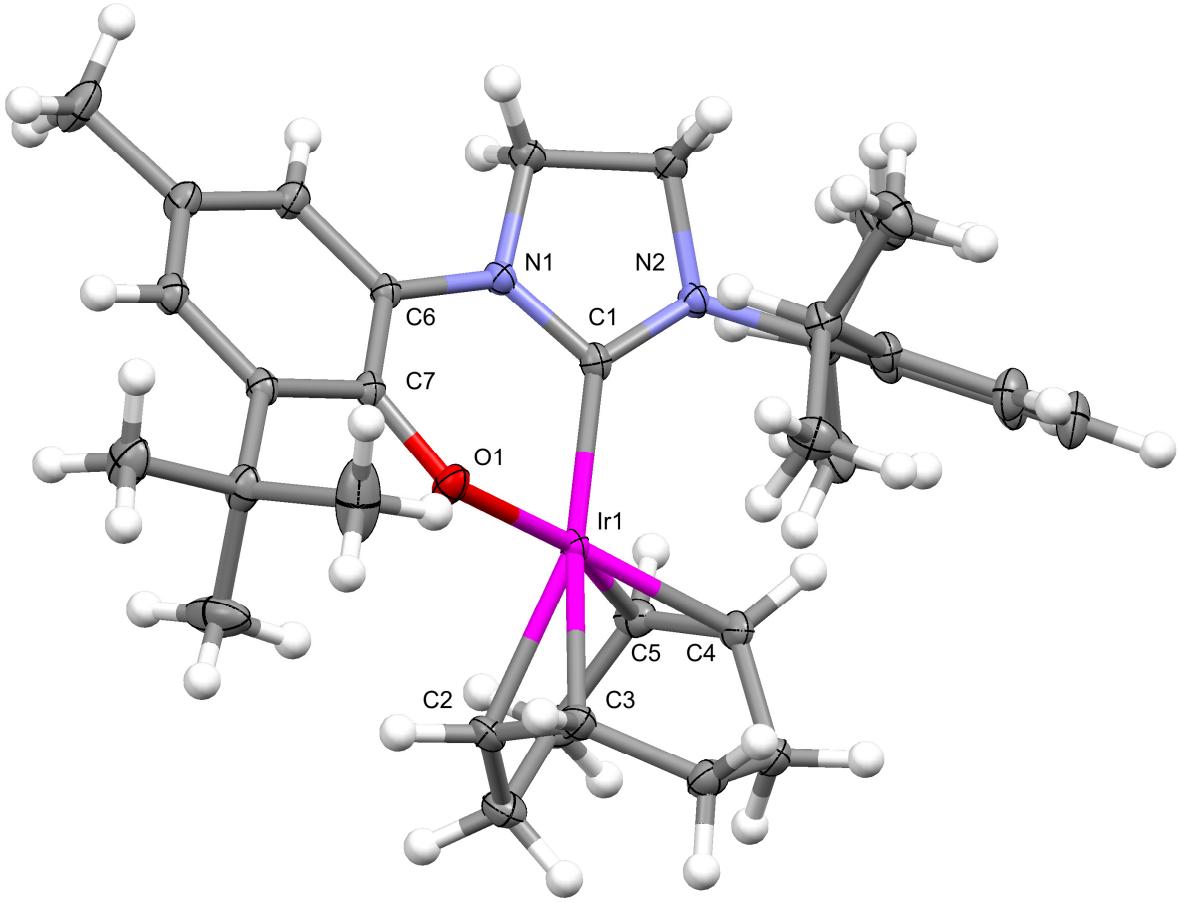

Figure 6.21: X-ray result from analysis of IrCOD-(3-(3-tert-butyl-5-methyl-phen-2-olate)-1-(2,6-diisoproylphenyl)-4,5-dihydroimidazol-2-ylidene); ***9****.*

The structure of the Ir(I) complex synthesized by Bercaw and co-workers is shown with complex **9** in Figure 6.22.[205] The potassium cation in **10** is in the crystal structure complexated by an 18-crown-6-ether. The 18-crown-6 ether is omitted for clarity in Figure 6.22. In Table 6.2 some bond lengths, angles and a torsion of **9** and **10** are compared.

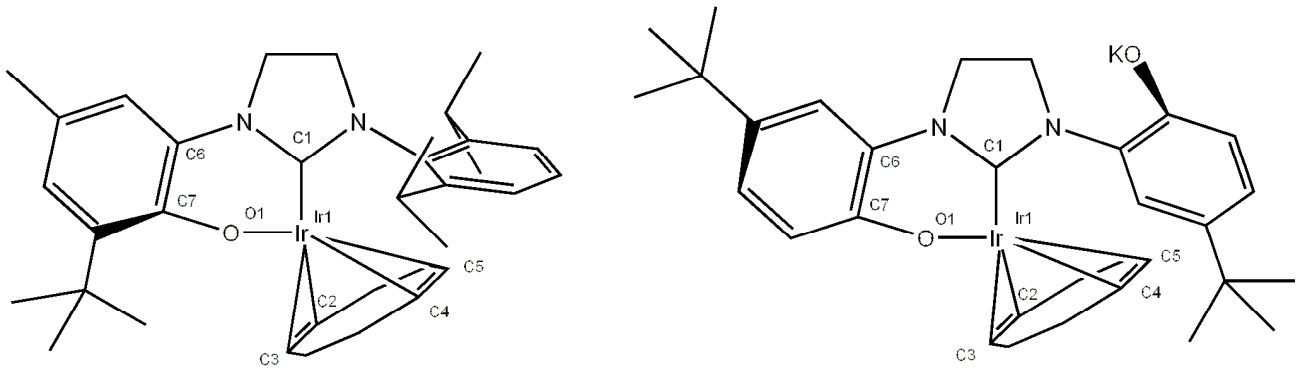

9 **10**

Figure 6.22: Comparison **9** *reported complex* **10**[205].

The most striking difference when comparing **9** and **10** is the orientation of the chelate ring in space. In Figure 6.21 we can see that the chelate ring is bending out of the plane, but in complex **10** it is bending into the plane. This is difference is shown by the torsional angle between C5-O1-Ir1-C1 which has a difference of almost most 80°. Some distances and angles of **9** and **10** are compared in Table 6.2.

Table 6.2: Comparison of complex **9** *and* **10**.

	Atoms	**Complex 9**	**Complex 10**[205]
Bonds(Å)	Ir1-C1	2.023	2.041
	Ir1-O1	2.019	2.042
	Ir1-C2	2.198	2.174
	Ir1-C3	2.179	2.159
	Ir1-C4	2.131	2.093
	Ir1-C5	2.101	2.145
	C2-C3	1.395	1.397
	C4-C5	1.427	1.418
Angles (°)	O1-Ir1-C1	87.07	87.57
	C1-Ir1-C2	157.96	164.28
	C1-Ir1-C3	163.01	156.84
	C1-Ir1-C4	101.89	93.29
	C1-Ir1-C5	94.96	100.69
Torsion(°)	C7-O1-Ir1-C1	**35.52**	**-42.31**

The big question in the end of this chapter is why would not the ligand bind to a ruthenium complex?
Catalysts **1** and **2** shown on Chart 6.1 have 8-membered NHC-phenoxy ruthenium chelates. An eight-membered rings have a sufficient flexibility to direct the NHC ring in the most sterically and electronically stable orientation,[144] namely with the plan of the imidazole ring approximately bisector of the Cl–Ru–O angle. On the contrary, a smaller ring (seven- or six-membered) will force an intrinsically less stable orientation of the NHC-ring providing so far unstable monosubstituted complexes.[137] **5** has some large steric moieties which was intended to interact with the alkylidene to stabilize the reactive conformer of the 14-electron active complex and the *tert*-butyl group that was intended to interact with the metallo-cylclobutane.

Most of the known second generation olefin metathesis catalysts have some similarities in their geometries. For example, the Cl-Ru-Cl angle usually around 170° and one would then expect the O-Ru-Cl angle to be similar. It is also usual that the plane of the imidazole ring lies perpendicularly above the ruthenium alkylidene bond. That means that the NHC-phenoxy chelate should bind to the metal centre in a really specific orientation. This can of course be problematic since there is a low

flexibility in its potential six-membered chelate, so probably it is impossible for the ligand to satisfy both these two geometrical specifications. In addition to this there are some sterical demanding groups that can hinder this specific orientation. It seems like the only possibility of using the NHC-phenoxy ligands with ruthenium based olefin metathesis catalysts is to use a larger ring as Hoveyda and co-workers.[62,183,184]

Two proposed isomers of our target complex **4** and of another hypothetical six-ring chelate complex **11** based on a less sterically demanding bidentate NHC ligand are shown in Figure 6.23. **4'** and **11'** have retained the condition with the angle between O-Ru-Cl at about 170° and **4''** and **11''**has retained the spatial orientation of the N–Ar moiety above the Ru=C bond.

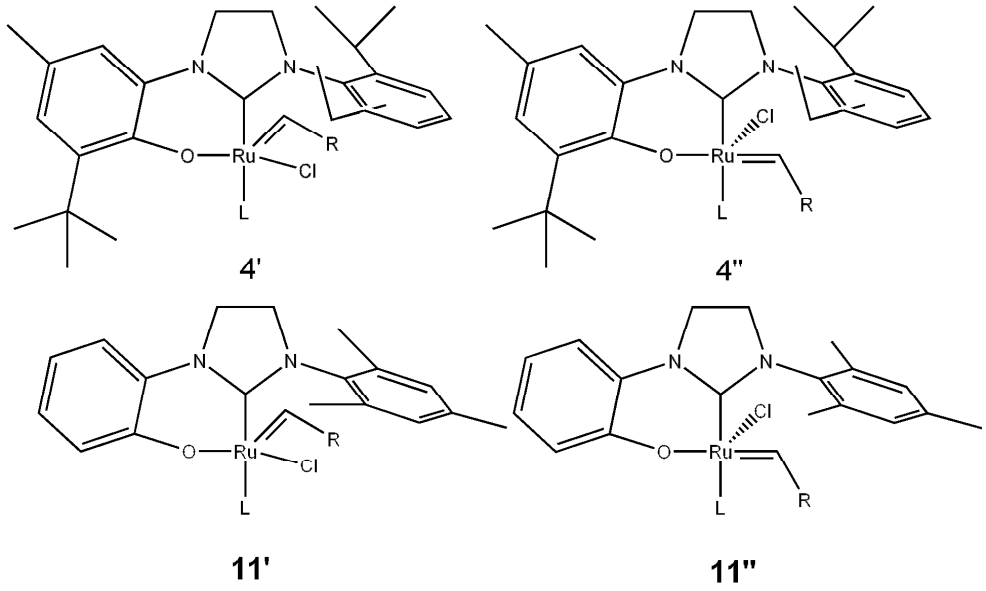

Figure 6.23: Structural conformations of **4** *and conformations with a simpler ligand* **11.**

One might wonder if it had been possible to complexate with a simpler NHC-phenoxy ligand with a potential six-ring chelate and form either **11'** or **11''**? A complex with a simple NHC-phenoxy chelate must probably also break these general geometry relations between the second generation ruthenium olefin metathesis catalysts. A potential problem with a less sterically hindered ligand can be that it in the same way as G. Occhipinti et al. could end up with a disubstituted inactive complex.[185] But these conformational challenges do not explain why the ligand could not bind to ruthenium in the simpler complexes. It might be that it is impossible to get such a ligand to bind to ruthenium in general.

Since the suggested complex **4** could not be formed and the fact that we were not able to synthesize a well defined ruthenium complex bearing the NHC-phenoxy ligand of **5**, the question might be raised if it is even possible to form such a six-ring NHC-phenoxy chelate with ruthenium in general. **11** has been made by Verpoort and co-workers who are working in the field olefin metathesis and reacted with **8** and fully characterized.[209]

Over the last eight years a lot of work has been focused on these NHC-phenoxy ligands. Hoveyda was the first who published his complexes with eight membered NHC-phenoxy chelating ligands.[62,184] Approximately two years after Hoveyda's first publication Grubbs published a series of complexes with six-membered NHC-phenoxy chelating ligands with palladium,[186] our group published some work with a seven-membered NHC-phenoxy ligand,[63] and Verpoort also published some work involving a six-membered NHC-phenoxy.[209] We also know that another significant group in the field has worked with such ligands and not been able to make a Grubbs type of catalyst bearing such a ligand. From all these results and including our last work described in this chapter it seems like such a design does not work for making a Grubbs type of catalyst. This is a bit disappointing since such ligands are very interesting from a stereoselectivity point of view.

It is only Hoveyda and co-workers who has been successful with their NHC-phenoxy forming an eight-membered chelate.[62,183,184] Such large chelates are not so interesting with regard of *Z*-stereoselectivity. This is due to their high flexibility which makes it harder to direct a sterical pressure on one of the faces of the metallo-cyclobutane intermediate. Large and advanced NHC-phenoxy ligands are very challenging to synthesize and very expensive to prepare, even the one in this work has been very time consuming and expensive. Probably if one was able to obtain a stereoselective catalyst with such a ligand it would have been too expensive to prepare that it would not have been of commercial interest.

6.3 Concluding remarks

During the search for a potential stereoselective Grubbs type of olefin metathesis catalyst we have synthesized and fully characterized a sterically demanding NHC-phenoxy ligand (**5**). We were not able to synthesize an olefin metathesis catalyst with the ligand, neither a ruthenium complex bearing the ligand. Such ligands are not suitable for these systems, both from our results and what is indirectly published in the literature by important scientist in the field as Verpoort and Grubbs. The synthesized NHC ligand is one of the most sterically demanding bi-dentate NHC-ligands made, and it was showed to be sterically demanding to form a six-membered chelate with ruthenium.

The ligand was able to coordinate to square planar complex of iridium(I) and similar ligands has been bound to square planar palladium(II)[186] and nickel(II) [190] complexes.

7 Conclusion and suggested further work

During the work involved with my master degree, I have synthesized and characterized two novel amine based olefin metathesis catalyst **A2** and **A3**. These catalysts together with **A1** (synthesized previously in the group[55]) have been studied theoretically by doing quantum chemical computations. Prior to studying the catalysts behaviour in the catalytic cycle by computations, a large benchmark was performed to find the most suited functional for geometry optimizations of amine based olefin metathesis catalysts. We found PBE to be the most suited functional for geometry optimizations of this class of catalyst. The results from the calculations correspond with the experimental results in a qualitative manner. The catalytic activity of **A1**, **A2** and **A3** have been tested. The results showed that the catalysts were labile catalyst with the following activity in decreasing order: **A3, A1** and **A2**. The stability of the catalysts was the opposite order: **A2, A1** and **A3**, which gives **A1** a higher turn over number (TON) than **A3**. Their catalytic activity is comparable with the activity of other labile catalysts with an imine decoordinating moiety. Five-membered chelates were found to be the most stabile for amine-carboxy ligands and the activity varied according to modifications of the chelate size and substitution of the amine. Three new potential catalysts with assumed higher activity; **A10**, **A13** and **A16**; are suggested for further analysis including both calculations and synthesis;

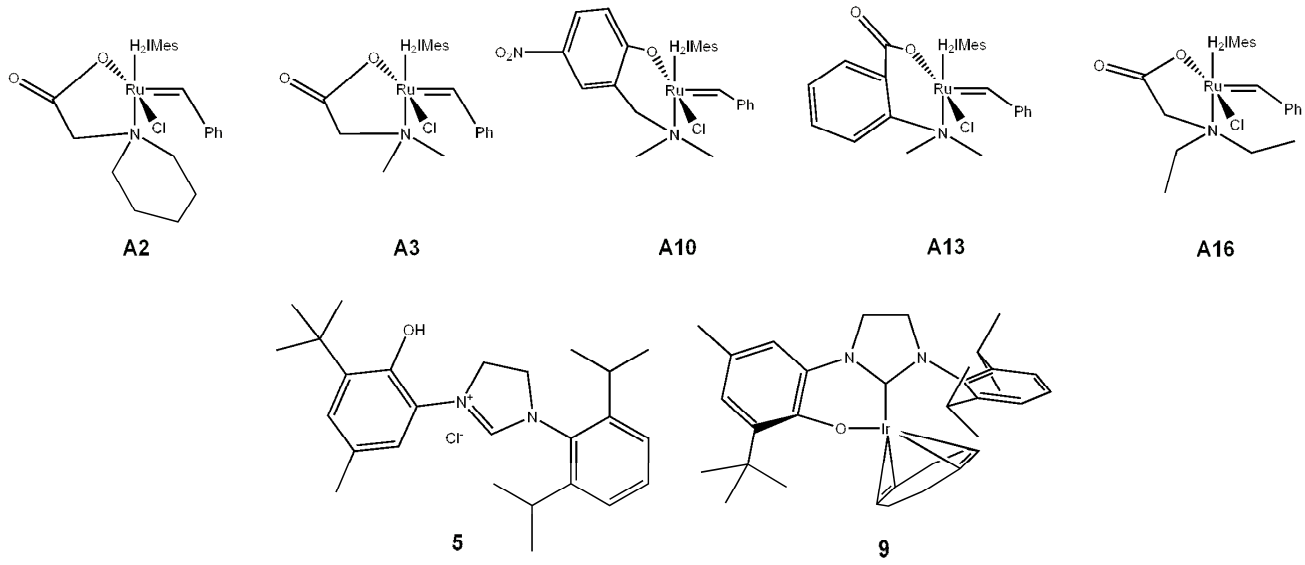

Figure 7.1: Main compounds in this work.

A novel six-mebered chelating NHC-phenoxy ligand precursor; the 4,5-dihydroimidzolium salt **5**; was successfully made and fully characterized. However, we were not able to use the ligand for a ruthenium based olefin metathesis catalyst or as a ligand for a ruthenium complex in general. We

managed to synthesize an iridium(I) complex (**9**). By oxidising the complex to an iridium(III) it might be able to catalyse hydrogenation of simple alkenes.

In the future, it might be productive to do further calculations on **A10**, **A13** and **A16** to see if they can show any interesting activities and differences compared to **A1-A3**. If so, they can easily be synthesized by existing procedures and by the inspirations of this work. When synthesized, I recommend that they undergo thorough testing together with **A1-A3** trying to locate any special and interesting application relevant to latent catalysts; perhaps even olefin metathesis activity in water. Olefin metathesis in water is one area which is getting a lot of attention at the moment.[210] If this testing shows some interesting results, a larger screening, like the one done in our group previously (quantitative structure-activity relationship),[44] should be considered. Further attempts to crystallize **A2** should be tried. In addition, some catalytic tests should a be done in C_6D_8 (d-toluene) to be more comparable with the calculations and the kinetic studies performed by Grubbs and co-workers.[149]

Another suggestion is to do a more detailed computational study of **A1-A3**, especially when it comes to model the first catalytic cycle, where the alkylidene is a benzylidene. It would be interesting to know the heights of the barriers in the first cycle, because these barriers might be higher than in the following catalytic.

As mentioned above the iridium(I) complex can be oxidised to an iridium(III) complex, and the complex might have some potential catalytic application. Perhaps one also should also consider a new attempt to complexate **5** with **8** by the procedure reported by Verpoort,[209] to exclude the possibility of the potential existence of such a ruthenium complex with the ligand.

There is also a large amount of data from the benchmark study with large potential for further analysis; 50 parameters per compound benchmarked for 8 functionals (approximately 6000 numbers!). It might be interesting to know how solvents in the crystal lattice are affecting such a benchmark, and to analyse functionals in more detail to discover their strengths and their weaknesses.

There is still a lot of interesting research left in this field, but my time is up for now. Good luck to you all!

8 List of references

(1) Truett, W. L.; Johnson, D. R.; Robinson, I. M.; Montague, B. A. *J. Am. Chem. Soc.* **1960**, *82*, 2337.
(2) Calderon, N.; Chen, H. Y.; Scott, K. W. *Tetrahedron Lett.* **1967**, 3327.
(3) Banks, R. L.; Bailey, G. C. *I&EC Product Research and Development* **1964**, *3*, 170.
(4) Grubbs, R. H. *Handbook of metathesis*; Wiley-VCH: Weinheim, 2003.
(5) Nobelprize.org *The Nobel Prize in Chemistry 2005*, Nobel Web AB. <http://nobelprize.org/nobel_prizes/chemistry/laureates/2005/> [per 23.3.2010]
(6) Herisson, J. L.; Chauvin, Y. *Makromol. Chem.* **1971**, *141*, 161.
(7) Chauvin, Y. *Angew. Chem. Int. Edn* **2006**, *45*, 3740.
(8) Wiberg, K. B. *Angew. Chem. Int. Ed. Engl.* **1986**, *25*, 312.
(9) Hoveyda, A. H.; Zhugralin, A. R. *Nature* **2007**, *450*, 243.
(10) Fürstner, A.; Ackermann, L.; Gabor, B.; Goddard, R.; Lehmann, C. W.; Mynott, R.; Stelzer, F.; Thiel, O. R. *Chem.-Eur. J.* **2001**, *7*, 3236.
(11) Thomas, R. M.; Grubbs, R. H. *Macromolecules* **2010**, *43*, 3705.
(12) Schrock, R. R. *Angew. Chem. Int. Edn* **2006**, *45*, 3748.
(13) Nguyen, S. T.; Johnson, L. K.; Grubbs, R. H.; Ziller, J. W. *J. Am. Chem. Soc.* **1992**, *114*, 3974.
(14) Schwab, P.; France, M. B.; Ziller, J. W.; Grubbs, R. H. *Angew. Chem. Int. Ed. Engl.* **1995**, *34*, 2039.
(15) Schwab, P.; Grubbs, R. H.; Ziller, J. W. *J. Am. Chem. Soc.* **1996**, *118*, 100.
(16) Grubbs, R. H. *Angew. Chem. Int. Edn* **2006**, *45*, 3760.
(17) Trnka, T. M.; Grubbs, R. H. *Acc. Chem. Res.* **2000**, *34*, 18.
(18) Scholl, M.; Ding, S.; Lee, C. W.; Grubbs, R. H. *Org. Lett.* **1999**, *1*, 953.
(19) Kingsbury, J. S.; Harrity, J. P. A.; Bonitatebus, P. J.; Hoveyda, A. H. *J. Am. Chem. Soc.* **1999**, *121*, 791.
(20) Garber, S. B.; Kingsbury, J. S.; Gray, B. L.; Hoveyda, A. H. *J. Am. Chem. Soc.* **2000**, *122*, 8168.
(21) Morrissey, S. R. *NIH director has steered agency through congressional inquiries and paltry budget increases with bold actions to position agency for future*, Chemical & Engineering News. <http://pubs.acs.org/cen/coverstory/84/8427zerhouni.html> [per 24.3.2010]
(22) Ege, S. N. *Organic chemistry: structure and reactivity*; Houghton Mifflin: Boston, 2004.
(23) Nicolaou, K. C.; Bulger, P. G.; Sarlah, D. *Angew. Chem. Int. Ed.* **2005**, *44*, 4490.
(24) Gradillas, A.; Perez-Castells, J. *Angew. Chem. Int. Ed.* **2006**, *45*, 8086.
(25) Hanessian, S.; Margarita, R.; Hall, A.; Johnstone, S.; Tremblay, M.; Parlanti, L. *Pure Appl. Chem.* **2003**, *75*, 209.
(26) Tanaka, K.; Itagaki, Y.; Satake, M.; Naoki, H.; Yasumoto, T.; Nakanishi, K.; Berova, N. *J. Am. Chem. Soc.* **2005**, *127*, 9561.
(27) Srihari, P.; Kumaraswamy, B.; Rao, G. M.; Yadav, J. S. *Tetrahedron-Asymmetry* **2010**, *21*, 106.
(28) Ghosh, S.; Rao, C. N. *Tetrahedron Lett.* **2010**, *51*, 2052.
(29) Marciniec, B. *Przem. Chem.* **2007**, *86*, 15.
(30) Deck, J. A.; Martin, S. F. *Org. Lett.* **2010**.
(31) Li, P.; Li, J.; Arikan, F.; Ahlbrecht, W.; Dieckmann, M.; Menche, D. *J. Org. Chem.* **2010**, *75*, 2429.
(32) Crimmins, M. T.; Shamszad, M.; Mattson, A. E. *Org. Lett.* **2010**.
(33) Nicolaou, K. C.; Xu, H. *Chem. Commun.* **2006**, 600.

(34) Cramer, C. J.; Truhlar, D. G. *Phys. Chem. Chem. Phys.* **2009**, *11*, 10757.
(35) Monsaert, S.; Lozano Vila, A.; Drozdzak, R.; Van Der Voort, P.; Verpoort, F. *Chem. Soc. Rev.* **2009**, *38*, 3360.
(36) Gessler, S.; Randl, S.; Blechert, S. *Tetrahedron Lett.* **2000**, *41*, 9973.
(37) Schrock, R. R.; Hoveyda, A. H. *Angew. Chem. Int. Edn* **2003**, *42*, 4592.
(38) Samojłowicz, C.; Bieniek, M.; Grela, K. *Chem. Rev.* **2009**, *109*, 3708.
(39) Straub, B. F. *Adv. Synth. Catal.* **2007**, *349*, 204.
(40) Correa, A.; Cavallo, L. *J. Am. Chem. Soc.* **2006**, *128*, 13352.
(41) Mathew, J.; Koga, N.; Suresh, C. H. *Organometallics* **2008**, *27*, 4666.
(42) Webster, C. E. *J. Am. Chem. Soc.* **2007**, *129*, 7490.
(43) Zhao, Y.; Truhlar, D. G. *Org. Lett.* **2007**, *9*, 1967.
(44) Occhipinti, G.; Bjørsvik, H.-R.; Jensen, V. R. *J. Am. Chem. Soc.* **2006**, *128*, 6952.
(45) Chung, C. K.; Grubbs, R. H. *Org. Lett.* **2008**, *10*, 2693.
(46) Kuhn, K. M.; Bourg, J.-B.; Chung, C. K.; Virgil, S. C.; Grubbs, R. H. *J. Am. Chem. Soc.* **2009**, *131*, 5313.
(47) Fournier, P.-A.; Collins, S. K. *Organometallics* **2007**, *26*, 2945.
(48) Vehlow, K.; Maechling, S.; Blechert, S. *Organometallics* **2006**, *25*, 25.
(49) Clark, P. G.; Guidry, E. N.; Chan, W. Y.; Steinmetz, W. E.; Grubbs, R. H. *J. Am. Chem. Soc.* **2010**, *132*, 3405.
(50) Lee, C. W.; Grubbs, R. H. *Org. Lett.* **2000**, *2*, 2145.
(51) Sattely, E. S.; Meek, S. J.; Malcolmson, S. J.; Schrock, R. R.; Hoveyda, A. H. *J. Am. Chem. Soc.* **2008**, *131*, 943.
(52) Fürstner, A.; Davies, P. W. *Chem. Commun.* **2005**, 2307.
(53) Fürstner, A.; Seidel, G. *J. Organomet. Chem.* **2000**, *606*, 75.
(54) Jiang, A. J.; Zhao, Y.; Schrock, R. R.; Hoveyda, A. H. *J. Am. Chem. Soc.* **2009**, *131*, 16630.
(55) Occhipinti, G.; Bjørsvik, H.-R.; Törnroos, K. W.; Jensen, V. R. *Unpublished material* **2010**.
(56) Occhipinti, G.; Bjørsvik, H.-R.; Törnroos, K. W.; Jensen, V. R. *Organometallics* **2007**, *26*, 5803.
(57) Samec, S. M.; Grubbs, R. H. *Chem. Commun.* **2007**, 2826.
(58) Samec, J. S.; Grubbs, R. H. *Chem.-Eur. J.* **2008**, *14*, 2686.
(59) Allaert, B.; Dieltiens, N.; Ledoux, N.; Vercaemst, C.; Van der Voort, P.; Stevens, C. V.; Linden, A.; Verpoort, F. *J. Mol. Catal. A-Chem.* **2006**, *260*, 221.
(60) De Clercq, B.; Verpoort, F. *Adv. Synth. Catal.* **2002**, *344*, 639.
(61) Strem Chemicals, I. *Strem Chemicals*, <http://www.strem.com/> [per 15.5.2010]
(62) Van Veldhuizen, J. J.; Garber, S. B.; Kingsbury, J. S.; Hoveyda, A. H. *J. Am. Chem. Soc.* **2002**, *124*, 4954.
(63) Occhipinti, G.; Bjørsvik, H.-R.; Törnroos, K. W.; Fürstner, A.; Jensen, V. R. *Organometallics* **2007**, *26*, 4383.
(64) Friebolin, H. *Basic One- and Two-Dimensional NMR Spectroscopy*; Wiley-VCH Verlag GmbH & Co. KGaA: Weinheim, 2005.
(65) Kühl, O. *Phosphorus-31 NMR Spectroscopy*; Springer-Verlag: Berlin Heidelberg, 2008.
(66) Keeler, J. *Understanding NMR Spectroscopy*; John Wiley & Sons Ltd: Chichester, 2005.
(67) Donald, L. P.; Gary, M. L.; Kriz, G. S. *INTRODUCTION TO SPECTROSCOPY*; 3 ed.; Thomson Learning, Inc.: Bellingham, 2001.
(68) Harris, R. K.; Becker, E. D.; Menezes, S. M. C. d.; Goodfellow, R.; Granger, P. *Magn. Reson. Chem.* **2002**, *40*, 489.
(69) CambridgeSoft; *Chemdraw Ultra 9.0*. 2005
(70) Holmes, D. *Basic NMR Concepts:*
A Guide for the Modern Laboratory, Michigan State University, 2007.
(71) Cookson, D. J.; Smith, B. E. *Anal. Chem.* **1982**, *54*, 2591.

(72) Evilia, R. F. *Anal. Lett.* **2001**, *34*, 2227
(73) Crabtree, R. H. *THE ORGANOMETALLIC CHEMISTRY OF THE TRANSITION METALS*; 4 ed.; John Wiley & Sons, Inc.: Hoboken, New Jersey, 2005.
(74) Gottlieb, H. E.; Kotlyar, V.; Nudelman, A. *J. Org. Chem.* **1997**, *62*, 7512.
(75) Harris, R. K.; Becker, E. D.; De Menezes, S. M. C.; Granger, P.; Hoffman, R. E.; Zilm, K. W. *Magn. Reson. Chem.* **2008**, *46*, 582.
(76) Cullity, B. D. *ELEMENTS OF X-RAY DIFFRACTION*; Addison-Wesley Publishing Company, Inc.: Reading, Massachusetts, 1956.
(77) Laue, M. V. *Nobel Lectures, Physics 1914* **1915**.
(78) Olsen, E. D. *Modern Optical Methods of Analysis*; McGraw-Hill, Inc.: London, 1975.
(79) Massa, W. *Crystall Structure Determination*; Springer Verlag: Berlin Heidelberg, 2004.
(80) Greibrokk, T.; Lundanes, E.; Rasmussen, K. E. *Kromatografi - Separasjon og deteksjon*; Universitetsforlaget: Oslo, 1984.
(81) Harris, D. C. *Quantitative Chemical Analysis*; W.H. Freeman and Company: New York, 2007.
(82) Leonard, J.; Lygo, B.; Procter, G. *Advanced Pratical Organic Chemistry*; Taylor and Francis Group: New York, 1998.
(83) Furniss, B. S.; Hannaford, A. J.; Smith, P. W. G.; Tatchell, A. R. *Vogel's Textbook of Practical Organic Chemistry*; 5 ed.; Longman Group UK Limited: London, 1989.
(84) Ziegler, T.; Autschbach, J. *Chem. Rev.* **2005**, *105*, 2695.
(85) Nobelprize.org *The Nobel Prize in Physics 1933*, Nobel Web AB. <http://nobelprize.org/nobel_prizes/physics/laureates/1933/schrodinger-bio.html> [per 29.4.2010]
(86) Levine, I. N. *Quantum Chemistry*; Prentince Hall: New Yersey, 2000.
(87) Koch, W.; Holthausen, M. C. *A Chemist's Guide to Density Functional Theory*; 2 ed.; Wiley-VCH Verlag: Weinheim, 2001.
(88) Cramer, C. J. *Essentials of Computational Chemistry*; 2 ed.; John Wiley & Sons, Ltd: Chichester, 2004.
(89) Hohenberg, P.; Kohn, W. *Phys. Rev.* **1964**, *136*, B864.
(90) Kohn, W.; Sham, L. J. *Phys. Rev.* **1965**, *140*, A1133.
(91) Kohn, W.; Becke, A. D.; Parr, R. G. *J. Phys. Chem.* **1996**, *100*, 12974.
(92) Contributors, W. *Jacob's ladder*, Wikipedia, The Free Encyclopedia. <http://en.wikipedia.org/w/index.php?title=Jacob%27s_Ladder&oldid=358417740> [per 6.5.2010]
(93) Perdew, J. P. *Phys. Rev. B* **1986**, *33*, 8822.
(94) Lee, C.; Yang, W.; Parr, R. G. *Phys. Rev. B* **1988**, *37*, 785.
(95) Perdew, J. P.; Burke, K.; Ernzerhof, M. *Phys. Rev. Lett.* **1996**, *77*, 3865.
(96) Tao, J.; Perdew, J. P.; Staroverov, V. N.; Scuseria, G. E. *Phys. Rev. Lett.* **2003**, *91*, 146401.
(97) Becke, A. D. *J. Chem. Phys.* **1993**, *98*, 5648.
(98) Zhao, Y.; Truhlar, D. G. *J. Chem. Theor. Comput.* **2005**, *1*, 415.
(99) Zhao , Y.; Truhlar, D. G. *J. Chem. Phys.* **2006**, *125*, 194101.
(100) Zhao, Y.; Truhlar, D. *Theor. Chim. Acta* **2008**, *120*, 215.
(101) Notur *Notur Programe*, <http://www.notur.no/> [per 30.5.2010]
(102) Zhurko, G. A. <http://www.chemcraftprog.com> [per 27.3.2010]
(103) Frisch, M. J. T., G. W.; Schlegel, H. B.; Scuseria, G. E.; Robb, M. A.; Cheeseman, J. R.; Scalmani, G.; Barone, V.; Mennucci, B.; Petersson, G. A.; Nakatsuji, H.; Caricato, M.; Li, X.; Hratchian, H. P.; Izmaylov, A. F.; Bloino, J.; Zheng, G.; Sonnenberg, J. L.; Hada, M.; Ehara, M.; Toyota, K.; Fukuda, R.; Hasegawa, J.; Ishida, M.; Nakajima, T.; Honda, Y.; Kitao, O.; Nakai, H.; Vreven, T.; Montgomery, Jr., J. A.; Peralta, J. E.; Ogliaro, F.; Bearpark, M.; Heyd, J. J.; Brothers, E.; Kudin, K. N.; Staroverov, V. N.; Kobayashi, R.; Normand, J.;

Raghavachari, K.; Rendell, A.; Burant, J. C.; Iyengar, S. S.; Tomasi, J.; Cossi, M.; Rega, N.; Millam, N. J.; Klene, M.; Knox, J. E.; Cross, J. B.; Bakken, V.; Adamo, C.; Jaramillo, J.; Gomperts, R.; Stratmann, R. E.; Yazyev, O.; Austin, A. J.; Cammi, R.; Pomelli, C.; Ochterski, J. W.; Martin, R. L.; Morokuma, K.; Zakrzewski, V. G.; Voth, G. A.; Salvador, P.; Dannenberg, J. J.; Dapprich, S.; Daniels, A. D.; Farkas, Ö.; Foresman, J. B.; Ortiz, J. V.; Cioslowski, J.; Fox, D. J. ; *Gaussian 09, Revision A.1, Gaussian, Inc.* 2009

(104) Bylaska, E. J. J., W. A. d.; Govind, N.; Kowalski, K.; Straatsma, T. P.; Valiev, M.; Wang, D.; Apra, E.; Windus, T. L.; Hammond, J.; Nichols, P.; Hirata, S.; Hackler, M. T.; Zhao, Y.; Fan, P.-D.; Harrison, R. J.; Dupuis, M.; Smith, D. M. A.; Nieplocha, J.; Tipparaju, V.; Krishnan, M.; Wu, Q.; Voorhis, T. V.; Auer, A. A.; Nooijen, M.; Brown, E.; Cisneros, G.; Fann, G. I.; Fruchtl, H.; Garza, J.; Hirao, K.; Kendall, R.; Nichols, J. A.; Tsemekhman, K.; Wolinski, K.; Anchell, J.; Bernholdt, D.; Borowski, P.; Clark, T.; Clerc, D.; Dachsel, H.; Deegan, M.; Dyall, K.; Elwood, D.; Glendening, E.; Gutowski, M.; Hess, A.; Jaffe, J.; Johnson, B.; Ju, J.; Kobayashi, R.; Kutteh, R.; Lin, Z.; Littlefield, R.; Long, X.; Meng, B.; Nakajima, T.; Niu, S.; Pollack, L.; Rosing, M.; Sandrone, G.; Stave, M.; Taylor, H.; Thomas, G.; Lenthe, J. v.; Wong, A.; Zhang, Z.; *NWChem Version 5.1 ed.; Pacific Northwest National Laboratory: Richland, Washington,*. 2007

(105) Summerfield, M. *Programming in Python 3: A complete introduction to the Python Language*; 2 ed.; Addison-Wesley Professional, 2009.

(106) Calhorda, M. J.; Pregosin, P. S.; Veiros, L. F. *J. Chem. Theor. Comput.* **2007**, *3*, 665.

(107) Karttunen, V. A.; Linnolahti, M.; Pakkanen, T. A.; Maaranen, J.; Pitkanen, P. *Theor. Chem. Acct.* **2007**, *118*, 899.

(108) Stewart, I. C.; Benitez, D.; O'Leary, D. J.; Tkatchouk, E.; Day, M. W.; Goddard, W. A.; Grubbs, R. H. *J. Am. Chem. Soc.* **2009**, *131*, 1931.

(109) Schneider, N.; Finger, M.; Haferkemper, C.; Bellemin-Laponnaz, S.; Hofmann, P.; Gade, L. H. *Chem.-Eur. J.* **2009**, *15*, 11515.

(110) Huang, H. S.; Zhang, T. L.; Zhang, J. G.; Wang, L. Q. *Chem. Phys. Lett.* **2010**, *487*, 200.

(111) Machura, B.; Jaworska, M.; Kruszynski, R. *Polyhedron* **2004**, *23*, 1819.

(112) Machura, B.; Jaworska, M.; Kruszynski, R. *Polyhedron* **2004**, *23*, 2005.

(113) Sieffert, N.; Buhl, M. *Inorg. Chem.* **2009**, *48*, 4622.

(114) Rydberg, P.; Olsen, L. *J. Phys. Chem. A* **2009**, *113*, 11949.

(115) Barbasiewicz, M.; Bieniek, M.; Michrowska, A.; Szadkowska, A.; Makal, A.; Wozniak, K.; Grela, K. *Adv. Synth. Catal.* **2007**, *349*, 193.

(116) Trnka, T. M.; Dias, E. L.; Day, M. W.; Grubbs, R. H. *Arkivoc* **2002**, 28.

(117) Lehman, S. E.; Wagener, K. B. *Organometallics* **2005**, *24*, 1477.

(118) Slugovc, C.; Burtscher, D.; Stelzer, F.; Mereiter, K. *Organometallics* **2005**, *24*, 2255.

(119) Ledoux, N.; Linden, A.; Allaert, B.; Mierde, H. V.; Verpoort, F. *Adv. Synth. Catal.* **2007**, *349*, 1692.

(120) Barbasiewicz, M.; Szadkowska, A.; Bujok, R.; Grela, K. *Organometallics* **2006**, *25*, 3599.

(121) Day, M. W.; Love, J. A.; Grubbs, R. H. *Private communication* **2005**.

(122) Boydston, A. J.; Xia, Y.; Kornfield, J. A.; Gorodetskaya, I. A.; Grubbs, R. H. *J. Am. Chem. Soc.* **2008**, *130*, 12775.

(123) Slugovc, C.; Perner, B.; Stelzer, F.; Mereiter, K. *Organometallics* **2004**, *23*, 3622.

(124) Fürstner, A.; Thiel, O. R.; Lehmann, C. W. *Organometallics* **2002**, *21*, 331.

(125) Lindner, E.; Geprags, M.; Gierling, K.; Fawzi, R.; Steimann, M. *Inorg. Chem.* **1995**, *34*, 6106.

(126) Adlhart, C.; Chen, P. *Angew. Chem. Int. Ed.* **2002**, *41*, 4484.

(127) Perdew, J. P.; Burke, K.; Ernzerhof, M. *Phys. Rev. Lett.* **1997**, *78*, 1396.

(128) Grimme, S. *J. Comput. Chem.* **2006**, *27*, 1787.

(129) Chai, J.-D.; Head-Gordon, M. *Phys. Chem. Chem. Phys.* **2008**, *10*, 6615.

(130) Heisterberg, D. J. *unpublished results* **1990**.
(131) Minenkov, Y.; *final_geometry_12.py*. 2010
(132) *Gaussian 09 User's Reference*, Gaussian Inc. <http://www.gaussian.com/g_tech/g_ur/k_integral.htm> [per 23.5.2010]
(133) Johnson, E. R.; Becke, A. D.; Sherrill, C. D.; DiLabio, G. A. *J. Chem. Phys.* **2009**, *131*, 034111.
(134) Minenkov, Y. *This project has been carried out together by me (Å. Singstad) and PhD. student Y.Minenkov. Under his guidance I have, myself, performed all the quantum chemical calculations. Y. Minenkov provided me with a number of valuable scripts and programs for efficient analysis and statistical treatment of the results, but again, the actual results have been obtained, treated and systemized by me. The figures in this section (Section 3.1.3) are made by Y. Minenkov unless otherwise stated. These figures have primarily been prepared for a joint publication based on the material contained in this chapter. Y. Minenkov has also written most of the computational details, also mainly prepared for this upcoming joint publication.* , UiB, 2010.
(135) Stallo *Supercomputer at University of Tromsø* Tromsø, 2007.
(136) Notur *Stallo*, <http://www.notur.no/hardware/stallo/> [per 27.5.2010]
(137) Straub, B. F. *Angew. Chem. Int. Ed.* **2005**, *44*, 5974.
(138) Truhlar, D. G.; Garrett, B. C.; Klippenstein, S. J. *J. Phys. Chem.* **1996**, *100*, 12771.
(139) Torker, S.; Merki, D.; Chen, P. *J. Am. Chem. Soc.* **2008**, *130*, 4808.
(140) Zhao, Y.; Truhlar, D. G. *J. Chem. Theor. Comput.* **2009**, *5*, 324.
(141) Yang, K.; Zheng, J. J.; Zhao, Y.; Truhlar, D. G. *J. Chem. Phys.* **2010**, *132*.
(142) Frisch, M. J. T., G. W.; Schlegel, H. B.; Scuseria, G. E.; Robb, M. A.; Cheeseman, J. R.; Montgomery, Jr., J. A.; Vreven, T.; Kudin, K. N.; Burant, J. C.; Millam, J. M.; Iyengar, S. S.; Tomasi, J.; Barone, V.; Mennucci, B.; Cossi, M.; Scalmani, G.; Rega, N.; Petersson, G. A.; Nakatsuji, H.; Hada, M.; Ehara, M.; Toyota, K.; Fukuda, R.; Hasegawa, J.; Ishida, M.; Nakajima, T.; Honda, Y.; Kitao, O.; Nakai, H.; Klene, M.; Li, X.; Knox, J. E.; Hratchian, H. P.; Cross, J. B.; Bakken, V.; Adamo, C.; Jaramillo, J.; Gomperts, R.; Stratmann, R. E.; Yazyev, O.; Austin, A. J.; Cammi, R.; Pomelli, C.; Ochterski, J. W.; Ayala, P. Y.; Morokuma, K.; Voth, G. A.; Salvador, P.; Dannenberg, J. J.; Zakrzewski, V. G.; Dapprich, S.; Daniels, A. D.; Strain, M. C.; Farkas, O.; Malick, D. K.; Rabuck, A. D.; Raghavachari, K.; Foresman, J. B.; Ortiz, J. V.; Cui, Q.; Baboul, A. G.; Clifford, S.; Cioslowski, J.; Stefanov, B. B.; Liu, G.; Liashenko, A.; Piskorz, P.; Komaromi, I.; Martin, R. L.; Fox, D. J.; Keith, T.; Al-Laham, M. A.; Peng, C. Y.; Nanayakkara, A.; Challacombe, M.; Gill, P. M. W.; Johnson, B.; Chen, W.; Wong, M. W.; Gonzalez, C.; and Pople, J. A; *Gaussian 03, Revision C.02, .; Gaussian, Inc., Wallingford CT*. 2004
(143) Aldhart, C.; Chen, P. *J. Am. Chem. Soc.* **2004**, *126*, 3496.
(144) Tsipis, A. C.; Orpen, A. G.; Harvey, J. N. *Dalton Trans.* **2005**, 2849.
(145) Tomasi, J.; Persico, M. *Chem. Rev.* **1994**, *94*, 2027.
(146) Cossi, M.; Scalmani, G.; Rega, N.; Barone, V. *J. Chem. Phys.* **2002**, *117*, 43.
(147) Tomasi, J.; Mennucci, B.; Cammi, R. *Chem. Rev.* **2005**, *105*, 2999.
(148) Woo, T. K.; Blochl, P. E.; Ziegler, T. *J. Phys. Chem. A* **1999**, *104*, 121.
(149) Sanford, M. S.; Love, J. A.; Grubbs, R. H. *J. Am. Chem. Soc.* **2001**, *123*, 6543.
(150) Laine, A.; Linnolahti, M.; Pakkanen, T. A.; Severn, J. R.; Kokko, E.; Pakkanen, A. *Organometallics* **2010**, *29*, 1541.
(151) Mellum, E. *Friedel*, <http://friedel.no/> [per 13.5.2010]
(152) ASA, Y. I. *Yara*, <http://www.yara.no/> [per 13.5.2010]
(153) International, V. *VWR*, <http://no.vwr.com/app/Home> [per 13.5.2010]
(154) Normag *NORMAG Labor- und Prozesstechnik*, <http://www.laboratory-glassware.com/> [per 13.5.2010]

(155) Shriver, D. F.; Drezdzon, M. A. *The Manipulation of Air-Sensitive Compounds*; John Wiley & Sons, Inc.: New York, 1986.
(156) Stefan, B.; Siegmar, B. *200 and more NMR Experiments*; WILEY-VCH Verlag GmbH & Co. KgaA: Weinheim, 2004.
(157) Sigma-Aldrich. *Sigma*, <http://www.sigmaaldrich.com/norway.html> [per 13.5.2010]
(158) Chang, S.; Jones, L.; Wang, C.; Henling, L. M.; Grubbs, R. H. *Organometallics* **1998**, *17*, 3460.
(159) De Clercq, B.; Verpoort, F. *Tetrahedron Lett.* **2002**, *43*, 9101.
(160) Clercq, B. D.; Verpoort, F. *J. Organomet. Chem.* **2003**, *672*, 11.
(161) Drozdzak, R.; Allaert, B.; Ledoux, N.; Dragutan, I.; Dragutan, V.; Verpoort, F. *Adv. Synth. Catal.* **2005**, *347*, 1721.
(162) Drozdzak, R.; Ledoux, N.; Allaert, B.; Dragutan, I.; Dragutan, V.; Verpoort, F. *Cent. Eur. J. Chem.* **2005**, *3*, 404.
(163) Drozdzak, R.; Allaert, B.; Ledoux, N.; Dragutan, I.; Dragutan, V.; Verpoort, F. *Coord. Chem. Rev.* **2005**, *249*, 3055.
(164) Ding, F.; Sun, Y.; Monsaert, S.; Drozdzak, R.; Dragutan, I.; Dragutan, V.; Verpoort, F. *Curr. Org. Synth.* **2008**, *5*, 291.
(165) IUPAC *Compendium of Chemical Terminology compiled by A. D. McNaught and A. Wilkinson*; 2 ed.; Blackwell Scientific Publications, 1997.
(166) Housecroft, C. E.; Sharpe, A. G. *Inorganic chemistry*; Pearson/Prentice Hall: Harlow, 2005.
(167) Pearson, R. R.; Songstad, J. *J. Am. Chem. Soc.* **1967**, *89*, 1827.
(168) Wang, H.; Li, Y.; Sun, F.; Feng, Y.; Jin, K.; Wang, X. *J. Org. Chem.* **2008**, *73*, 8639.
(169) Lai, M. Y. H.; Brimble, M. A.; Callis, D. J.; Harris, P. W. R.; Levi, M. S.; Sieg, F. *Bioorg. Med. Chem.* **2005**, *13*, 533.
(170) Bernhard, P.; Sargeson, A. M. *J. Am. Chem. Soc.* **1989**, *111*, 597.
(171) Dinger, M. B.; Mol, J. C. *Organometallics* **2003**, *22*, 1089.
(172) Grisi, F.; Mariconda, A.; Costabile, C.; Bertolasi, V.; Longo, P. *Organometallics* **2009**, *28*, 4988.
(173) Binder, J. B.; Guzei, I. A.; Raines, R. T. *Adv. Synth. Catal.* **2007**, *349*, 395.
(174) Wakamatsu, H.; Blechert, S. *Angew. Chem. Int. Ed.* **2002**, *41*, 2403.
(175) Kawai, T.; Komaki, M.; Iyoda, T. *J. Mol. Catal. A-Chem.* **2002**, *190*, 45.
(176) Pietraszuk, C.; Marciniec, B.; Fischer, H. *Organometallics* **2000**, *19*, 913.
(177) Kawai, T.; Shida, Y.; Yoshida, H.; Abe, J.; Iyoda, T. *J. Mol. Catal. A-Chem.* **2002**, *190*, 33.
(178) SDBSWeb National Institute of Advanced Industrial Science and Technology. <http://riodb01.ibase.aist.go.jp/sdbs/> [per 2.5.2010]
(179) Hall, H. K. *J. Am. Chem. Soc.* **1957**, *79*, 5441.
(180) Diesendruck, C. E.; Tzur, E.; Lemcoff, N. G. *Eur. J. Inorg. Chem.* **2009**, 4185.
(181) Mitchell, L.; Parkinson, J. A.; Percy, J. M.; Singh, K. *J. Org. Chem.* **2008**, *73*, 2389.
(182) Gillingham, D. G.; Kataoka, O.; Garber, S. B.; Hoveyda, A. H. *J. Am. Chem. Soc.* **2004**, *126*, 12288.
(183) Van Veldhuizen, J. J.; Campbell, J. E.; Giudici, R. E.; Hoveyda, A. H. *J. Am. Chem. Soc.* **2005**, *127*, 6877.
(184) Van Veldhuizen, J. J.; Gillingham, D. G.; Garber, S. B.; Kataoka, O.; Hoveyda, A. H. *J. Am. Chem. Soc.* **2003**, *125*, 12502.
(185) Occhipinti, G.; Jensen, V. R.; Törnroos, K. W.; Frøystein, N. Å.; Bjørsvik, H.-R. *Tetrahedron* **2009**, *65*, 7186.
(186) Waltman, A. W.; Grubbs, R. H. *Organometallics* **2004**, *23*, 3105.
(187) Kuhn, K. M.; Grubbs, R. H. *Org. Lett.* **2008**, *10*, 2075.
(188) Vougioukalakis, G. C.; Grubbs, R. H. *Chem.-Eur. J.* **2008**, *14*, 7545.

(189) Fürstner, A.; Alcarazo, M.; Cesar, V.; Krause, H.; Hopkins, C.; Wipf, P. *Org. Synth.* **2008**, *85*, 34.
(190) Waltman, A. W.; Ritter, T.; Grubbs, R. H. *Organometallics* **2006**, *25*, 4238.
(191) Herrmann, W. A. *Angew. Chem. Int. Ed.* **2002**, *41*, 1290.
(192) Albert, H. E. *J. Am. Chem. Soc.* **1953**, *76*, 4985.
(193) Zeynizadeh, B.; Setamdideh, D. *Synth. Commun.* **2006**, *36*, 2699.
(194) Occhipinti, G.; Jensen, V. R.; Bjørsvik, H.-R. *J. Org. Chem.* **2007**, *72*, 3561.
(195) Wang, H. M. J.; Lin, I. J. B. *Organometallics* **1998**, *17*, 972.
(196) Garrison, J. C.; Youngs, W. J. *Chem. Rev.* **2005**, *105*, 3978.
(197) Gandelman, M.; Rybtchinski, B.; Ashkenazi, N.; Gauvin, R. M.; Milstein, D. *J. Am. Chem. Soc.* **2001**, *123*, 5372.
(198) Shaw, A. P.; Ryland, B. L.; Norton, J. R.; Buccella, D.; Moscatelli, A. *Inorg. Chem.* **2007**, *46*, 5805.
(199) Vougioukalakis, G. C.; Grubbs, R. H. *Chem. Rev.* **2009**.
(200) Jensen, S. B.; Rodger, S. J.; Spicer, M. D. *J. Organomet. Chem.* **1998**, *556*, 151.
(201) Hodson, E.; Simpson, S. J. *Polyhedron* **2004**, *23*, 2695.
(202) Wilhelm, T. E.; Belderrain, T. R.; Brown, S. N.; Grubbs, R. H. *Organometallics* **1997**, *16*, 3867.
(203) Grunwald, C.; Gevert, O.; Wolf, J.; Gonzalez-Herrero, P.; Werner, H. *Organometallics* **1996**, *15*, 1960.
(204) Esteruelas, M. A.; Lahoz, F. J.; Onate, E.; Oro, L. A.; Zeier, B. *Organometallics* **1994**, *13*, 4258.
(205) Weinberg, D. R.; Hazari, N.; Labinger, J. A.; Bercaw, J. E. *Organometallics* **2009**.
(206) Wold, A.; Ruff, J. K. *Inorganic syntheses*; Wiley: New York, 1973; page 94; Vol. 14.
(207) Goodall, B. L.; Grubbs, R. H.; Waltman, A. W.; (Rohn and Haas Company, USA). Application: US, 2005, p 12 pp.
(208) Yang, D.; Long, Y.; Wang, H.; Zhang, Z. *Org. Lett.* **2008**, *10*, 4723.
(209) Ledoux, N.; Allaert, B.; Verpoort, F. *Eur. J. Inorg. Chem.* **2007**, *2007*, 5578.
(210) Burtscher, D.; Grela, K. *Angew. Chem. Int. Ed.* **2009**, *48*, 442.
(211) Becke, A. D. *Phys. Rev. A* **1988**, *38*, 3098.
(212) Becke, A. D. *J. Chem. Phys.* **1997**, *107*, 8554.
(213) Zhao, Y.; Truhlar, D. G. *Acc. Chem. Res.* **2008**, *41*, 157.
(214) Seeger, R.; Pople, J. A. *J. Chem. Phys.* **1977**, *66*, 3045.
(215) Bauernschmitt, R.; Ahlrichs, R. *J. Chem. Phys.* **1996**, *104*, 9047.
(216) Bergner, A.; Dolg, M.; Kuchle, W.; Stoll, H.; Preuss, H. *Mol. Phys.* **1993**, *80*, 1431.
(217) Dolg, M.; Wedig, U.; Stoll, H.; Preuss, H. *J. Chem. Phys.* **1987**, *86*, 866.
(218) Andrae, D.; Haussermann, U.; Dolg, M.; Stoll, H.; Preuss, H. *Theor. Chim. Acta* **1990**, *77*, 123.
(219) Dunning Jr., T. H.; Hay, P. J. In *Methods of Electronic Structure Theory*; Schaefer III, H. F., Ed.; Plenum Press: New York, 1977, p 1-27.
(220) Feller, D. *J. Comput. Chem.* **1996**, *17*, 1571.
(221) Schuchardt, K. L.; Didier, B. T.; Elsethagen, T.; Sun, L. S.; Gurumoorthi, V.; Chase, J.; Li, J.; Windus, T. L. *J. Chem. Inf. Model.* **2007**, *47*, 1045.
(222) Martin, J. M. L.; Sundermann, A. *J. Chem. Phys.* **2001**, *114*, 3408.
(223) Tomasi, J.; Persico, M. *Chem. Rev.* **1994**, *94*, 2027.
(224) Tomasi, J. *Theor. Chem. Acct.* **2004**, *112*, 184.
(225) Hoffman, P. R.; Caulton, K. G. *J. Am. Chem. Soc.* **1975**, *97*, 4221.
(226) Abbel, R.; Abdur-Rashid, K.; Faatz, M.; Hadzovic, A.; Lough, A. J.; Morris, R. H. *J. Am. Chem. Soc.* **2005**, *127*, 1870.
(227) Sakaguchi, S.; Mizuta, T.; Ishii, Y. *Org. Lett.* **2006**, *8*, 2459.

LIST OF REFERENCES

A Appendix

Supporting information for the computational studies is given in A1. The experimental sections are preceding in A.2-A.6. In A.6 the most important spectra from the characterizations of **A2, A3, 5** and **9** are shown.

A.1 Supporting information on theoretical work

Computational details[134]

Geometry optimizations

All computations were performed with Gaussian 09 suite of programs. The functionals set included the standard generalized gradient approximation (GGA) functionals BP86[93,211] and PBEPBE,[95,127] GGA functional B97-D[128,212] which includes an empirical correction for dispersion interactions, hybrid meta-GGA wB97X-D[128,129,212] which also corrected both for dispersion and long-range interactions, the meta-GGA functionals TPSS,[96] popular hybrid-GGA B3LYP,[97] recently developed and dispersion-accounted meta-GGA (M06-L) and hybrid counterpart thereof (M06) [95,100,127,213] which were both fitted to the datasets included non-covalently bounded complexes and TM energetics.[100,213] Numerical grids for the integration of exchange-correlation (XC) DFT potentials, self-consistent-field (SCF) and geometry optimization criteria were set to their default values of Gaussian 09. The X-Ray geometries were taken as input structures to corresponding computations. Multiplicity equal to 1 and restricted formalism was applied to all the compounds because practically all similar Ru (IV) complexes have been shown to be singlets. The SCF solutions were routinely tested for instabilities,[214,215] both prior to and subsequent to geometry optimization. All optimized geometries were characterized by the eigenvalues of analytically calculated Hessian matrix, no negative eigenvalues were found for the optimized structures.

Effective core potentials (ECPs) of Stuttgart type were used for all non-hydrogen elements, thereby reducing the computational cost, and in the case of Ru taking care of relativistic effects. The ECPs accounted for the inner electrons of C (two-electron ECP), N (2), O (2), P (10), Cl (10) and were used in combination with their corresponding [2s2p] (C, N, P) and [2s3p] (O, Cl) contracted valence basis sets.[216] Similarly, ECP was applied for Ru (10 electron ECP) and accomplished by (8s7p6d)/[6s5p3d] contracted valence basis set.[217,218] Hydrogen atoms were described by a Dunning

double-ζ basis set.[219] Single sets of polarization functions, obtained from the EMSL basis set exchange Web site,[220,221] were added to basis sets of all elements bonded to Ru and to the elements directly bonded to those elements (two layers around metal), namely P (exponent $\alpha_d = 0.465$), Cl ($\alpha_d = 0.619$), C ($\alpha_d = 0.720$), N ($\alpha_d = 0.980$), O ($\alpha_d = 1.280$), H ($\alpha_p = 1.000$).

To investigate the effect of a basis sets size on the structural parameters, all structures were reoptimized with PBEPBE and M06 functionals and improved valence basis sets, whereas ECPs described above were retained. For Ru, two f-functions[222] were added to (8s7p6d) primitive basis set.[217,218] The resulting (8s7p6d2f) primitive basis set was contracted to [7s6p4d2f]. The valence basis sets of all non-metal, non-carbon and non-hydrogen elements described above[216]have been supplemented by single sets of diffuse s and diffuse p functions obtained even-temperedly and, for those elements for which such functions were not part of the geometry optimization basis set, also by polarization d functions (P ($\alpha_d = 0.465$), Cl ($\alpha_d = 0.619$), C ($\alpha_d = 0.720$), N ($\alpha_d = 0.980$), O ($\alpha_d = 1.280$)). The resulting 4s4p1d (C), 5s5p1d (N), 5s6p1d (O), 5s5p1d (P), 5s6p1d (Cl) primitive basis sets were contracted to [3s3p1d] (C), [4s4p1d] (N), [4s5p1d] (O), [4s4p1d] (P), [4s5p1d] (Cl). Hydrogen atoms were described by a Dunning triple-ζ basis set[219] augmented by a polarization p function ($\alpha_p = 1.000$).

Local minima were calculated using PBEPBE as implemented in the Gaussian 09. Integrations were performed using the default fine grid of Gaussian 09, and the Gaussian 09 default values were adopted for the selfconsistent-field (SCF) and geometry optimization convergence criteria. The SCF solutions were routinely tested for instabilities, both prior to and subsequent to geometry optimization. Stationary geometries were characterized by the eigenvalues of the analytically calculated Hessian matrix. Translational, rotational, and vibrational partition functions for thermal corrections to give total Gibbs free energies were computed within the ideal-gas, rigid-rotor, and harmonic oscillator approximations following standard procedures. The same basis sets as mentioned in A.1.1 were used.

Potential energy surface evaluations were done using PBEPBE as implemented in the Gaussian 09 and MODREDUNDANT and linearly scanning the reaction coordinate.

Transition states were calculated using PBEPBE as implemented in the Gaussian 09 using the standard basis set mentioned above. Integrations were performed using the default fine grid of

Gaussian 09, and the Gaussian 09 default values were adopted for the selfconsistent-field (SCF) and geometry optimization convergence criteria. The SCF solutions were routinely tested for instabilities, both prior to and subsequent to geometry optimization. NOEIGENTEST and TS were specified in the input files to use the Berny optimization to locate transition states.[132] The imaginary frequency was checked and the motion of the frequency followed (should be along the reaction coordinate) and structures obtained at the end points and optimized to see whether the converged to the intermediate states located around the transition state.

Potential energy surface evaluations were done using PBEPBE as implemented in the Gaussian 09 and MODREDUNDANT and linearly scanning the reaction coordinate.

Single-Point Energy Evaluations.

The energy was re-evaluated at the optimized geometry, using the meta-GGA functional M06-L using Gaussian 09. Whereas the ECPs described above were retained in the single-point (SP) evaluations, the valence basis sets were improved compared to those used in the geometry optimizations. For the Ruthenium, two f-functions[222] were added to the (8s7p6d) primitive basis sets.[217,218] The resulting (8s7p6d2f) primitive basis sets were contracted to [7s6p4d2f]. The valence basis sets of all non-metal and non-hydrogen elements described above[216] have been supplemented by single sets of diffuse s and p functions obtained even-temperedly and, for those elements for which such functions were not part of the geometry optimization basis set, also by polarization d functions (C, α_d = 0.72; N, α_d = 0.72 0.98; O, α_d = 1.28). The resulting (5s5p1d) (C, N, P) and (5s6p1d) (O, Cl, Br) primitive basis sets were contracted to [4s4p1d] (C, N, P) and [4s5p1d] (O, Cl, Br). Hydrogen atoms were described by a Dunning triple-*zeta* basis set[219] augmented by a diffuse s function (α_s= 0.043152), obtained even-temperedly, and a polarization p function (α_p = 1.00).

Electrostatic and nonelectrostatic solvent terms for effects were calculated by the polarizable continuum model (PCM)[223,224] as implemented in Gaussian 03.

The Gibbs free energy was calculated as the sum of single-point energy from single-point energy evaluation, gibbs free energy correction from the geometry optimization and solvation energy from the PCM.

A.1.1 Benchmarking project

Before the benchmarking started the X-ray structures had to be prepared for analysis. This involved removing solvent molecules from some of the structures. Information about the X-ray structures and pretreatment is given in Table A.1.

Table A.1: Information about X-ray structures used in the benchmark.

Crystal	Manipulations done on the structure	R-factor (%)	Temperature (K)	Number of d-functions
ABEJUM01[115]	Removed a DCM	2.1	103	9
BIBREK[116]	Removed a pyridine	2.79	98	9
CAZVEE[19]	-	7.28	183	6
GALGOQ[117]	Removed a methanol	3.41	193	6
GALGUW[117]	Removed a DCM	3.29	173	12
GAQGAH[118]	Removed 4 alt. pos.	5.86	283-303	9
GIOAMIN (A1)[55]	Removed a DCM	3.69	100	13
JOFREC[45]	Removed a benzene	4.45	100	9
KIJFIT[119]	-	4.92	160	9
LEMRAX[120]	Removed a benzene	4.34	200	9
NALTIE[121]	Removed two DCMs	2.69	98	11
ROHHAY[122]	-	5.21	100	9
STEWART[108]	Removed an isomer	5.38	100	12
TIHLIF[10]	-	5.44	100	6
XACYOQ[123]	Removed two DCM	3.69	283-303	9
YIQWUQ[124]	-	2.62	100	6
ZETLOZ[14]	-	3.5	158	3
ZIPLEP[125]	-	3.31	173	6

A.2 Supporting information on amine ligand sythesis.

Synthesis of L2 (2-(piperidin-1-yl)acetic acid)[169]

In a 250 mL reaction flask 3.24 g (23.3 mmol, 1.2 equiv) of 2-bromoacetic acid was dissolved in 20 mL water. 10 mL 2.8M NaOH was added, and pH read to be almost 14. The solution was then cooled on ice. 2 mL (20.2 mmol, 1 equiv) of piperidine was added dropwise and the reaction mixture stirred on melting ice until the next morning. The next morning the reaction mixture was refluxed for 2 hours and then the solvent removed with a rotavap. The resulting oil was dissolved in 40 mL ethanol and stirred at 50°C for 15 minutes and filtered. The solvent was again removed on rotavap to yield 4.86 g of a yellow powder. This was however more than a 100% yield; probably a mixture of NaBr and the product. It was therefore redissolved in 20 mL methanol and put in the freezer over night. This gave no precipitate, added therefore 30 mL ether to yield 1.45 g (43 %) of a pure white powder, which was showed to be the product from ^{1}H-NMR. It was characterized by:

^{1}H-NMR (400.0MHz, D_2O; 4.79 ppm): δ 3.69 (s, 2H) 3.58 (d, J=12.0Hz, 2H) 3.01 (dt, J=3.0Hz;12.0Hz, 2H) 1.84 (m, 5H) 1.51 (m, 1H).

^{13}C-NMR (100.6MHz, D_2O): δ 170.6, 60.0, 54.3, 23.0, 21.3.

Synthesis of the potassium salt of L2

In a dry 100 mL schlenk flask 274 mg (1.91 mmol, 1 equiv) of **L2** and 283 mg (2.48 mmol, 1.3 equiv) of potassium *tert*-butoxide were dissolved in 10 mL THF and heated to 40°C. The reaction mixture; a suspension; was stirred vigorously overnight. The following morning the solvent was removed under reduced pressure to yield a white potassium 2-(piperidin-1-yl)acetate, which was dried under vacuum for 24 hours. Yield 250 mg (72 %)

It was characterized by:

^{1}H-NMR (400MHz, D_2O; 4.79 ppm): δ 2.98 (s, 2H) 2.49 (s, 4H) 1.57 (quintet, J=5.5Hz , 4H) 1.43 (m, 2H).

Mol weight: 181.27 g/mol.

Synthesis of the potassium salt of L3

In a dry 100 mL schlenk flask 1.09 g (10.49 mmol, 1 equiv) of **L3** and 1.62 g (13.64 mmol, 1.3 equiv) potassium *tert*-butoxide were dissolved in 20 mL THF and heated to 40°C. The reaction mixture; a suspension was stirred vigorously overnight. The following morning the solvent was

removed under reduced pressure to yield a white potassium N,N-dimethylglycinate, which was dried under vacuum for 24 hours. Yield 1.40 g (94 %). It was characterized by:
^{1}H-NMR (400MHz, D_6-DMSO; 2.50 ppm): δ 2.48 (s, 1H) 2.09 (s, 6H) 1.08 (s, 1H).
Mol weight: 141.21 g/mol.

A.3 Supporting information of amine complex synthesis

Attempted synthesis of A0 from L0 with silver carbonate and G2

In a dry schlenk flask 2 mg (0.012 mmol, 1 equiv) of **L0** and 2 mg (0.007 mmol, 0.6 equiv) were dissolved in 0.5 mL THF and stirred vigorously for 10 minutes. 10 mg (0.011 mmol, 1 equiv) of **G2** was dissolved in 1 mL toluene and added to the ligand. The reaction mixture was stirred at room temperature for 1 hour and followed by TLC (8:2 hexane:ether). After 1 hour the TLC showed no new compound and the reaction mixture was heated to 50°C and added a small amount of AgCl and stirred vigorously for 1 hour, still the TLC did not show any new compound. The solvent was removed under reduced pressure and the solids analysed by ^{1}H-NMR.

Comments:

The important peaks were 19.14 ppm (2.4); 2.gen. Grubbs; and 19.09 ppm (1). The conclusion from this reaction was that it was possible to make a new complex. The reaction was repeated in a larger scale, but it was impossible to isolate the product with a peak at 19.09 ppm. It was unstable in silica and decomposed faster than 2. gen. Grubbs. The colour of the reaction mixture went from red to brown-green.

Attempted synthesis of A0 from L0 with potassium *tert*-butoxide and G2.

2.8 mg (0.017 mmol, 1 equiv) of **L0** and 2 mg (0.017 mmol, 1 equiv) potassium *tert*-butoxide were dissolved in THF and stirred vigorously for 1 hour at 50°C and then the solvent removed under reduced pressure. 14 mg (0.017 mmol, 1 equiv) of **G2** was dissolved in 1 mL toluene and transferred to the dry solid ligand and added 0.5 mL THF, plus a small amount of AgCl. The reaction mixture was heated to 50°C and stirred vigorously for 2.5 hours. In the beginning the reaction mixture was red and in the end brown. The solvent was removed under reduced pressure and the remaining solid analysed by ^{1}H-NMR. The spectra showed three peaks in the alkylidene area: 19.21 ppm (2.6 %), 19.14 ppm (92.5 %) and 19.09 ppm (4.9 %).

Comments:

This reaction proved to be worse than the first attempt; described above.

Attempted synthesis of A3 with Grubbs' method with Cu_2O as the base[58]

In a dry 25 mL schlenk flask 23 mg (0.027 mmol, 1 equiv) of 2.gen Grubbs, 43 mg (0.300, 11 equiv) of Cu_2O and 17 mg (0.165 mmol, 6 equiv) of **L3** were dissolved in 1 mL DCM and stirred at room temperature for 2 hours. The TLC showed no new product. The reaction mixture turned green.

Comments:

It was concluded as a failure. This conclusion was later shown to be wrong by repeating the experiment and comparing the ^{1}H-NMR of the reaction mixture with the ^{1}H-NMR-spectra of **A3**. The synthesis actually gave the right product.

From the salt of the corresponding ligand

Synthesis of A2 from the potassium salt of L2 and G2

In a dry 50 mL schlenk flask in the glovebox 294 mg (0.346 mmol, 1 equiv) of **G2** and 150 mg (1.05 mmol, 3 equiv) AgCl were loaded. The schlenk flask was brought out and connected to the schlenk line and added 180 mg of the potassium salt of **L2**. 4 mL THF and 4 mL toluene were added and the reaction mixture heated to 50°C and stirred vigorously for 2 hours, while following the reaction by TLC; 9:1 ether:methanol. After the reaction had gone to completion according to TLC the solvent was removed under reduced pressure and the solids redissolved in dichloromethane. The brown solution was filtered over celite to yield a green transparent solution. This solution was characterized by ^{1}H-NMR which showed some rests of phosphines. A short silica column (7.5 cm) under argon was done. The first eluent was chosen to be ether and the column eluated with 50 mL ether prior to using the second eluent; methanol. The column was then eluated with methanol and the green fraction collected in a schlenk flask. Yield 120 mg (51 %) Characterized by:

^{1}H-NMR (400MHz, $CDCl_3$; 7.26 ppm): δ 19.46 (s, 1H) 7.71 (d, J=7.4Hz, 2H) 7.46 (t, J=7.4Hz, 1H) 7.17 (t, J=7.8Hz, 2H) 7.08 (s, 1H), 7.06 (s,1H) 6.52 (s, 1H) 6.10 (s, 1H) 4.26 (m, 1H) 4.17 (m, 1H) 4.09 (m, 1H) 3.97 (m, 1H) 3.7 (t, J=13.5Hz, 2H) 3.51 (d, J=15.8Hz, 1H) 2.70 (s, 3H) 2.51 (s, 3H) 2.44 (t, J=12.5Hz, 1H) 2.31 (d, J=15.8Hz, 1H) 2.29 (s, 3H) 2.21 (s, 3H) 2.01 (s, 3H) 1.93 (s, 3H)

1.87 (d,J=13.5Hz, 4H) 1.53 (m, 2H) 1.38(d,12.5Hz, 1H) 1.29 (m, 2H) 1.05 (m, 2H) . ^{13}C-NMR(150MHz, $CDCl_3$; 77.16 ppm): δ 299.2 (t, J= 36.5Hz), 222.0, 180.5, 151.9, 141.2, 140.8, 139.6, 138.2, 137.2, 136.8, 135.7, 133.5, 129.6, 129.2, 128.95, 128.90, 128.86, 128.4, 58.3, 58.0, 51.7, 50.6, 46.2, 23.0, 21.0, 20.9, 20.6, 20.2, 19.1, 18.7, 18.3, 18.2.

Elemental analysis: N 5.47 % C 61.51 % H 7.06 % Teoretical: N 6.22 % C 62.25 % H 6.57

MS(IS=PEG+H, 250C DART): 676.22554 m/z Theoretical: 676.22501 (<1 ppm)

Mol weight: 675.26 g/mol. Green

Comments:

Main mass spectrum peak is the protonated molecule. Main fragment in MS is the protonated molecule, method related. The same for **A3**.

Synthesis of A3 from the potassium salt of L3 and G2.

In a dry 50 mL schlenk flask in the glovebox 310 mg(0.365 mmol, 1 equiv) **G2** and 200 mg of AgCl were loaded. The flask was taken out of the glovebox and under argon added 64 mg (0.474 mmol, 1.3 equiv) of potassium salt of **L3**. The flask was filled with 3 mL THF and 12 mL toluene. The reaction mixture was heated to 50°C for 1 hour and then the solvent removed under reduced pressure. The reaction was followed by TLC; 9:1 ether:methanol. The solid was dissolved in dichloromethane and filtered over celite. Some mL of the solution was taken out and dried in a separate schlenk for NMR-analysis, which showed a new alkylidene at 19.44ppm. The product was purified by column chromatography with first eluent diethyl ether which eluated impurities and then methanol which eleuated the wanted complex. Crystals with a good enough quality for x-ray diffraction analysis were made by diffusion of pentane into a concentrated solution of complex in fluorobenzene. It was characterized by:

^{1}H-NMR (400MHz, $CDCl_3$; 7.26 ppm): δ 19.44 (s, 1H) 7.72 (d, J=7.4Hz, 2H) 7.49 (t, J=7.4Hz, 1H) 7.18 (t, J=7.4Hz, 2H) 7.08 (d, J=1.9Hz, 2H) 6.52 (s, 1H) 6.13 (s, 1H) 4.23 (m, 2H) 4.10 (m, 2H) 2.69 (d+s J=14Hz, 4H) 2.54 (d+s J=14Hz 4H) 2.30 (s, 3H) 2.24 (s, 3H) 2.20 (s, 3H) 2.02 (s, 3H) 1.95 (s, 3H) 1.58 (s, 3H).

^{13}C-NMR (150MHz, $CDCl_3$; 77.16 ppm): δ 298.5, 221.4, 152.0, 140.9, 140.5, 140.0, 138.1, 137.0, 136.6, 135.5, 133.3, 129.5, 129.4, 129.2, 128.96, 128.94, 128.7, 128.2, 66.5, 51.5, 51.0, 50.4, 20.9, 20.7, 20.0, 18.9, 18.1, 18.0, 17.8.

Element analysis: N 4.71 % C 60.58 % H 7.28 % Theoretical: N 6.62 % C 60.51 % H 6.35 %

MS(IS=PEG+H, 250C DART): 636.19502 m/z Theoretical: 636.19363 m/z (2.2 ppm)

Prod: 635.20 g/mol. Green

X-ray data for A3

Table 1. Crystal data and structure refinement for A3.

Identification code	A3	
Empirical formula	C35 H42.50 Cl F0.50 N3 O2 Ru	
Formula weight	683.24	
Temperature	103(2) K	
Wavelength	0.71073 Å	
Crystal system	Monoclinic	
Space group	P2(1)/c	
Unit cell dimensions	a = 17.4269(12) Å	α= 90°.
	b = 9.4125(6) Å	β= 107.115(1)°.
	c = 20.2894(13) Å	γ = 90°.
Volume	3180.7(4) $Å^3$	
Z	4	
Density (calculated)	1.427 Mg/m^3	
Absorption coefficient	0.616 mm^{-1}	
F(000)	1420	
Crystal size	0.32 x 0.22 x 0.10 mm^3	
Theta range for data collection	2.10 to 26.72°.	
Index ranges	-22<=h<=22, -11<=k<=11, -25<=l<=25	
Reflections collected	40003	
Independent reflections	6729 [R(int) = 0.0562]	
Completeness to theta = 26.72°	99.8 %	
Absorption correction	None	
Max. and min. transmission	0.9410 and 0.8273	
Refinement method	Full-matrix least-squares on F^2	
Data / restraints / parameters	6729 / 4 / 391	
Goodness-of-fit on F^2	1.044	
Final R indices [I>2sigma(I)]	R1 = 0.0492, wR2 = 0.1285	
R indices (all data)	R1 = 0.0567, wR2 = 0.1369	
Largest diff. peak and hole	2.962 and -1.033 $e.Å^{-3}$	

Table 2. Bond lengths [Å] and angles [°] for AS3.

Ru(1)-C(26)	1.834(3)
Ru(1)-C(1)	2.015(3)
Ru(1)-O(1)	2.099(2)

Ru(1)-N(3)	2.162(2)
Ru(1)-Cl(1)	2.3946(8)

C(26)-Ru(1)-C(1)	98.14(13)
C(26)-Ru(1)-O(1)	87.00(11)
C(1)-Ru(1)-O(1)	96.23(10)
C(26)-Ru(1)-N(3)	101.19(11)
C(1)-Ru(1)-N(3)	159.97(11)
O(1)-Ru(1)-N(3)	79.69(9)
C(26)-Ru(1)-Cl(1)	104.60(10)
C(1)-Ru(1)-Cl(1)	88.01(9)
O(1)-Ru(1)-Cl(1)	167.01(6)
N(3)-Ru(1)-Cl(1)	92.12(7)
C(25)-O(1)-Ru(1)	115.1(2)
N(1)-C(1)-N(2)	107.5(3)
N(1)-C(1)-Ru(1)	118.6(2)
N(2)-C(1)-Ru(1)	133.6(2)

Table 3. Torsion angles [°] for AS3.

C(26)-Ru(1)-O(1)-C(25)	-88.9(2)
C(1)-Ru(1)-O(1)-C(25)	173.2(2)
N(3)-Ru(1)-O(1)-C(25)	13.0(2)
Cl(1)-Ru(1)-O(1)-C(25)	64.6(4)
C(26)-Ru(1)-C(1)-N(1)	-172.8(2)
O(1)-Ru(1)-C(1)-N(1)	-85.0(2)
N(3)-Ru(1)-C(1)-N(1)	-8.0(5)
Cl(1)-Ru(1)-C(1)-N(1)	82.7(2)
C(26)-Ru(1)-C(1)-N(2)	13.1(3)
O(1)-Ru(1)-C(1)-N(2)	101.0(3)
N(3)-Ru(1)-C(1)-N(2)	177.9(3)
Cl(1)-Ru(1)-C(1)-N(2)	-91.3(3)
N(2)-C(1)-N(1)-C(4)	-169.5(3)
Ru(1)-C(1)-N(1)-C(4)	15.0(4)
N(2)-C(1)-N(1)-C(3)	-0.7(4)
Ru(1)-C(1)-N(1)-C(3)	-176.1(3)
N(1)-C(1)-N(2)-C(13)	173.2(3)
Ru(1)-C(1)-N(2)-C(13)	-12.3(5)
N(1)-C(1)-N(2)-C(2)	1.9(4)
Ru(1)-C(1)-N(2)-C(2)	176.4(2)

C(1)-N(2)-C(2)-C(3)	-2.2(4)
C(13)-N(2)-C(2)-C(3)	-174.0(3)
C(26)-Ru(1)-N(3)-C(24)	57.9(2)
C(1)-Ru(1)-N(3)-C(24)	-106.8(3)
O(1)-Ru(1)-N(3)-C(24)	-26.97(18)
Cl(1)-Ru(1)-N(3)-C(24)	163.19(18)
C(26)-Ru(1)-N(3)-C(22)	172.7(2)
C(1)-Ru(1)-N(3)-C(22)	8.1(4)
O(1)-Ru(1)-N(3)-C(22)	87.87(19)
Cl(1)-Ru(1)-N(3)-C(22)	-81.97(18)
C(26)-Ru(1)-N(3)-C(23)	-66.5(2)
C(1)-Ru(1)-N(3)-C(23)	128.9(3)
O(1)-Ru(1)-N(3)-C(23)	-151.3(2)
Cl(1)-Ru(1)-N(3)-C(23)	38.8(2)

Catalytic testing procedures of A1, A2 and A3.

Ring closing metathesis of diethyl 2,2-diallylmalonate.

In the glovebox 0.017 μmol (~1 mg, 1 equiv) of catalyst was weighted and put in a young NMR-tube. The NMR-tube was taken out of the glovebox and connected to the schlenk line and filled with 0.5 mL of the wanted deuterated solvent. After the addition of the solvent 40 μL (0.165 mmol, 100 equiv) of diethyl 2,2-diallylmalonate(0.3 M) was added by a microsyringe, this gives about 1 mol% catalyst. The NMR-tube was heated on an oil-bath and measured by NMR. The conversion was measured by the ratio between the singlet at 3.00 ppm and the sum of this singlet plus the doublet at 2.62 ppm. The peak at 3.00 ppm is the signal from the product.

RCM in CD_3OD was done with 2.5 mol% catalyst.

RCM in CD_2Cl_2 was done with 2.0 mol% catalyst.

Cross metathesis of styrene.

In the glovebox 0.050 μmol (~3 mg) of catalyst was weighted and put in a young NMR-tube. The NMR-tube was taken out of the glovebox and connected to the schlenk line and filled with 0.5 mL of the wanted deuterated solvent. After the addition of solvent 30 μL (0.26 mmol) of styrene was added by a microsyringe; gives about 2 % catalyst. The NMR-tube was heated on an oil-bath and measured by NMR. The reference peak for the *Z*-isomer is at 6.57 ppm and the reference peak for *E*-isomer at 7.15 ppm in $CDCl_3$.[178] The substrate peak is a doublet of a doublet at 6.69 ppm.

APPENDIX

A.4 Supporting information NHC ligand synthesis.

Most of these reactions were done several times to yield a total of 1.3 g of the target molecule **5**; 3-(3-*tert*-butyl-2-hydroxy-5-metylphenyl)-1-(2,6-diisopropylphenyl)-4,5-dihydro-1*H*-imidazolium chloride.

The synthesis was in general inspired by the work done by Grubbs' co-workers[186].

Synthesis of 6-*tert*-butyl-4-methyl-2-nitrophenol[192]

4.39 g of 2-*tert*-butyl-4-methylphenol, bought from Aldrich(B97208), was dissolved in 40 mL concentrated acetic acid and cooled to ~0ºC. After sufficient cooling, 1 equivalent of 65% HNO_3, dissolved in 40 mL acetic acid, was added drop wise under vigorous stirring. When half the amount of nitric acid had been added the colour of the solution changed from colourless to a brownish colour. The solution was stirred for 2.5 h and in the meantime the ice melted and the reaction mixture heated to ambient temperature. At this point 12 mL distilled water was added to precipitate the product; note that adding to much water will precipitate by-products. The product was crystallized from 50 mL technical ethanol to yield 2.25 g (40 %) pure yellow thread crystals. It was characterized by:

^{1}H-NMR (400MHz, $CDCl_3$; 7.26 ppm): δ 11.41 (s, 1Ar-O**H**), 7.79 (t, 1Ar**H**), 7.38 (d, 2.1Hz,1Ar**H**), 2.32 (s, 3Ar-C$\mathbf{H_3}$) and 1.43 (s ,9 C($\mathbf{CH_3)_3}$,).

Melting point: 91-91.5°C

Synthesis of 2-amino-6-*tert*-butyl-4-methylphenol[193]

5.52 g of 6-*tert*-butyl-4-methyl-2-nitrophenol was dissolved in a 1:2 mixture of THF:H_2O; 15ml:30mL. 3.2 g of fine powdered activated charcoal was added to the solution. The solution was heated to 50ºC under a stream of argon. 8.42 g (8 equivalents) $NaBH_4$ tablets was added six portions every half hour until TLC confirmed completion of the reduction (eluent 1:1 diethyl ether:hexane). The reaction mixture was then allowed to cool down to room temperature and filtered on celite under argon, additional solvent ethyl acetate was used to wash the celite. The solution was then washed 2 times with 10 mL brine, dried over $MgSO_4$. Afterwards the solvent was evaporated in a schlenk flask and stirred in hexane to remove oxidation products. Isolated product: 3.63 g (77 %). It was then characterized by:

^{1}H-NMR (400MHz, $CDCl_3$; 7.26 ppm): δ 6.67 (d, J=1.6Hz, 1H,Ar**H**), 6.61 (d, J=1.6Hz, 1H, Ar**H**), 5.59 (b, 1H, ArO**H**), 3.19 (b, 2H, ArN$\mathbf{H_2}$), 2.22 (s,3H, Ar-C$\mathbf{H_3}$), 1.40 (s, 9H, Ar-C(C$\mathbf{H_3}$)$_3$).

Synthesis of ethyl 2-(2,6-diisopropylphenylamino)-2-oxoacetate

2 mL 2,6-diisopropylaniline (97 %,Sigma; 374733) and 1.8 mL ethyldiisopropylamine(Et-DIPA) were dissolved in 30 mL THF and cooled on ice to ~0ºC. Ethyl chloro oxoacetate (98 %, Sigma; E43101) was added to the solution drop wise under vigorous stirring, during the addition a white precipitate formed; Et-DIPA·HCl. It was left stirring until the ice had melted and the temperature had reached ambient. The reaction mixture was filtrated over cotton. Washed with 2×10 mL 2M HCl and then with 2×10 mL brine. The water phase was then washed with ethyl acetate; EtOAc. Dried the organic solution over $MgSO_4$ and evaporated the solvent on a rotavapour. The solids were crystallized from 30 mL of a heated 9:1 mixture of hexane and ethyl acetate to yield 2.13 g (89 %) of white thread like crystals. It was characterized by:

^{1}H-NMR (400MHz, $CDCl_3$; 7.26 ppm): δ 8.36 (b, 1H, ArN**H**), 7.34 (t, J=7.6Hz, *p*-Ar**H**), 7.20 (d, J=7.6Hz, 2H, *m*-ArH), 4.45 (q, J=7.1Hz, 2H, -OC$\mathbf{H_2}$CH3), 3.01 (sep, J=6.9Hz, 2H, ArC**H**$(CH_3)_2$), 1.47 (t, J=7.1Hz, 3H, -OCH2C$\mathbf{H_3}$), 1.21 (d, J=6.9Hz, 12H, ArCH(C$\mathbf{H_3})_2$).

MS (IS=PEG+H, 350C DART) 278.17365m/z main peak, which gives exact mass 277.16582, expected 277.168; $C_{16}H_{23}NO_2$.

Molecular weight: 277.359.

IR(Nicolet Protege 460 FTIR): 3266mb, 3071w, 2955m, 2926m, 2857m, 1737s, 1685s, 1502s, 1457m, 1301s, 1281s, 1205s, 1176m, 1159s, 1020s, 944m, 732s.

Synthesis of N^1-(3-*tert*-butyl-2-hydroxy-5-metylphenyl)-N^2-(2,6-diisopropylphenyl)oxalamide

Dissolved 2-amino-6-*tert*-butyl-4-methylphenol (1.01 g, 5.65 mmol, 1.1 equiv) and ethyl 2-(2,6-diisopropylphenylamino)-2-oxoacetate (1.43 g, 5.13 mmol, 1.0 equiv) in 20 mL toluene. It was allowed to stir for 10 min until all was dissolved and then Et-DIPA was added (1.7 mL, 1.33 g, 2.0 equiv). It was then heated to reflux and refluxed for 16 h. After it had cooled down EtOAc was added to dissolve solids and washed with 2×10mL 2M HCl and then with 2×10 mL brine. The solvent was evaporated on a rotavapour to yield a white/grey powder. It was then dissolved in 40 mL diethyl ether and 40 mL pentane and allowed to sit in the freezer to precipitate a white powder; insoluble in pentane. After crystallization it is possible to get a higher yield by doing a column with 9:1 Hexane:EtOAc. Yield: 1.68 g; (79 %). It was characterized by:

^{1}H-NMR(400MHz, $CDCl_3$; 7.26 ppm): δ 9.51 (s, 1H, ArN**H**), 8.77 (s, 1H, ArN**H**), 7.91 (s, 1H, ArO**H**), 7.36 (t, J=7.8Hz, 1H, Ar**H**), 7.23 (d, J=7.8Hz, 2H, Ar**H**), 3.01 (sep, J=6.9Hz, 2H,

ArC**H**$(CH_3)_2$), 2.29 (s, 3H, ArC**H$_3$**), 1,46 (s, 9H, ArC(C**H$_3$**)$_3$), 1.22 (d, J=6.9Hz, 12H, ArCH(C**H$_3$**)$_2$). ^{13}C-NMR(100MHz, $CDCl_3$; 77.16 ppm): 158.5, 158.4 146.1 145.9 140.6 129.9 129.4 129.3 126.9 124.8 124.0 121.3 35.3 31.1 29.9 29.1 23.8 20.9.

Melting point: 174-175 °C.

MS (IS=PEG, 350C DART) 411.31669m/z main peak, which gives exact mass 410.30886m/z, expected 410.257; $C_{25}H_{34}N_2O_3$. Molecular weight: 410.549.

IR(Nicolet Protege 460 FTIR): 3353mb, 3259mb, 2926m, 2927m, 2865m, 1651s, 1593w, 1506s, 1470s, 1449m, 1383w, 1365m, 1232w, 1206m, 1177w, 1061w, 932w, 855w, 801m, 736s.

Comments:

Mass spectroscopy to concentrated; hard to get good results.

Synthesis of N^1-(3-*tert*-butyl-2-hydroxy-5-metylphenyl)-N^2-(2,6-diisopropylphenyl)ethane-1,2-diaminium dichloride[188]

N^1-(3-tert-butyl-2-hydroxy-5-metylphenyl)-N^2-(2,6-diisopropylphenyl)oxalamide 0.56 g (1,37 mmol, 1 equiv) was placed in a dry high pressure tube under a stream of argon. 1 M Borane in THF (16 mL, 16 mmol, 12 equiv) was added with a syringe under a stream of argon. The tube was closed and heated to 90°C and stirred for 18 h. It was then removed from the heating source and cooled down on ice before 10 mL methanol was added drop wise to quench any remaining borane; forms $B(OMe)_3$. Concentrated aqua's HCl (0.5 mL;12 M, 6 mmol, 4.5 equiv) was then added to protonate the N^1-(3-*tert*-butyl-2-hydroxy-5-metylphenyl)-N^2-(2,6-diisopropylphenyl)ethane-1,2-diamine. The solution was then transferred to a dry 50 mL schlenk flask and the solvent evaporated. It was then redissolved in 5 mL methanol and evaporated thrice. This yielded 0.59 g white powder (95 %). It was characterized by:

^{1}H-NMR (400MHz, $CDCl_3$; 7.26 ppm): δ 7.95 (broad, 1H, ArO**H**), 7.41 (t, J=7.7Hz, 1H, Ar**H**), 7.32 (s, 1H, Ar**H**), 7.27 (s, 1H, Ar**H**), 7.25 (s, 1H, Ar**H**), 7.10 (s, 1H, Ar**H**), 4.45 (b, 2H, ArN**H$_2$**), 3.90 (b, 2H, ArN**H$_2$**), 3.65 (~t, J=6.6 Hz, 2H, NC**H$_2$**), 3.46 (m, 4H, NCH_2 + ArC**H**$(CH_3)_2$), 2.19 (s, 3H, ArC**H$_3$**), 1.36 (s, 9H, ArC(C**H$_3$**)$_3$), 1.31(d, J=6.2Hz, 12H, ArCH(C**H$_3$**)$_2$).

^{13}C-NMR (100MHz, $CDCl_3$; 77.16 ppm): δ 146.1, 143.0, 142.3, 131.2, 130.8, 129.1, 126.1, 71.0, 49.9, 35.3, 29.9, 28.7, 25.1.

Melting point: decomposes.

MS (IS=PEG, 350C DART) 383.30708m/z main peak, which fits with first abstraction one chloride from the molecule and then one HCl molecule which would give expected m/z at 383.30637 (1.9 ppm); $C_{25}H_{39}N_2O$. Molecular weight 455.504: $C_{25}H_{40}Cl_2N_2O$.

IR(Nicolet Protege 460 FTIR): ~3350wb, ~3200wb, 2963s, 2927s, 2865m, 2713mb, 2568mb, 1571s, 1499m, 1459s, 1441s, 1361m, 1235m, 1206s, 1058m, 1040m, 805s, 751s.

Comments:

This compound is usually not characterized in the literature. The NMR-peaks were a bit unclear, with some overlapping peaks.

Synthesis of 5

IUPAC name: (3-(3-*tert*-butyl-2-hydroxy-5-metylphenyl)-1-(2,6-diisopropylphenyl)-4,5-dihydro-1*H*-imidazolium chloride)

N^1-(3-tert-butyl-2-hydroxy-5-metylphenyl)-N^2-(2,6-diisopropylphenyl)ethane-1,2-diaminium chloride 0.50 g (1.1 mmol, 1.0 equiv) was dissolved in triethyl orthoformiate 3mL, (2.67g , 18 mmol, 16 equiv) and heated to 110°C under argon and stirred vigorous for 10 min. It was then cooled down and the product was precipitated from the reaction mixture by adding pentane under vigorous stirring. Was then separated by filtration to yield 0.33 g white powder; 70%. It was characterized by:

^{1}H-NMR(400MHz, $CDCl_3$; 7.26ppm): δ 9.65 (s, 1H, CH), 8,34 (s, 1H, ArO**H**), 7.46 (t, J=7.8Hz, 1H, Ar**H**), 7.29 (d, J=7.8Hz, 2H, Ar**H**), 7.11 (d, J=1.9Hz, 1H, Ar**H**), 6.81 (d, J=1.9Hz, 1H, Ar**H**), 4.89 (t, J=10.5 Hz, 2H, NC$\mathbf{H_2}$), 4.46 (t, J=10.5 Hz, 2H, NC$\mathbf{H_2}$), 3.41 (sep, J=6.8Hz, 2H, ArC**H**$(CH_3)_2$), 2.29 (s, 3H, ArC$\mathbf{H_3}$), 1.43 (s, 9H, ArC(C$\mathbf{H_3})_3$), 1.35 (d, J=6.8Hz, 6H, ArCH(C$\mathbf{H_3})_2$), 1.31 (d, J=6.8Hz, 6H, ArCH(C$\mathbf{H_3})_2$).

^{13}C-NMR(100MHz, $CDCl_3$; 77.16ppm): δ 158.4, 147.8, 147.2, 144.4, 131.4, 130.7, 130.1, 128.6, 127.9, 125.1, 121.2, 53.9, 52.4, 35.6, 30.1, 28.7, 25.4, 24.3, 21.0 .

Melting point: decomposes at 260°C.

MS (IS=PEG, 350C DART) main peak 393.29040, which fits with the molecule being protonated and losing one HCl molecule; expected peak 393.2901 (0.8 ppm): $C_{26}H_{37}N_2O$.

Molecular weight: 429.038.

IR(Nicolet Protege 460 FTIR): 2970m, 2915m, 2858m, 2760m, 2637m, 2530m, 1636s, 1578w, 1463m, 1445m, 1260m, 1246m, 1069m, 1043m, 808m, 758m.

Element analysis: N 6.36 % C 70.95 % H 8.47 % Theoretical N 6.53 % C 72.79 % H 8.69 %

A.5 Supporting information on complex synthesis.

In-situ complexation

Complexation of 5 with H1 with Ag_2O as base

In a dry 25 mL schlenk flask 5.8 mg (0.014 mmol, 1 equiv) of **5**, 8.1 mg (0.014 mmol, 1 equiv) of **H1** and 3.4 mg (0,015 mmol, 1.1 equiv) Ag_2O were dissolved/suspended in 1 mL dry dichloromethane with a couple of activated 4Å molecular sieves; to remove formed water. After stirring for 19 hours the solvent was removed under reduced pressure and a ^{1}H-NMR in $CDCl_3$ (7.26 ppm) was done of the reaction mixture. The typical alkylidene duplet for **H1** was located at 17.43 ppm (d, J=4.3Hz).

Comments:

Since this was the only peak in the alkylidene area it was concluded that the reaction did not yielded a Ru-complex containing both å-NHC and an alkylidene. This reaction was therefore concluded as a failure.

Complexation of 5 with H1 with Ag_2CO_3 as base

In a dry 25 mL schlenk flask 4.8 mg (0.011 mmol, 1 equiv) of **5**, 6.7 mg(0.011 mmol, 1 equiv) of **H1** and 3.8 mg (0.012 mmol, 1.1 equiv) Ag_2CO_3 were dissolved/suspended in 1 mL dry dichloromethane with a couple of 4Å molecular sieves; to remove formed water. After stirring for 24 hours the solvent was removed under reduced pressure and a ^{1}H-NMR in $CDCl_3$ (7.26 ppm) was done of the reaction mixture. The typical alkylidene doublet for **H1** was located at 17.43 ppm (d, J=4.3Hz).

Comments

Since this was the only peak in the alkylidene area, it was concluded that the reaction did not yielded a Ru-complex containing both å-NHC and an alkylidene. This reaction was therefore concluded as a failure.

Free carbene reactions

5 as free carbene with G1 in THF.

A dry 25 mL schlenk flask was introduced to the glovebox and loaded with 10 mg (0.023 mmol, 1 equiv) of **5** and 10 mg (0.049 mmol, 2.1 equiv) KBTSA. The schlenk flask was then closed and brought out of the glovebox and connected to the schlenk line. 1 mL of THF was added and stirred vigorously for 10 minutes. 15.5 mg (0.019 mmol, 0.8 equiv) of **G1** was dissolved in 1 mL THF and transferred by canulla to the free carbene. The reaction mixture was allowed to stir for 1 hour at ambient temperature. After 1 hour the solvent was removed under reduced pressure and the reaction mixture redissolved in dichloromethane and filtered over celite. The solution was concentrated and pentane added and the solution put in the freezer over night. The next day ^{1}H-NMR was done in C_6D_6. This showed only one peak in the alkylidene area; 20.61 ppm. This was rests of **G1**, but most of it had decomposed due to the harsh reaction conditions. **G1** was also observed on TLC.

Comments:

Reaction concluded as a failure from NMR results.

5 as free carbene with G1 in toluene.

A dry 25 mL schlenk flask was introduced to the glovebox and loaded with 10 mg (0.023 mmol, 1 equiv) of **5** and 10 mg (0.049 mmol, 2.1 equiv) KBTSA. The schlenk flask was brought out of the glovebox and connected to the schlenk line and filled with 1 mL THF. The suspension was stirred vigorously for 30 minutes and then the solvent was removed under reduced pressure. 13 mg (0.015 mmol, 0.7 equiv) of **G1** was dissolved in 2 mL toluene and transferred by canulla to the free carbene. The reaction mixture was heated to 60°C and stirred over night. The reaction mixture was cooled to ambient temperature and filtered over celite with dichloromethane. The solvent was evaporated and the raw product analysed by ^{1}H-NMR, ^{13}C-NMR and ^{31}P-NMR. The only alkylidene bearing Ru-complex was from ^{1}H-NMR in $CDCl_3$ some traces (~5 %) of **G1** at 19.99 ppm.

Comments:

This reaction was from NMR concluded as a failure.

5 as free carbene with H1 in toluene

A dry 25 mL schlenk flask was introduced to the glovebox and loaded with 15 mg (0.035 mmol, 1 equiv) of **5** and 10 mg (0.071 mmol, 2.1 equiv) KBTSA. The schlenk flask was brought out the glovebox and filled with 1 mL THF and stirred for 30 minutes at room temperature and then the solvent was removed at reduced pressure. 20 mg (0.033 mmol, 1.0 equiv) of **H1** was dissolved in 2 mL toluene in a separate schlenk flask and transferred by canulla to the free carbene. 10 mg AgCl was added as a phosphine scavenger. The reaction mixture was stirred vigorously at room temperature for 30 minutes and then heated to 50°C and stirred over night. The next day the reaction mixture was filtered over celite which was washed with dichloromethane. The solvent was removed under reduced pressure and ^{1}H-NMR, ^{13}C-NMR and ^{31}P-NMR taken of the raw product. The only peak from the ^{1}H-NMR in the typical alkylidene area was the peak for **H1**; 17.43 ppm (d, J=4.3Hz)

Comments:

Reaction concluded as a failure from NMR.

Transmetalation

Synthesis of 6 from 5 and Ag_2O

In a dry 50 mL schlenk flask 83.4 mg (0.20 mmol, 1 equiv) **5** and 48.7 mg (0.21 mmol, 1.05 equiv) Ag_2O were suspended in dichloromethane and heated to 37°C for 16h. The reaction mixture was then filtered over celite and the solvent removed under reduced pressure to yield 78 mg of **6**; which was a foam-like white substance. The product was extremely soluble in almost every solvent and was tried crystallized from hexane in the freezer. Before filtration the reaction mixture was white and cloudy, but after filtration it turned green; might be due to some oxidation. The product was characterized by: ^{1}H-NMR(400MHz, CD_2Cl_2; 5.32ppm): δ 7.31 (t, J=7.8Hz, 1H, Ar**H**), 7.21 (d, 7.8Hz, 2H, Ar**H**), 6.61 (t, J=9.7Hz|, 2H, Ar**H**), 3.71 (t, J=5.9 Hz, 2H, NC**H$_2$**), 3.39 (m, 4H, NC**H$_2$+** ArC**H**$(CH_3)_2$), 2.29 (s, 3H, ArC**H$_3$**), 1.39 (s, 9H, ArC(C**H$_3$)$_3$**), 1.29 (d, J=6.9Hz, 6H, ArCH(C**H$_3$)$_2$**), 1.19 (d, J=6.9Hz, 6H, ArCH(C**H$_3$)$_2$**).

^{13}C-NMR(100MHz, CD_2Cl_2; 53.4ppm): δ 149.6, 147.4, 140.4, 138.4, 131.2, 128.9, 127.9, 124.1, 120.4, 113.9, 112.5, 55.2, 50.3, 33.7, 29.7, 29.3, 28.1, 25.0, 23.9, 21.0. MS (IS=PEG+H, 350C DART) main peaks 800.55112, 799.54733, 393.28984. The last peak fits with the two times protonation of the free **5**$^{-}$. The two first peaks can fit with **6** (891.46) losing to water molecules(2×18.01) and *tert*-butyl group(57.07) which would give 798.37.

IR(Nicolet Protege 460 FTIR): 3057w, 2959s, 2915s, 2869m, 1687w, 1651w, 1593w, 1485m, 1455s, 1423s, 1394s, 1337m, 1289m, 1293w, 1199m, 1174m, 1091w, 1074s, 1019m, 834s, 812s, 766s, 729m.

Transmetalation with 6 and G1

In a dry 25 mL schlenk flask 15.1 mg (0.015 mmol, 1 equiv) of **6** and 24 mg (0.029 mmol, 2 equiv) **G1** were dissolved in toluene and stirred at 40°C for 2 hours and then heated to 50°C and stirred for 20 hours. The reaction was followed with a TLC-system; 8:2 hexane: ether. The reaction mixture turned violet. ^{1}H-NMR showed a new alkylidene at 19.73 ppm (J=9.1Hz) in $CDCl_3$. There was about 7% of this compared with **G1**.

Comments:

A similar reaction to what is described above was tried in dichloromethane at 30°C lasting 20h. This reaction did not yield any new alkylidene at 19.73ppm (J=9.1Hz) in $CDCl_3$. Due to these two experiments this approach was concluded as a failure.

Transmetalation with 6 and H1

In a dry 25 mL schlenk flask 30.0 mg (0.03mmol, 1 equiv) of **6** and 18.5 mg (0.06mmol, 2 equiv) **H1** were dissolved in toluene and stirred at 50°C for 19h. After 19h the solvent was removed and the reaction mixture dissolved in $CDCl_3$ to take a ^{1}H-NMR spectra. The only significant peak in the alkylidene area was the doublet at 17.43ppm, J=4.6Hz.

Comments:

This reaction was therefore concluded as a failure.

Precursors synthesis

Synthesis of 7 ($RuCl_2(PPh_3)_3$) **from $RuCl_3$.**[198]

14 g of Triphenylphophine; PPh_3; was crystallized from 100 mL methanol to yield 12.4 g pure PPh_3. 100 mL methanol was degassed by bubbling argon through it for 30 min. In a 500 mL round bottom schlenk flask 587.5 mg (2.24 mmol, 1.0 equiv) $RuCl_3 \cdot 3H_2O$ was added and dissolved in the degassed methanol, and then 3.958 g (15.19 mmol, 6.8 equiv) PPh_3 was added. The reaction mixture was heated to reflux, oil bath at 80°C. It was refluxed for 2.5h. During the reaction time the product precipitated. The reaction mixture was removed from the oil bath and filtered by canulla while the solvent was still warm. The black product was then washed with 3×5 mL dry diethyl ether. The product was dried under vacuum to yield 1.955 g (90%) of black micro crystals; 958.87 g/mol. The product is unstable in silica and in solution when exposed to air; oxidised to a blue unknown compound. The product was characterized by:

^{13}C-NMR (100MHz, $CDCl_3$; 77.16ppm): δ 135.4 134.9(d, J=9.2Hz) 132.3(d, J=10Hz) 129.4 128.6(m) 127.5.

^{31}P-NMR (216MHz, $CDCl_3$, Ref: 85 % H_3PO_4; 0.00 ppm): δ 29.8(m)

Comments:

NMR peaks corresponds with the literature.[198] -4.7 (free PPh_3; can be seen in $CDCl_3$ due to decoordination from the complex.[225])

Synthesis of 8 [(η^6-*p*-cymene)$RuCl_2$]$_2$**.**[200,201]

Absolute ethanol was degassed by bubbling argon through for 20 min. 2.995 g (14.43 mmol, 1 equiv) of $RuCl_3 \cdot 3H_2O$ was dissolved in the degassed ethanol. 19 mL(115.5 mmol, 8 equiv) of *α*-terpine was added to the mixture. The reaction mixture was then heated to reflux and stirred vigorously over night. After 18.5h the reaction mixture was allowed to cool down to ambient temperature and then the solvent was removed by canulla filtration, washed with 2×20 mL ice cold methanol and filtered by canulla. The solid which remained was dried under vacuum to yield a first crop of 2.2 g of pure product;49%. It was characterized by:

^{1}H-NMR(400MHz, $CDCl_3$; 7,26ppm): δ 5.43 (d, 2H, J=6.1Hz) 5.30 (d, 2H, J=6.1Hz) 2.87 (sep, 1H, J=6.9Hz) 2.11 (s, 3H) 1.23 (d, 6H, J=6.9Hz).

Comments:

The NMR-data corresponds with the literature.[200,201] A second crop was obtained from removing the solvent from the methanol, which had been used for the washing, and washing it with diethyl ether and redissolving it in ethanol. This solution was put in the freezer.

Ru-based complexes with NHC-phenoxy

Attempted transmetalation with 6 and 7 in toluene

In a dry 25 mL schlenk flask 80 mg (0.08 mmol, 0.75 equiv) of **6** was dissolved in 3 mL toluene. In another dry 25 mL schlenk flask 104 mg (0.11mmol, 1 equiv) **7** was dissolved in 1 mL toluene. The solution of **6** was transferred to the **7**-solution slowly by canulla under vigour stirring. The reaction was followed by TLC (1:1 hexane:ether). The reaction temperature was first ambient for 30 minutes, it was then increased to 30°C for 45 minutes and when nothing changed on the TLC system the temperature was increased to 40°C for 12 hours. The colour changed from brown to dark purple. The solvent was removed under reduced pressure and the solids dissolved in ether. The corresponding solution was filtered by canulla and concentrated to a saturated solution. Pentane was then added to precipitate a brown solid; which was shown by NMR to be $RuCl_2(PPh_3)_3$. The solution over the precipitate was filtrated and filtrate was cooled down on liquid nitrogen. From the cold dark purple solution there was a precipitate. This precipitate was analysed by ^{1}H-NMR, ^{13}C-NMR and ^{31}P-NMR. ^{31}P-NMR(216MHz, CD_2Cl_2, Ref: 85 % H_3PO_4; 0.00 ppm): δ 51.2 (13 %) 46.6 (11 %) 25.9 (59 %) 24.0 (10 %) -4.4 (7 %).

Comments:

According to 7 ^{1}H-NMR spectra there were no evidence of claiming that the ligand had coordinated to the ruthenium metal centre. There were no significant changes in chemical shift for the all the peaks corresponding to ligand. The same conclusion was reached from two ^{13}C-NMR experiments. The ^{31}P-NMR showed some new species, but in connection with both ^{1}H-NMR and ^{13}C-NMR we have to conclude that no new ruthenium complex bearing the ligand has been formed.

Attempted transmetalation with 6 and 7 in THF.

In a dry 25 mL schlenk flask 4.2 mg (0.004 mmol, 0.5 equiv) of **6** was dissolved in 0.5 mL toluene. In another dry 25 mL schlenk flask 8.3 mg (0.008 mmol, 1 equiv) **7** was dissolved in 0.5 mL THF. The solution of **6** was transferred to **7**-solution slowly by canulla under vigour stirring. 4 mg AgCl was used as phosphine scavenger. The reaction mixture was heated to 50°C and stirred vigorously for 4 hours. After cooling to ambient temperature the reaction mixture was filtered over celite and the solvent removed under reduced pressure. The solids were dissolved in ether and filtered by canulla and the solvent was evaporated. The solids were analysed by ^{1}H-NMR and ^{13}C-NMR the conclusion was again that the **6** had not reacted.

Comment:

Failure

Attempted reaction with 5 and 8.

In a dry 25 mL schlenk flask 30 mg (0.07 mmol, 1 equiv) **5** was dissolved in 1 mL THF and cooled down on ice. A oven dried micro syringe was loaded with 50 µL(0.13 mmol, 1.8 equiv) 2.5 M butyl lithium, in hexane, and added dropwise to the solution; substrate still on ice. The reaction mixture was allowed to stir on ice for 30 minutes, removed the solvent. Then 19 mg (0.03mmol, 0.05 equiv) of **8** was dissolved in 1 mL THF and transferred by canulla to the free carbene, which was still on ice. It was allowed to stir for 4 hours, while the ice was melting making the temperature go slowly to ambient. The solvent was removed under reduced pressure and the raw product dissolved in dichloromethane and filtered over celite. The solvent was then again removed under reduced pressure and the raw product characterized by ^{1}H-NMR which gave the conclusion that the dimeric structure of **8** had not been broken. This was due to the fact that all the peaks for the precursor complex were still there.

Comment:

Failure

Attempted reaction with the free carbene of 5 and 7

A dry 25 mL schlenk flask was introduced to the glovebox and loaded with 20 mg (0.047 mmol, 1 equiv) of **5** and 20 mg(0.095 mmol, 2.0 equiv) KBTSA. 47 mg(0.049 mmol, 1.0 equiv) of **7** was weighted in the glovebox and put in another 25 mL schlenk flask. Both schlenk flasks were brought out of the glovebox and connected to the schlenk line. To both of the schlenk flasks 2 mL THF were added and stirred vigorously. After 30 min the solvent was removed under reduced from the flask with the ligand. The complex was added to the free carbene by canulla. The reaction mixture was stirred at room temperature for 1 hour and was followed by TLC(8:2 Hexane:Ether). When the TLC did not show any change after 1 hour the reaction mixture was heated to 40°C and stirred over night. The TLC the next morning did not show any change and therefore after 16 hours AgCl was added to scavenge some of the triphenylphosphine. It was allowed to stir for 6 hours while following the reaction by 2D-TLC. A brown spot developed on the TLC. When the brown spot did not seem to grow in extent the reaction was stopped, after 22.5 hours in total. The solvent was removed under reduced pressure and the raw product dissolved in ether and filtered over celite. The solution was the concentrated and filtered by canulla. Pentane was then added until a precipitate started to form. It was left in the freezer over night and then filtered by canulla the next day. It was again concentrated and filtered by canulla and put in the freezer over night. It was again filtrated by canulla and characterized by ^{1}H-NMR and ^{31}P-NMR. It was hard to make any conclusions from ^{1}H-NMR but from ^{31}P-NMR gave some results.

^{31}P-NMR (216MHz, $CDCl_3$, Ref: 85% H_3PO_4; 0.00 ppm): δ 51.3 (51 %) 50.7 (22 %) 48.5 (2 %) 48.2 (2 %) 29.7 (12 %) 10.3 (5 %) 6.5(6 %).

Comment:

It showed impossible to isolate the peaks which were thought to be the product from the starting material; 29.7 ppm. By this reason concluded as a failure.

Attempted reaction with the free carbene of 5 and $RuHCl(PPh_3)_3$

A dry 25 mL schlenk flask was introduced to the glovebox and loaded with 20 mg (0.047 mmol, 1 equiv) of **5** and 20 mg (0.095 mmol, 2.0 equiv) KBTSA. 43 mg (0.049 mmol, 1.0 equiv) of $RuCl_2(PPh_3)_3$ was weighted in the glovebox and put in another 25 mL schlenk flask. Both schlenk flasks were taken out of the glovebox and connected to the schlenk line. 2 mL THF was added to the schlenk flask containing the ligand and the mixture was stirred for 30 minutes at room temperature and then the solvent removed under reduced pressure. $RuHCl(PPh_3)_3$ was dissolved in 2 mL THF and transferred by canulla to the free carbene. The reaction mixture was stirred at room temperature for

2.5 hours. The reaction was monitored by TLC, and when nothing seemed to happen 10 mg AgCl was added and the reaction mixture heated to 40°C. After 24 hours the solvent was removed under reduced pressure and the raw product dissolved in dichloromethane and filtered over celite. It was characterized by ^{1}H-NMR and when the spectra only showed peak in the upfield area; a quartet at -17.80ppm (q, $^{2}J_{H,P}$=26Hz), which is know to be the starting material from the literature.[226]

Comments:

Failure. From the integration most of the starting material had decomposed.

Iridium complex with å-NHC

Synthesis of $[IrClCOD]_2$

30 mL of a 2:1 mixture of isopropanol:water was put in a 500 mL round bottom schlenk flask and degassed by bubbling argon through for 30 minutes. 1.27 g(2.27 mmol, 1 equiv) of $IrCl_3 \cdot H_2O$ was added to the solvent under argon. 3 mL(24.5 mmol, 11 equiv) COD was added by a syringe through a septum on the flask. A condenser was attached to the flask and the reaction mixture heated to reflux; ~90°C; under argon. It was allowed to reflux over night. The next day the reaction mixture was removed from the heating source and allowed to cool to ambient temperature. A red-orange precipitate was the product. The product was washed with cold 2×5mL cold methanol to yield: 0.608 g; 79 %. Characterized by:

^{1}H-NMR (400MHz, $CDCl_3$; 7.26ppm): δ 4.24 (m) 2.26 (m) 1.53 (m).

Comment:

The integration does not make sense, but the peaks correspond nicely with the literature.[227] The reason might be due to incorrect NMR-settings; to short delay time.[71,72]

Reaction of free carbene of 5 with $[IrClCOD]_2$[205]

A dry 100 mL schlenk flask was introduced to the glovebox and loaded with 190 mg(0.44 mmol, 2.0 equiv) of **5** and 190 mg(0.90 mmol, 4.0 equiv) KBTSA. The flask was brought out of the glovebox and connected to the schlenk line and put on ice. It was filled with 5 mL THF and stirred on ice for 1 hour. The solvent was then removed under reduced pressure. During this reaction the colour went from colourless to red. 148 mg (0.22 mmol, 1 equiv) $[IrClCOD]_2$ was dissolved in 5 mL THF and

transferred to the free carbene by canulla; the reaction was cooled on ice. The reaction was ongoing for 2 hours on melting ice. The colour in the start was orange and in the end darkly red. The solvent was removed under reduced pressure, redissolved in dichloromethane and then filtered over celite. The solvent was then removed under reduced pressure. Yield 263.4 mg (86%). Then it was made a concentrated solution in hexane. This solution was filtrated by canulla into a crystallization tube and put in the freezer, this solution yielded good enough crystals for x-ray diffraction analysis. The solids which were left in the schlenk flask were characterized by ^{1}H-NMR.

^{1}H –NMR (600MHz, $CDCl_3$; 7.26 ppm): δ 7.36 (t, J=7.8Hz, 1H) 7.18 (d, J=7.8Hz, 2H) 6.90 (d, J=1.5Hz, 1H) 6.70 (d, J=1.5Hz, 1H) 4.89 (m, 2H) 4.30 (t, J=9.9Hz, 2H) 3.66 (t, J=9.9Hz, 2H) 3.08 (sep, J=6.9Hz) 2.33 (s, 3H) 2.30 (m, 2H) 2.01 (m, 2H) 1.84 (m, 2H) 1.62 (m, 2H) 1.51 (d, J=6.9Hz, 6H) 1.46 (m, 2H) 1.43 (s, 9H) 1.17 (d, J=6.9Hz, 6H).

^{13}C-NMR (150.9MHz, $CDCl_3$; 77.16 ppm): δ 188.3, 153.7, 147.0, 138.3, 137.8, 130.6, 129.0, 124.7, 122.9, 121.3, 116.8, 87.3, 54.5, 49.8, 47.9, 35.3, 33.9, 30.2, 28.5, 26.3, 24.3, 21.2.

Element analysis: N 4.15 % C 58.02 % H 6.82 % Theoretical: N 4.05 % C 59.01 % H 6.85 %

MS (IS=PEG+H, 250C DART) 693.34300 m/z Theoretical: 693.33976 m/z (4.7 ppm)

Mol weight: 691.94 g/mol.

Comment:

Main fragment in MS is the protonated molecule, method related. This fits with the isotopic distribution of iridium.

Crystall data:

Identification code	**9**	
Empirical formula	C34 H47 Ir N2 O	
Formula weight	691.94	
Temperature	123(2) K	
Wavelength	0.71073 Å	
Crystal system	Triclinic	
Space group	P-1	
Unit cell dimensions	a = 8.8707(4) Å	α= 79.3883(4)°.
	b = 12.9730(5) Å	β= 83.4457(5)°.
	c = 13.2928(5) Å	γ = 83.7041(4)°.
Volume	1487.57(10) Å^3	
Z	2	
Density (calculated)	1.545 Mg/m^3	
Absorption coefficient	4.516 mm^{-1}	

F(000)	700
Crystal colour	Purple
Crystal habit	Triangular prism
Crystal size	0.25 x 0.125 x 0.125 mm^3
Theta range for data collection	2.04 to 30.51°.
Index ranges	-12<=h<=12, -18<=k<=18, -18<=l<=18
Reflections collected	25472
Independent reflections	9037 [R(int) = 0.0235]
Completeness to theta = 30.51°	99.6 %
Absorption correction	None
Max. and min. transmission	0.6021 and 0.3981
Refinement method	Full-matrix least-squares on F^2
Data / restraints / parameters	9037 / 0 / 351
Goodness-of-fit on F^2	1.061
Final R indices [I>2sigma(I)]	R1 = 0.0170, wR2 = 0.0437
R indices (all data)	R1 = 0.0180, wR2 = 0.0442
Largest diff. peak and hole	2.288 and -0.729 e.$Å^{-3}$

Bond lengths:

Ir(1)-O(1)	2.0191(12)
Ir(1)-C(1)	2.0231(16)
Ir(1)-C(32)	2.1010(17)
Ir(1)-C(31)	2.1314(16)
Ir(1)-C(28)	2.1792(16)
Ir(1)-C(27)	2.1981(16)

Angles:

O(1)-Ir(1)-C(1)	87.07(6)
O(1)-Ir(1)-C(32)	157.34(7)
C(1)-Ir(1)-C(32)	94.97(6)
O(1)-Ir(1)-C(31)	161.28(6)
C(1)-Ir(1)-C(31)	101.88(6)
C(32)-Ir(1)-C(31)	39.37(7)
O(1)-Ir(1)-C(28)	85.75(6)
C(1)-Ir(1)-C(28)	163.01(7)
C(32)-Ir(1)-C(28)	97.58(6)
C(31)-Ir(1)-C(28)	81.05(6)
O(1)-Ir(1)-C(27)	88.84(6)
C(1)-Ir(1)-C(27)	157.96(7)
C(32)-Ir(1)-C(27)	80.83(7)
C(31)-Ir(1)-C(27)	88.62(6)

C(28)-Ir(1)-C(27)	37.17(6)
C(5)-O(1)-Ir(1)	126.78(10)
N(1)-C(1)-N(2)	107.15(13)
N(1)-C(1)-Ir(1)	121.59(11)
N(2)-C(1)-Ir(1)	131.16(12)

Torsions:

C(1)-Ir(1)-O(1)-C(5)	35.52(13)
C(32)-Ir(1)-O(1)-C(5)	-60.4(2)
C(31)-Ir(1)-O(1)-C(5)	154.93(17)
C(28)-Ir(1)-O(1)-C(5)	-159.90(14)
C(27)-Ir(1)-O(1)-C(5)	-122.81(14)
O(1)-Ir(1)-C(1)-N(1)	-29.95(13)
C(32)-Ir(1)-C(1)-N(1)	127.43(13)
C(31)-Ir(1)-C(1)-N(1)	166.66(12)
C(28)-Ir(1)-C(1)-N(1)	-95.0(2)
C(27)-Ir(1)-C(1)-N(1)	49.7(2)
O(1)-Ir(1)-C(1)-N(2)	154.15(15)
C(32)-Ir(1)-C(1)-N(2)	-48.47(15)
C(31)-Ir(1)-C(1)-N(2)	-9.24(16)
C(28)-Ir(1)-C(1)-N(2)	89.1(2)
C(27)-Ir(1)-C(1)-N(2)	-126.24(18)
N(2)-C(1)-N(1)-C(4)	-170.12(14)
Ir(1)-C(1)-N(1)-C(4)	13.1(2)
N(2)-C(1)-N(1)-C(3)	8.76(18)
Ir(1)-C(1)-N(1)-C(3)	-168.01(11)
N(1)-C(1)-N(2)-C(15)	159.50(14)
Ir(1)-C(1)-N(2)-C(15)	-24.2(2)
N(1)-C(1)-N(2)-C(2)	6.03(18)
Ir(1)-C(1)-N(2)-C(2)	-177.62(12)
C(1)-N(2)-C(2)-C(3)	-17.31(17)
C(15)-N(2)-C(2)-C(3)	-172.83(13)
C(1)-N(1)-C(3)-C(2)	-18.93(17)
C(4)-N(1)-C(3)-C(2)	160.06(14)
N(2)-C(2)-C(3)-N(1)	20.28(16)
C(1)-N(1)-C(4)-C(9)	-169.22(15)
C(3)-N(1)-C(4)-C(9)	12.0(2)
C(1)-N(1)-C(4)-C(5)	14.7(2)
C(3)-N(1)-C(4)-C(5)	-164.15(14)
Ir(1)-O(1)-C(5)-C(4)	-20.8(2)
Ir(1)-O(1)-C(5)-C(6)	158.08(11)

A.6 Spectras

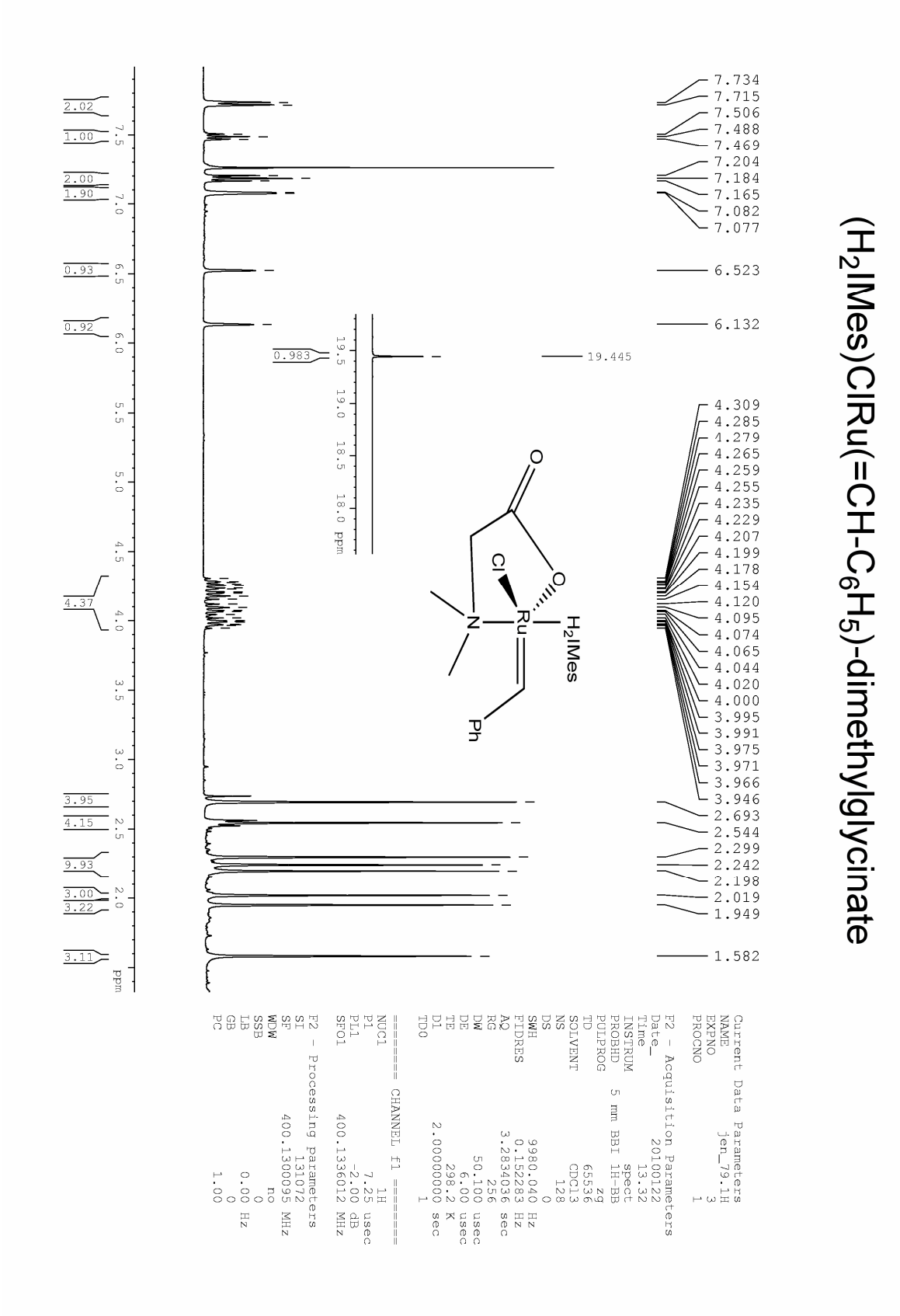
(H2IMes)ClRu(=CH-C6H5)-dimethylglycinate
H2IMes
Cl
Ru
N
O
Ph
7.734
7.715
7.506
7.488
7.469
7.204
7.184
7.165
7.082
7.077
6.523
6.132
19.445
4.309
4.285
4.279
4.265
4.259
4.255
4.235
4.229
4.207
4.199
4.178
4.154
4.120
4.095
4.074
4.065
4.044
4.020
4.000
3.995
3.991
3.975
3.971
3.966
3.946
2.693
2.544
2.299
2.242
2.198
2.019
1.949
1.582
2.02
1.00
2.00
1.90
0.93
0.92
0.983
4.37
3.95
4.15
9.93
3.00
3.22
3.11
ppm
Current Data Parameters
NAME jen_79.1H
EXPNO 3
PROCNO 1
F2 - Acquisition Parameters
Date_ 20100122
Time_ 13.32
INSTRUM spect
PROBHD 5 mm BBI 1H-BB
PULPROG zg
TD 65536
SOLVENT CDCl3
NS 128
DS 0
SWH 9980.040 Hz
FIDRES 0.152283 Hz
AQ 3.2834036 sec
RG 256
DW 50.100 usec
DE 6.00 usec
TE 298.2 K
D1 2.00000000 sec
TD0 1
======== CHANNEL f1 ========
NUC1 1H
P1 7.25 usec
PL1 -2.00 dB
SFO1 400.1336012 MHz
F2 - Processing parameters
SI 131072
SF 400.1300095 MHz
WDW no
SSB 0
LB 0.00 Hz
GB 0
PC 1.00

$(H_2IMes)ClRu(=CH\text{-}C_6H_5)$-dimethylglycinate

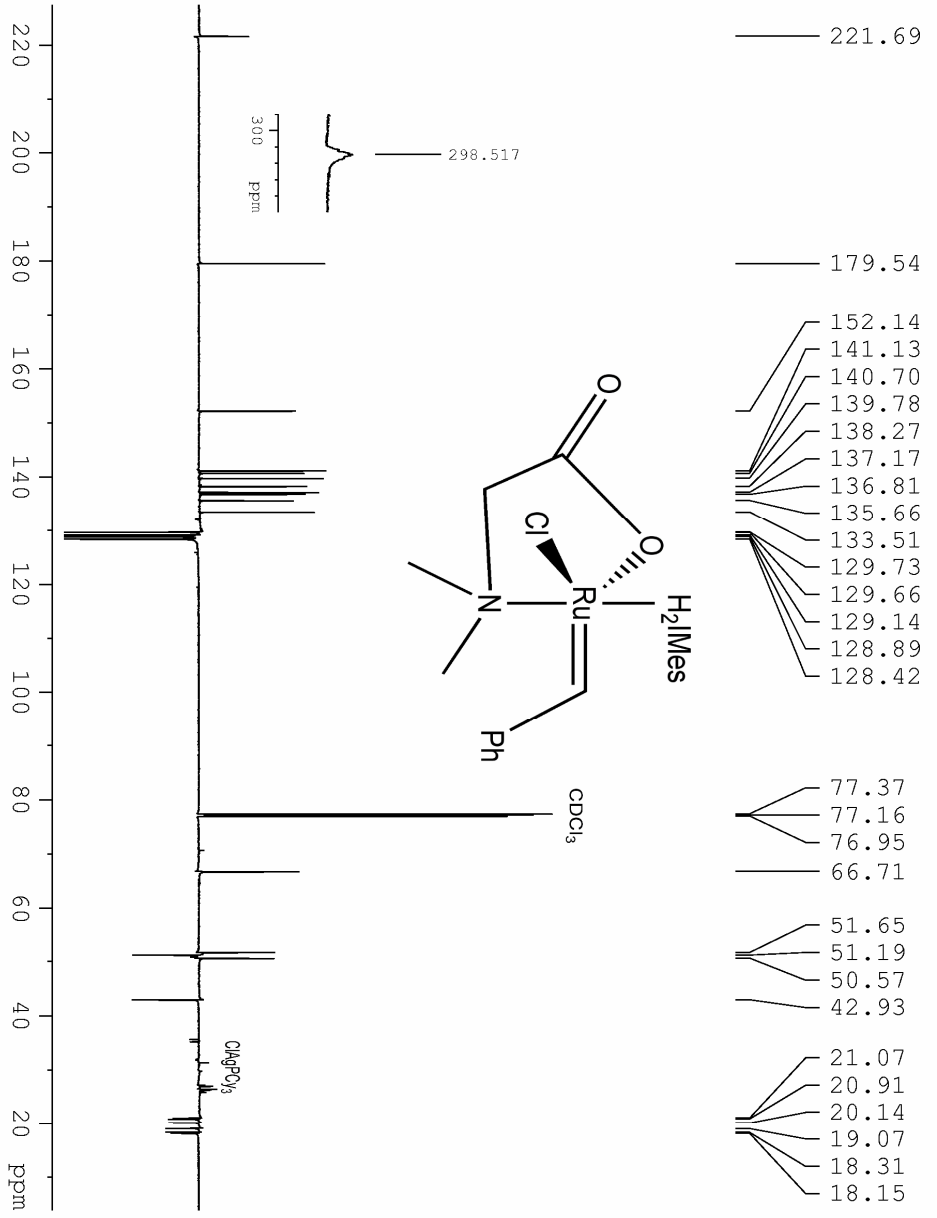


```
Current Data Parameters
NAME          jen_79_600.capt
EXPNO                       1
PROCNO                      1

F2 - Acquisition Parameters
Date_                20100410
Time                    13.04
INSTRUM                  spect
PROBHD     5 mm CPTCI 1H-
PULPROG                  aptjc
TD                       65536
SOLVENT                  CDCl3
NS                       10240
DS                           8
SWH                  52910.055 Hz
FIDRES                0.807343 Hz
AQ                    0.6193746 sec
RG                       10300
DW                     9.450 usec
DE                     6.00 usec
TE                      300.8 K
CNST2               145.0000000
D1                    6.0000000 sec
d2                    0.0034828 sec
d4                    0.0017241 sec
d11                   0.0300000 sec
P1                      12.50 usec
TD0                         1

========== CHANNEL f1 ==========
NUC1                       13C
PO                     10.00 usec
P2                     25.00 usec
PL1                    -1.80 dB
SFO1             150.9238595 MHz

========== CHANNEL f2 ==========
CPDPRG2                waltz16
NUC2                        1H
P3                      6.75 usec
P4                     13.50 usec
PCPD2                 100.00 usec
PL2                    3.00 dB
PL12                  20.00 dB
SFO2             600.1342000 MHz

F2 - Processing parameters
SI                      131072
SF               150.9027960 MHz
WDW                         EM
SSB                          0
LB                        2.00 Hz
GB                           0
PC                        1.40
```

Acq. Data Name: 200510AS
Internal Sample Id: IS=PEG,250
Ionization Mode: ESI+
MS Calibration Name: PEG_ESI+_16mars10
Orifice1 Volt Sweep: 20V
Acquired m/z Range: 7.0..1000.0
Spec. Record Interval: 0.4[s]
Ring Lens Volt: 4[V]
Time of Maximum: 2.749[min]
Reduction History: Determine m/z[Peak Detect[Centroid,80,Area];Correct Base[5.0%]];Correct Base[5.0%];Average(MS[1] 2.743..2.755)
Experiment Date/Time: 5/20/2010 11:41:09 AM
Operator Name: Accutof

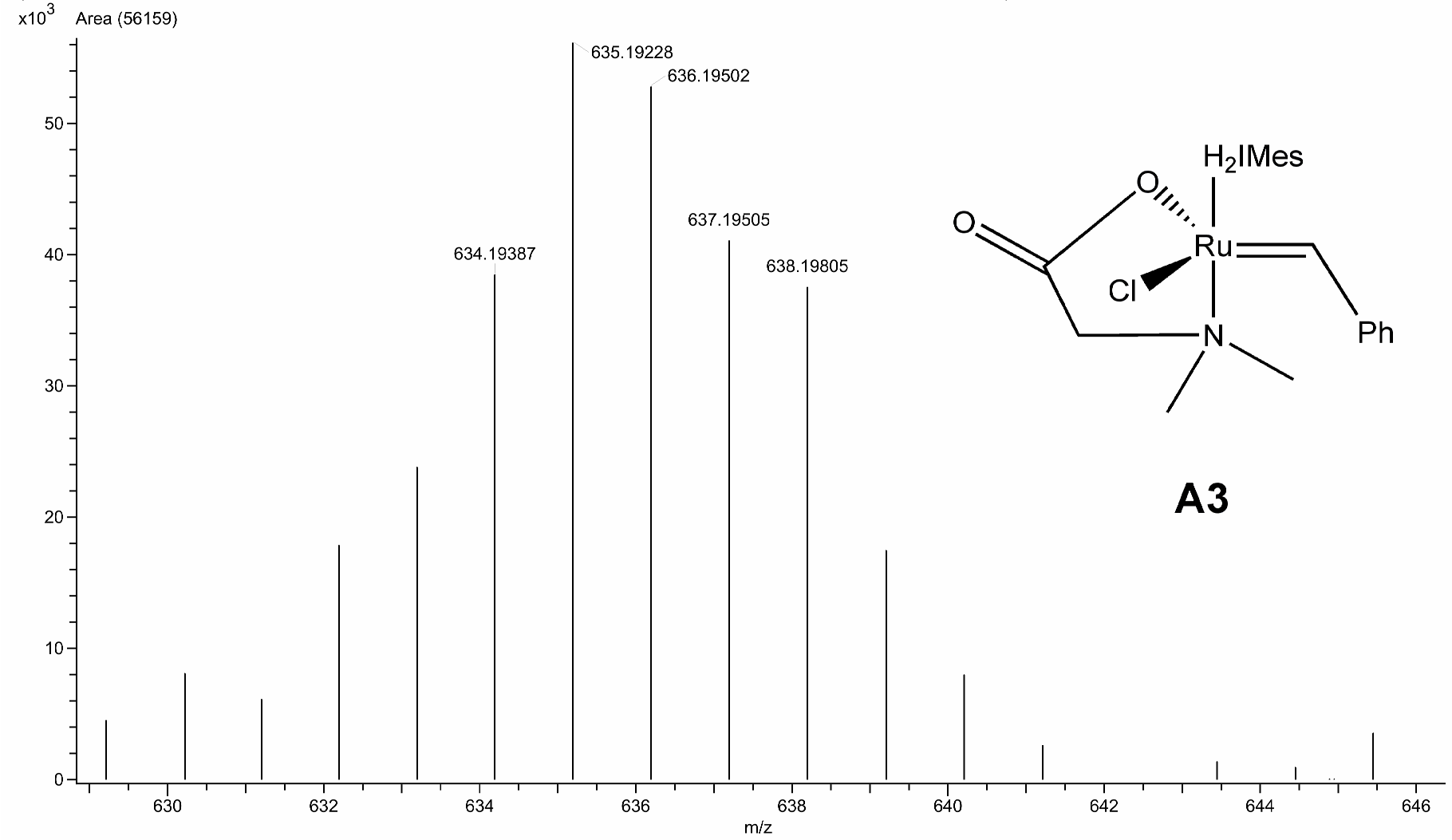

A3

$H_2IMesClRu(=CH\text{-}C_6H_5)\text{-}(2\text{-piperidin-acetate})$

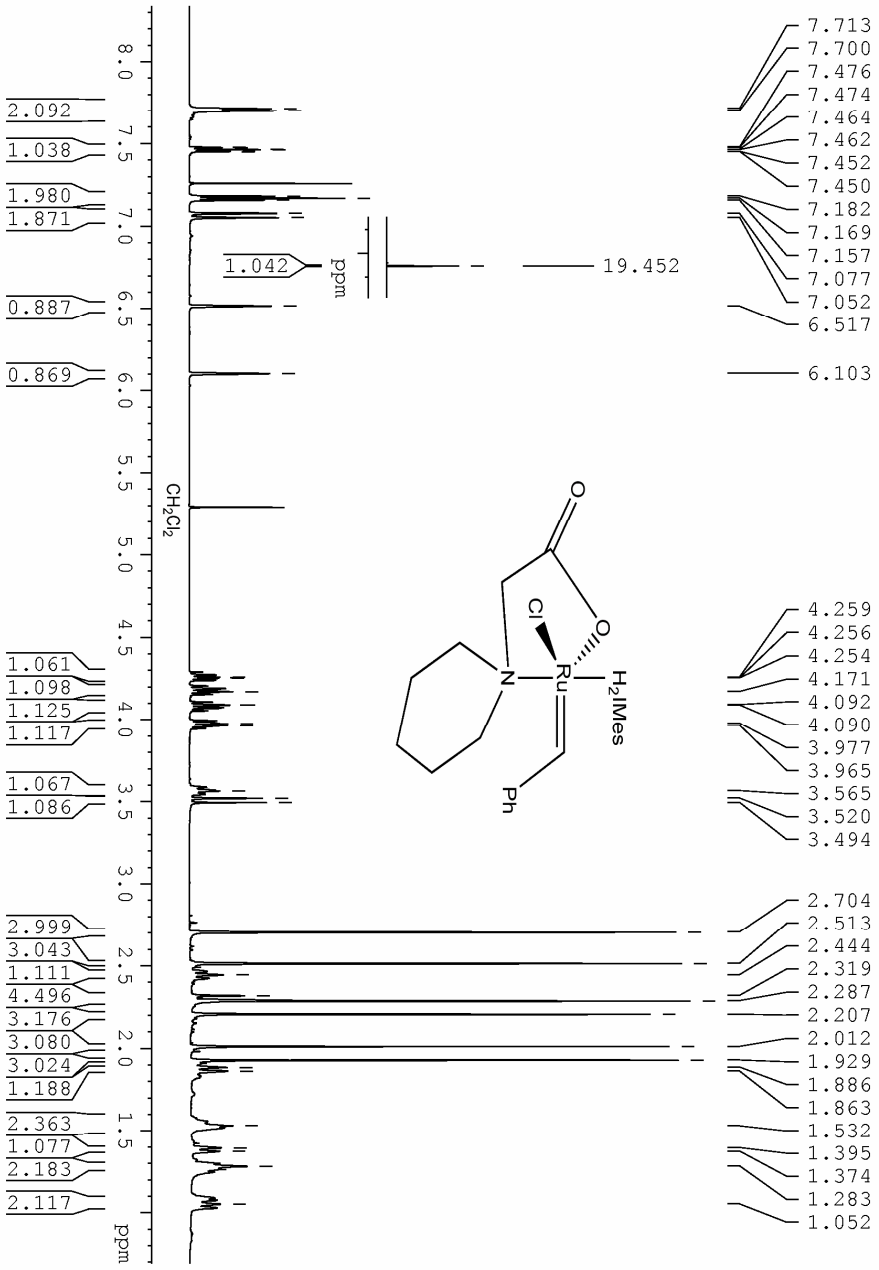


```
Current Data Parameters
NAME                  jen_86.600_1H
EXPNO                            1
PROCNO                           1

F2 - Acquisition Parameters
Date_                     20100417
Time                         15.48
INSTRUM                      spect
PROBHD     5 mm CPTCI 1H-
PULPROG                         zg
TD                           65536
SOLVENT                     CDCl3
NS                              32
DS                               0
SWH                    13550.136 Hz
FIDRES                     0.206759 Hz
AQ                         2.4183652 sec
RG                            11.3
DW                        36.900 usec
DE                         6.00 usec
TE                           300.8 K
D1                     1.00000000 sec
TD0                              1

========== CHANNEL f1 ========
NUC1                           1H
P1                         6.75 usec
PL1                        3.00 dB
SFO1                600.1364844 MHz

F2 - Processing parameters
SI                           131072
SF                  600.1300176 MHz
WDW                             no
SSB                              0
LB                            0.00 Hz
GB                               0
PC                            1.00
```

$H_2IMesClRu(=CH\text{-}C_6H_5)\text{-}(2\text{-piperidin-acetate})$

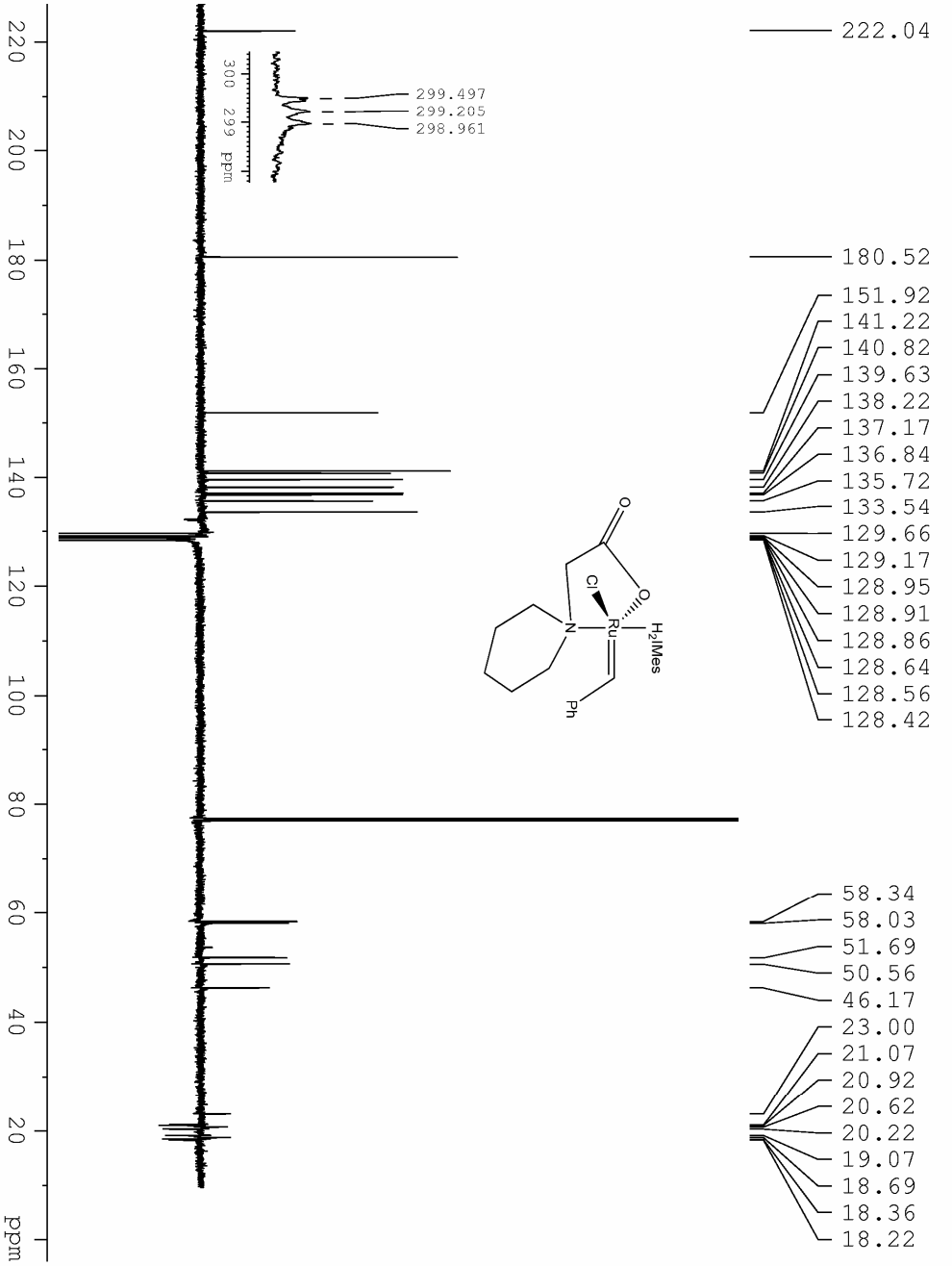


```
Current Data Parameters
NAME                  Jen_89_600.capt
EXPNO                              1
PROCNO                             1

F2 - Acquisition Parameters
Date_                       20100417
Time                           16.12
INSTRUM                         spect
PROBHD     5 mm CPTCI 1H-
PULPROG                        aptjc
TD                             65536
SOLVENT                        CDCl3
NS                               909
DS                                 8
SWH                        45454.547 Hz
FIDRES                      0.693581 Hz
AQ                          0.7209570 sec
RG                             10300
DW                            11.000 usec
DE                             6.00 usec
TE                            300.8 K
CNST2                      145.0000000
D1                          10.00000000 sec
d2                           0.00344828 sec
d4                           0.00172414 sec
d11                          0.03000000 sec
P1                             12.00 usec
TD0                                1

========== CHANNEL f1 ==========
NUC1                             13C
P0                             10.00 usec
P2                             24.00 usec
PL1                            -1.80 dB
SFO1                    150.9269456 MHz

========== CHANNEL f2 ==========
CPDPRG2                      waltz16
NUC2                             1H
P3                             6.62 usec
P4                            13.24 usec
PCPD2                        100.00 usec
PL2                            3.00 dB
PL12                          20.00 dB
SFO2                    600.1342000 MHz

F2 - Processing parameters
SI                            131072
SF                      150.9027934 MHz
WDW                               EM
SSB                                0
LB                              2.00 Hz
GB                                 0
PC                              1.40
```

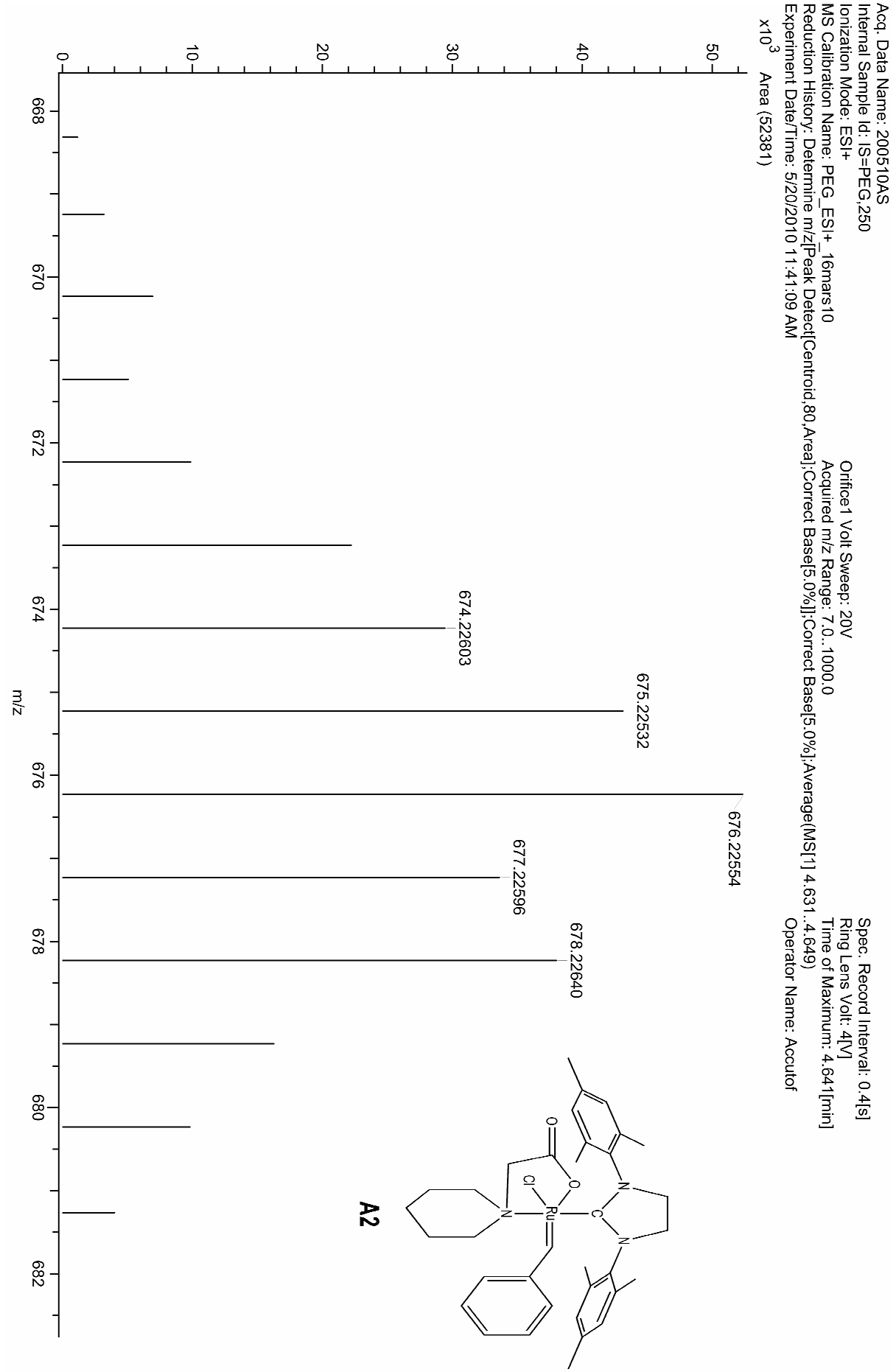
Acq. Data Name: 200510AS
Internal Sample Id: IS=PEG,250
Ionization Mode: ESI+
MS Calibration Name: PEG_ESI+_16mars10
Reduction History: Determine m/z[Peak Detect[Centroid,80,Area];Correct Base[5.0%]];Correct Base[5.0%];Average(MS[1] 4.631..4.649)
Experiment Date/Time: 5/20/2010 11:41:09 AM
Orifice1 Volt Sweep: 20V
Acquired m/z Range: 7.0..1000.0
Spec. Record Interval: 0.4[s]
Ring Lens Volt: 4[V]
Time of Maximum: 4.641[min]
Operator Name: Accutof
x10^3 Area (52381)
50
40
30
20
10
0
668
670
672
674
676
678
680
682
m/z
674.22603
675.22532
676.22554
677.22596
678.22640
A2

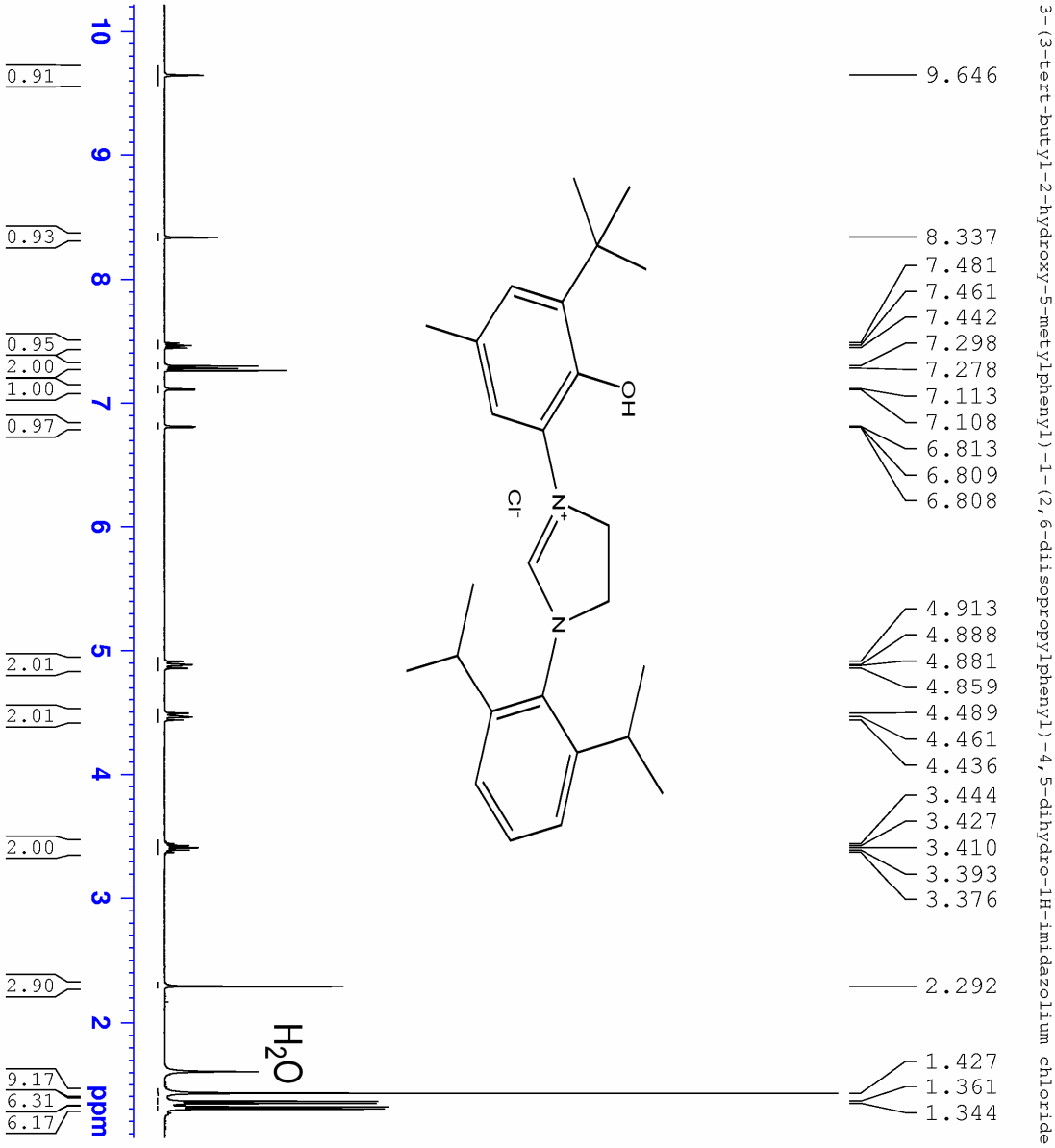
3-(3-tert-butyl-2-hydroxy-5-methylphenyl)-1-(2,6-diisopropylphenyl)-4,5-dihydro-1H-imidazolium chloride
9.646
8.337
7.481
7.461
7.442
7.298
7.278
7.113
7.108
6.813
6.809
6.808
4.913
4.888
4.881
4.859
4.489
4.461
4.436
3.444
3.427
3.410
3.393
3.376
2.292
1.427
1.361
1.344
OH
Cl⁻
N
N
H2O
0.91
0.93
0.95
2.00
1.00
0.97
2.01
2.01
2.00
2.90
9.17
6.31
6.17
10
9
8
7
6
5
4
3
2
ppm
Current Data Parameters
NAME jen_58.1h
EXPNO 3
PROCNO 1
F2 - Acquisition Parameters
Date_ 20090917
Time 17.41
INSTRUM spect
PROBHD 5 mm BBI 1H-BB
PULPROG zg
TD 19722
SOLVENT CDCl3
NS 32
DS 0
SWH 4930.966 Hz
FIDRES 0.250024 Hz
AQ 1.9998608 sec
RG 161.3
DW 101.400 usec
DE 6.00 usec
TE 299.2 K
D1 2.00000000 sec
TD0 1
======== CHANNEL f1 ========
NUC1 1H
P1 7.25 usec
PL1 -2.00 dB
SFO1 400.1322602 MHz
F2 - Processing parameters
SI 32768
SF 400.1300094 MHz
WDW no
SSB 0
LB 0.00 Hz
GB 0
PC 1.00

3-(3-tert-butyl-2-hydroxy-5-metylphenyl)-1-(2,6-diisopropylphenyl)-4,5-dihydro-1H-imidazolium chloride

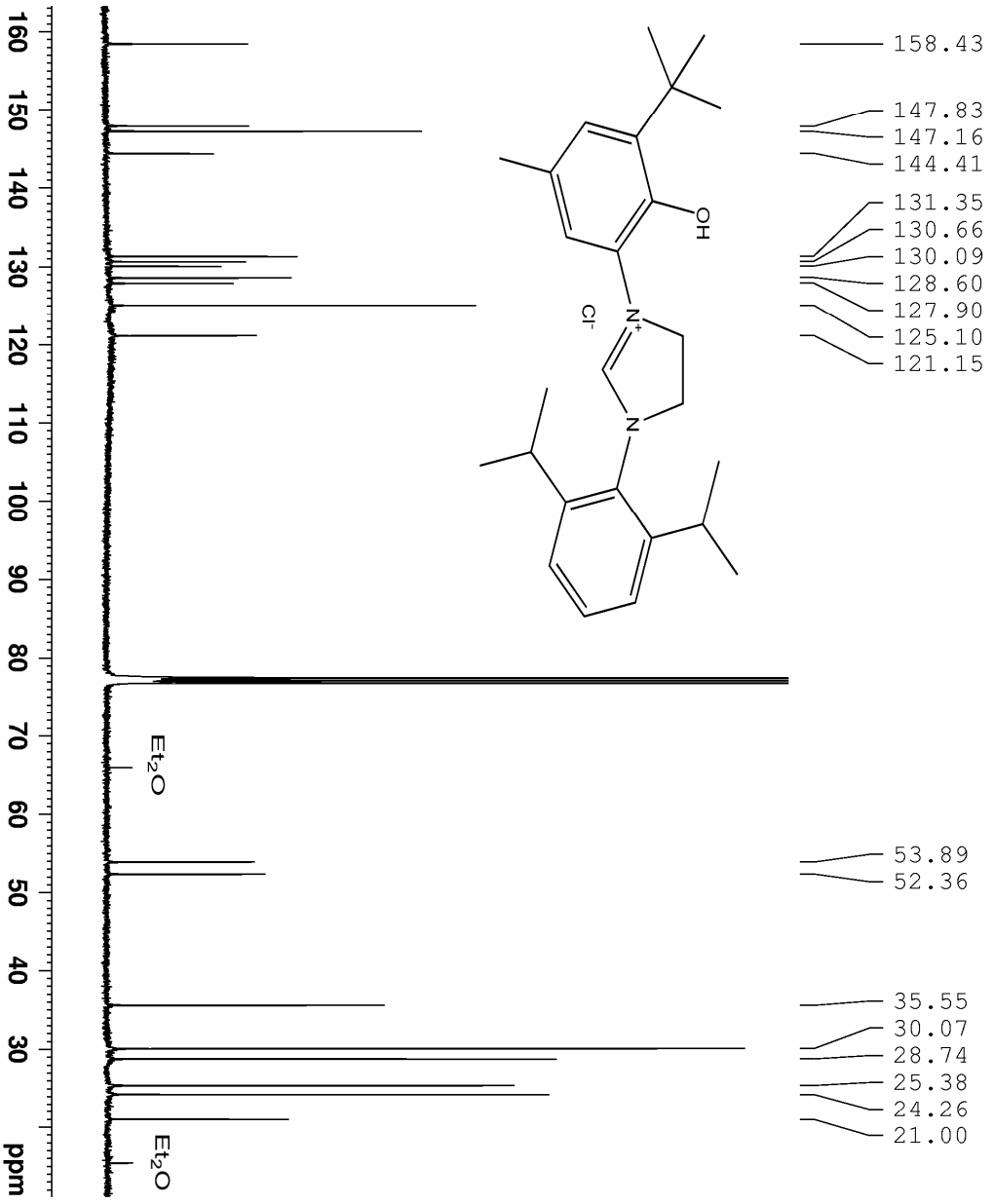


```
Current Data Parameters
NAME                  jen_34.13C
EXPNO                          2
PROCNO                         1

F2 - Acquisition Parameters
Date_                   20090511
Time                       18.17
INSTRUM                    spect
PROBHD     5 mm BBI 1H-BB
PULPROG                    zgdc
TD                       119756
SOLVENT                  CDCl3
NS                         4000
DS                            0
SWH                   29940.119 Hz
FIDRES                 0.250009 Hz
AQ                     1.9999752 sec
RG                          8192
DW                        16.700 usec
DE                         6.00 usec
TE                        298.2 K
D1                    10.00000000 sec
d11                    0.03000000 sec
TD0                           1

========== CHANNEL f1 ==========
NUC1                         13C
P1                         10.00 usec
PL1                        -4.00 dB
SFO1                 100.6228298 MHz

========== CHANNEL f2 ==========
CPDPRG2                  waltz16
NUC2                          1H
PCPD2                     100.00 usec
PL2                        -2.00 dB
PL12                       18.00 dB
SFO2                 400.1319540 MHz

F2 - Processing parameters
SI                         32768
SF                   100.6127571 MHz
WDW                           EM
SSB                            0
LB                          1.00 Hz
GB                             0
PC                          1.40
```

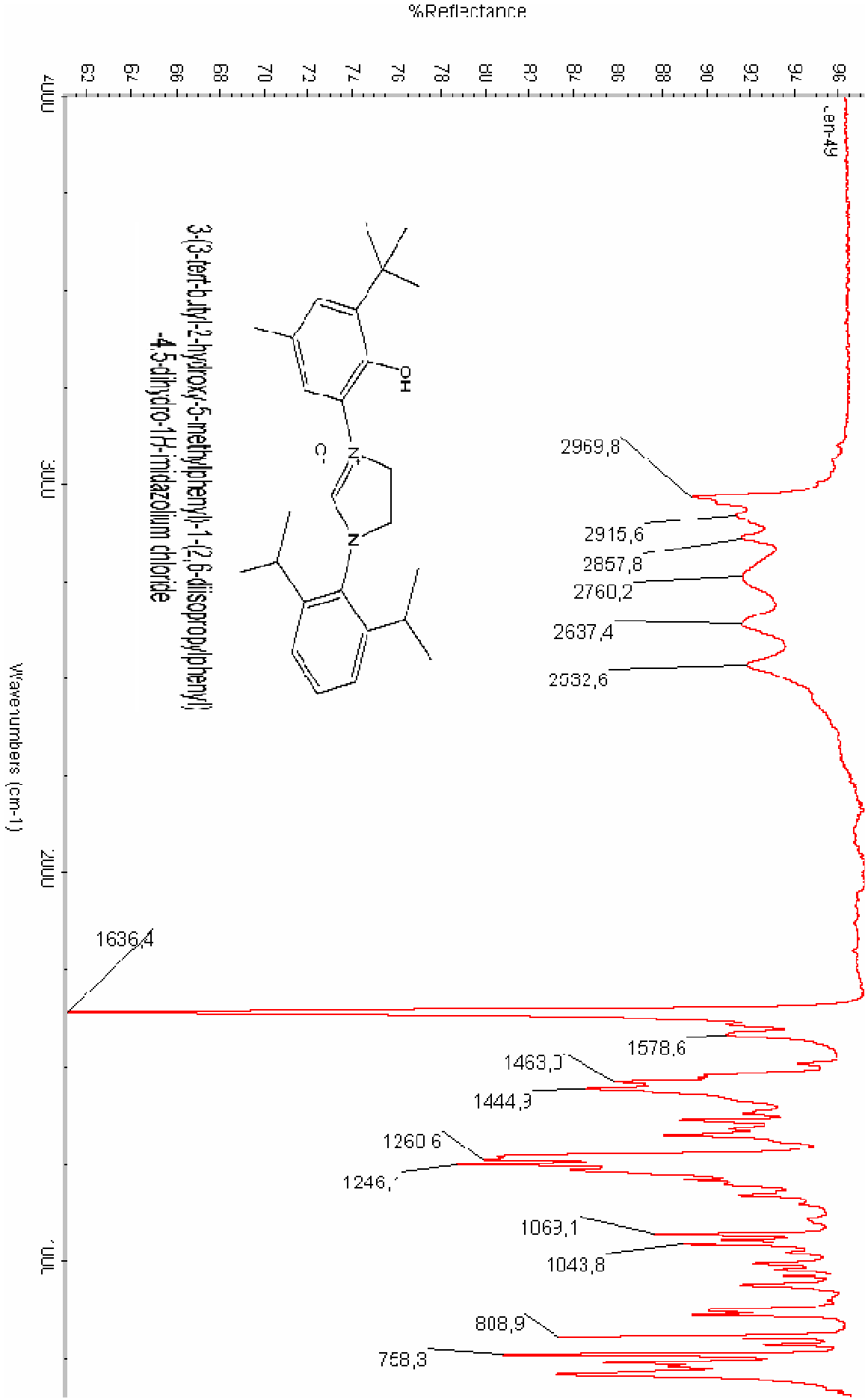
%Reflectance
Wavenumbers (cm-1)
4000
3000
2000
1000
96
94
92
90
88
86
84
82
80
78
76
74
72
70
68
66
64
62
Leu-49
3-(3-tert-butyl-2-hydroxy-5-methylphenyl)-1-(2,6-diisopropylphenyl)
-4,5-dihydro-1H-imidazolium chloride
OH
N
N
Cl
2969,8
2915,6
2857,8
2760,2
2637,4
2532,6
1636,4
1578,6
1463,0
1444,3
1260,6
1246,
1069,1
1043,8
808,9
758,3

IrCOD(3-(3-*tert*-butyl-5-methyl-phen-2-olate)-1-(2,6-diisopropyl) -4,5-dihydo-imidazol-2-yllidene

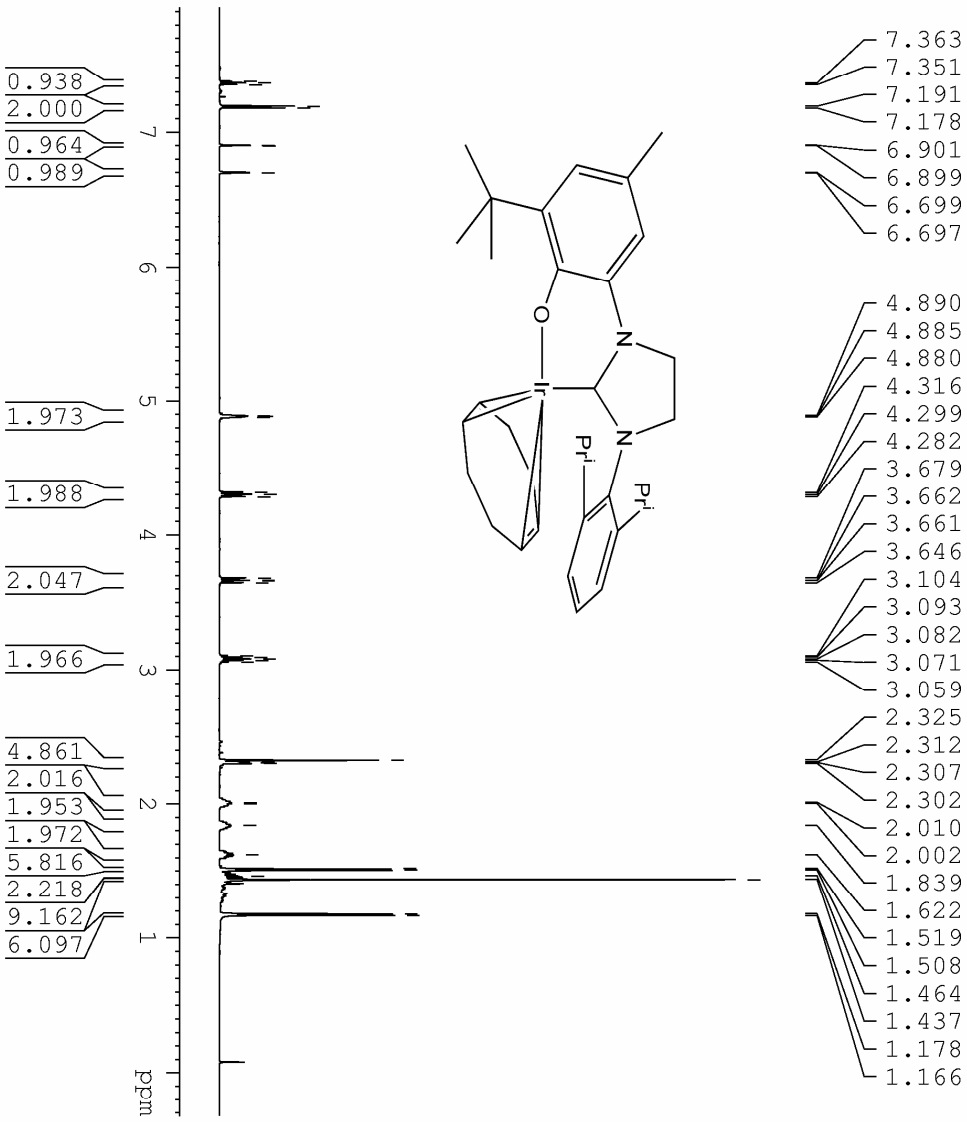


```
Current Data Parameters
NAME                  jen_87.600_1H
EXPNO                            1
PROCNO                           1

F2 - Acquisition Parameters
Date_                     20100314
Time                         14.39
INSTRUM                      spect
PROBHD     5 mm CPTCI 1H-
PULPROG                         zg
TD                           65536
SOLVENT                     CDCl3
NS                              32
DS                               0
SWH                    8992.806 Hz
FIDRES                 0.137219 Hz
AQ                     3.6439073 sec
RG                           11.3
DW                     55.600 usec
DE                      6.00 usec
TE                         300.8 K
D1                     1.00000000 sec
TD0                              1

========== CHANNEL f1 ==========
NUC1                           1H
P1                       6.75 usec
PL1                      3.00 dB
SFO1                600.1342000 MHz

F2 - Processing parameters
SI                           131072
SF                  600.1300172 MHz
WDW                            no
SSB                             0
LB                       0.00 Hz
GB                              0
PC                           1.00
```

IrCOD(3-(3-*tert*-butyl-5-methyl-phen-2-olate)-1-(2,6-diisopropyl) -4,5-dihydo-imidazol-2-yllidene

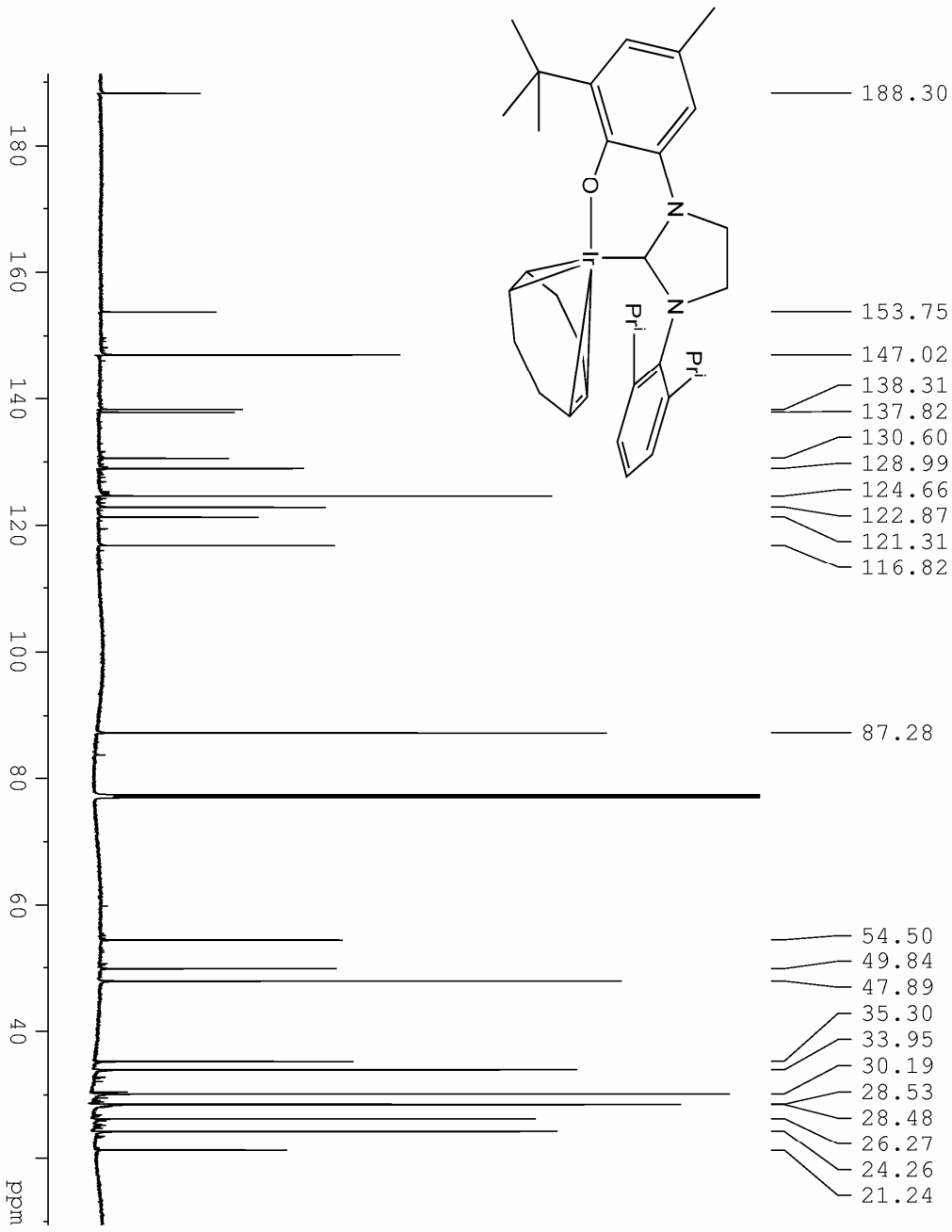


```
Current Data Parameters
NAME                  jen_87_600.13c
EXPNO                              1
PROCNO                             1

F2 - Acquisition Parameters
Date_                       20100314
Time                            14.51
INSTRUM                         spect
PROBHD     5 mm CPTCI 1H-
PULPROG                         zgdc
TD                             65536
SOLVENT                        CDCl3
NS                               758
DS                                 0
SWH                        42372.883 Hz
FIDRES                      0.646559 Hz
AQ                          0.7733866 sec
RG                                 10300
DW                             11.800 usec
DE                             256.00 usec
TE                              300.8 K
D1                         6.00000000 sec
d11                        0.03000000 sec
TD0                                1

======== CHANNEL f1 ========
NUC1                              13C
P1                              10.00 usec
PL1                             -1.80 dB
SFO1                  150.9238595 MHz

======== CHANNEL f2 ========
CPDPRG2                       waltz16
NUC2                              1H
PCPD2                          100.00 usec
PL2                             120.00 dB
PL12                             20.00 dB
SFO2                  600.1342000 MHz

F2 - Processing parameters
SI                            131072
SF                  150.9027892 MHz
WDW                               EM
SSB                                0
LB                              2.00 Hz
GB                                 0
PC                              1.40
```

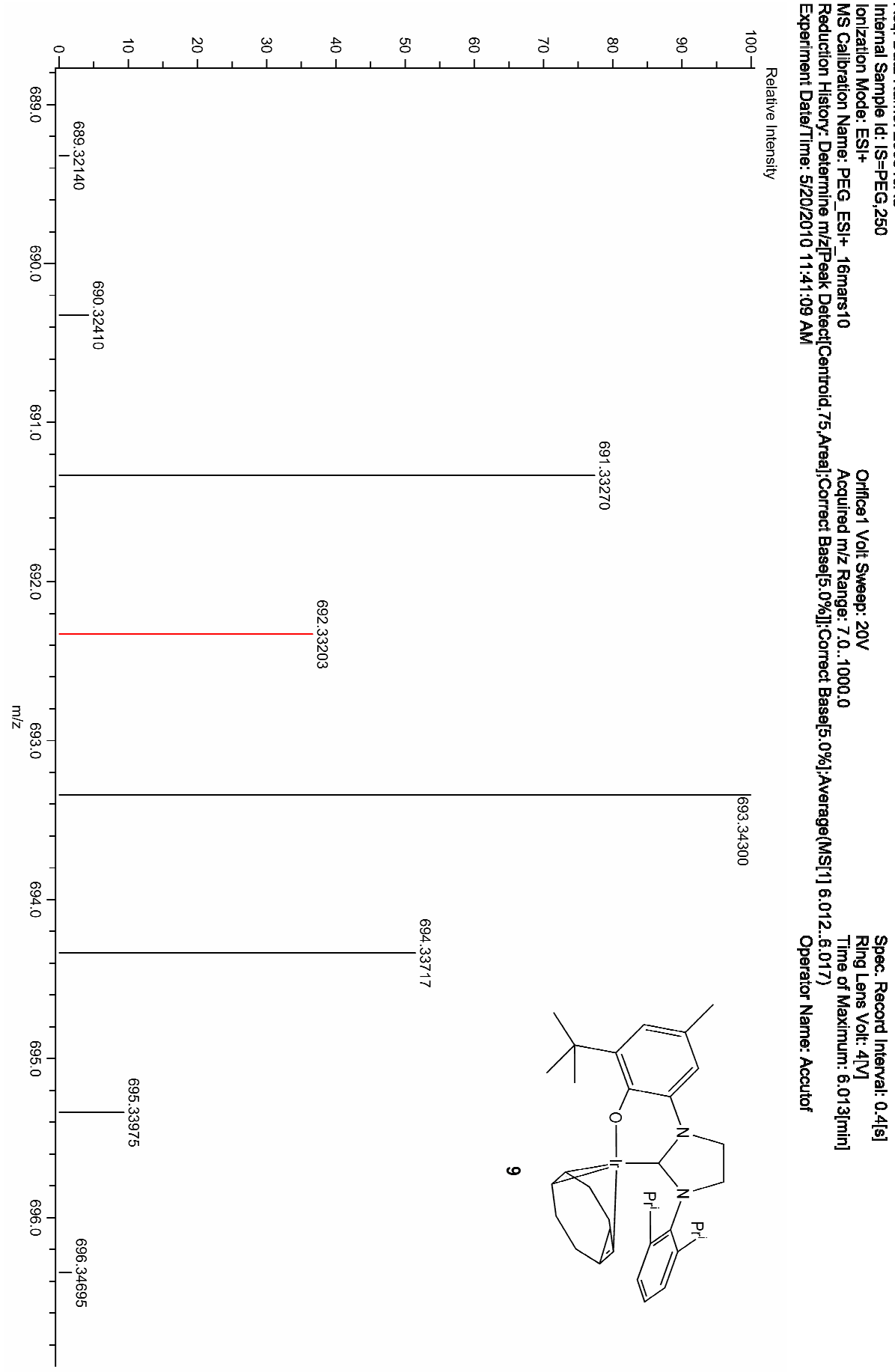
Acq. Data Name: 200510AS
Internal Sample Id: IS=PEG,250
Ionization Mode: ESI+
MS Calibration Name: PEG_ESI+_16mars10
Reduction History: Determine m/z[Peak Detect[Centroid,75,Area]:Correct Base[5.0%]]:Correct Base[5.0%];Average(MS[1] 6.012..6.017)
Experiment Date/Time: 5/20/2010 11:41:09 AM
Orifice1 Volt Sweep: 20V
Acquired m/z Range: 7.0..1000.0
Spec. Record Interval: 0.4[s]
Ring Lens Volt: 4[V]
Time of Maximum: 6.013[min]
Operator Name: Accutof
Relative Intensity
m/z
689.32140
690.32410
691.33270
692.33203
693.34300
694.33717
695.33975
696.34695
9